NON-SPATIAL INFORMATION ENCODING IN HIPPOCAMPAL CA1

By
William Hockeimer

A dissertation submitted to Johns Hopkins University in conformity with the requirements for the degree of Doctor of Philosophy

Baltimore, Maryland
January, 2021

Abstract

Pyramidal neurons of the hippocampus have spatial receptive fields, called place fields, which are thought to subserve both episodic memory and spatial navigation by instantiating a cognitive map. Crucial to the cognitive map is the non-spatial information which imbues the map with rich detail about the external world. However, the details and mechanisms of this multiplexing between spatial and non-spatial information is poorly understood. This thesis reports electrophysiological data taken from tetrode recordings of rat CA1 as rodents completed two different foraging tasks; the data from each of which forms a chapter here. Each task sought to address a specific question regarding non-spatial information coding in CA1. The first explored the rate remapping hypothesis that firing rate modulations in an otherwise stable place field multiplex cue information with spatial location. It was found that rate remapping can occur even in the absence of an association between cues and rewards, supporting the idea that any information the rat attends to is encoded, regardless of salience. Second, it was found that cue-evoked changes to place fields manifested as localized regions of rate change within the field, suggesting a new mechanism for infield computations. The second task explored the phenomenon of place field repetition, in which neurons display multiple firing fields at similar locations. Intriguing temporal dynamics, as well as effects of time and direction, were observed within repeating fields. These effects have begun to be characterized, however more study is the goal of future work. Taken together, these data

expand our understanding of how non-spatial cues are encoded in CA1 and the mechanistic underpinnings of the cognitive map.

Primary Reader: Dr. James Knierim

Secondary Reader: Dr. Shreesh Mysore

To the memory of my grandfather,

Henry Hockeimer

Acknowledgements

The support of many people made this dissertation possible and their role will be briefly acknowledged here. First, I would like to thank my family for their tireless support as I completed this project. They followed the trials and tribulations of the project, and I am grateful that they shared in this experience with me. Next, I would like to thank my adviser, Jim Knierim, and our lab manager, Geeta Rao. The lab is science as it should be done and it was a privilege to be a part of it. Their support was indispensable throughout the project and I look forward to taking what I have absorbed of the methods of science – both technical and cultural – into future work. I would like to thank all of my friends, many of whom are also in science, and so who understood the work needed to complete such an undertaking. I'd like to thank my friends in my cohort, including Alice Berners-Lee, Erika Dunn-Weiss, and Kevin Monk. I'd like to thank my friends in lab, including Vyash Puliyadi, Ravi Jayakumar, and Manu Madhav. I would like to thank Beth Wood-Roig and Rita Ragan, the department administrators, who make the department run as well as it does. I am also grateful to have worked with talented students, including William Snider, a fellow graduate student on rotations, and Ruo-Yah Lai, an undergraduate who has been an integral part of the project for some time now. I'd like to thank those whose technical assistance helped me at so many points along the way, including Cheng Wang, Heekung Lee, The Bills, Zitong Wang, and Dr. Scott Zeger. I would like to thank my committee – Dr. Shreesh Mysore, Dr. Marshall Shuler, and Dr. Kechen Zhang – whose advice and feedback were so essential and appreciated. I would like to thank the NSF and NIH for their support. Lastly, I

would like to thank the institution of Johns Hopkins University itself for giving me the opportunity to contribute, in however modest a way, to the tradition of science done within its walls.

Table of Contents

List of Tables

List of Figures

General Introduction

Anatomy of the Hippocampus

The hippocampus is a structure found in the medial temporal lobe of the mammalian brain with a curved, oblong-shape that inspired its name – Greek for *seahorse*. Two primary axes define the hippocampus. The first is the longitudinal axis from the septal pole of the hippocampus, at the dorsal end of the rodent brain, to the temporal pole of the hippocampus, on the ventral side of the rodent brain. This defines the long axis of the hippocampus and follows its curved route through the interior of the brain. The second axis, the transverse axis, is an axis that is perpendicular to the longitudinal axis such that it yields a cross-section of the hippocampus (Fig 1.1).

There are four major sub-regions of the hippocampus: CA1 (*cornu ammonis* 1; horn of Ammon region 1), CA2, CA3, and DG (dentate gyrus). Further details of these regions and their anatomical inter-relations can be found in (Amaral and Lavenex, in Andersen et al., 2007). These regions exist as bands along the longitudinal axis and bear a characteristic anatomical relationship to one another across the transverse axis (Fig 1.1). The primary input to the hippocampus is the entorhinal cortex (EC). The entorhinal cortex receives input from a variety of polymodal association areas which allows the entorhinal cortex to exhibit complex, high-dimensional firing patterns related to environmental variables. Thus, the EC is thought of as the gateway through which the rest of the brain accesses the hippocampus. The EC is divided into two major

subregions – the lateral (LEC) and medial (MEC) entorhinal cortices. Traditionally, the lateral entorhinal cortex has been more strongly associated with non-spatial information due to the presence of responses to cues such as objects (see section on Landmark and Object Vector cells). Conversely, the medial entorhinal cortex has traditionally been more associated with spatial signals, owing in large part to the presence of grid cells within the MEC. This is an extension of the “what” versus “where” distinction that is key to the ‘two stream’ hypothesis of visual processing (Goodale and Milner, 1992). However, more recent theories posit the division between the two subregions may be better explained by a difference between the representations of content (LEC) versus spatial context (MEC) (Wang et al., 2018).

The traditional, simplified circuit through the hippocampus is the trisynaptic loop (region in roman font, pathway in italics): layer II EC → *Perforant Path* → DG granule cells → *mossy fibers* → CA3 → *Schaffer collaterals* → CA1 → *alveus* → subiculum. However, other feedforward and feedback connections also exist between the different regions of the hippocampal formation. The primary EC input to the hippocampus is the perforant path which connects layer II of the EC to DG and CA3. Layer III of the EC also connects directly to CA1 and CA3 via a secondary perforant path (sometimes called the temporo-ammonic path). Granule cells in DG then send unmyelinated fibers, termed mossy fibers, to CA3 (as well as to cells in the hilus of DG to another cell type within DG, called hilar cells). CA3, in turn, sends projections, called Schaffer collaterals, to ipsilateral (same hemisphere) CA1. CA3 connects to the contralateral (opposite

hemisphere) CA1 via the commissural pathway. In addition, CA3 exhibits rich recurrent connections within the region. CA2 is a less studied region, present between CA1 and CA3 along the transverse axis, which is driven by Schaffer collaterals and connects to CA1. CA1 connects via the alveus to the subiculum, which is the primary output of the hippocampus. The subiculum sends projections to layer V of the EC as well as subcortical targets. The subicular-EC connection thus makes the trisynaptic pathway a loop from EC to the hippocampus and back again (although originating and terminating in different EC layers). A secondary output pathway, the fimbria, forms from fibers gathered along the longitudinal axis of the hippocampus that connect the hippocampus to a variety of regions. These fibers form into a bundle called the fornix. There is a topographical organization within the fimbria/fornix output system. More septal CA1 neurons connect via the fimbria to cortical regions, such as the retrosplenial cortex and perirhinal cortex. More temporal CA1 neurons connect to sensory regions via the fimbria, such as the olfactory regions, and subcortical structures such as the amygdala and the hypothalamus.

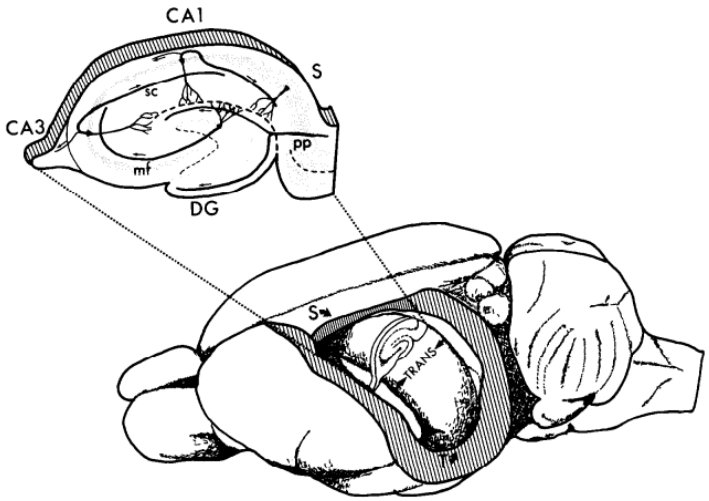

Fig 1.1 Hippocampal Anatomy. Three-dimensional anatomy of the rat hippocampus (Amaral and Witter, 1989).

The excitatory neurons of the hippocampus CA1, the focus of this thesis, are pyramidal cells. The dendritic arbor of CA1 pyramidal neurons is divided into four cytoarchitectural layers (from apical to basal): *stratum lacunosum-moleculare* which receives entorhinal inputs (from layer III), *stratum radiatum* which receives commissural inputs and Schaffer collaterals*, stratum pyramidale* where the cell body is located, and *stratum oriens*, where other Schaffer collaterals arrive. An important physiological characteristic of these pyramidal cells is that they are complex spiking. Complex spiking refers to a decaying burst wherein multiple spikes occur in a short train and the instantaneous frequency of the spiking decreases over the course of the burst. This short spike train exists on top of a membrane potential plateau which then decays back to baseline when the complex spike epoch is completed.

Overview of the Cognitive Map

A fundamental problem all mobile organisms face is how to navigate the world adaptively. To navigate, an organism must be able to sense, or construct a sense, of space. This is made conceptually challenging by the fact that space does not physically exist in the same manner as a photon (sensed by the retina) or a gravitational field (inferred by the motion of otoliths). Because space is not a physical quantity, it is constructed as the coordinate system, or embedding, within which the objects of the world exist and are interrelated. According to the cognitive map theory, the mammalian nervous contains an explicit representation of space based on the relationships between landmarks in the world, and the way the animal moves among them. This map was formed over the evolutionary history of the animals currently imbued with a cognitive map. Two processes are

fundamental for this construction: path integration and landmark recognition. Path integration is the process by which an organism maintains an estimate of its current position by integrating the changes in self-motion cues over time. These cues, such as optic flow and vestibular input, help the animal estimate how long it has traveled in a certain direction, and at what speed; by integrating these signals over time, a neural form of vector addition allows the animal to estimate where it currently is. However, any integrative process is subject to noise and uncertainty – “Have I taken 100 steps or 102?” – and this error will accumulate without bound unless corrected. Landmarks are used to correct the error of the path integration estimate by providing checkpoints with known positions along the trajectory which can be used to correct a drifting estimate. The relationship between an organism and a given landmark can be expressed in either allocentric or egocentric coordinates. The former expresses position in absolute terms in relation to an imaginary origin on the map while the latter does so in terms of the relationship of the landmark to the organism. Thus, as the animal traverses an environment it maintains an online estimation of its position within an allocentric framework that is periodically updated based on known reference points.

The cognitive map hypothesis proposes the existence of a metrical, topographical map instantiated within the medial temporal lobe of the mammalian brain. This map supports non-spatial modifications to provide a flexible system for organizing future navigational decisions based on current conditions (O’Keefe and Nadel, 1978). The map can be considered to be made up of two

components: the allocentric topographical map (the ‘chart’) (Samsonovich 1997), and the dynamic set of modifications to the chart which represent the objects and cues of experience (the ‘annotations’). Therefore, a cognitive map uses spatial location in allocentric coordinates as the organizing substrate upon which information about the content of the world is represented; in the words of the authors: “the hippocampus is the core of a neural memory system providing an objective spatial framework within which the items and events of an organism's experience are located and interrelated.” (O’Keefe and Nadel, 1978).

To better appreciate the utility of a map-based system, it is helpful to compare it to other ways space may be represented. The following is based on the discussion in Section 2.2 of (O’Keefe and Nadel, 1978). The main source of comparison is the route, or taxon, system which, as the name suggests, represents space as a complicated series of interlocking paths. A map differs from a route system in at least the following ways: the coordinate system used, the continuity of coordinate transformations, the role of landmarks, the degree of flexibility upon learning new information or encountering degraded or missing input, and its efficiency.

First, a map represents space in allocentric coordinates, while a route system tends to represent the space within each route in an egocentric manner. Further, a map represents space using a two (or three) dimensional set of continuous coordinates, whereas a route system uses a series of routes which do not exist in a common, continuous framework. Within each route the coordinate system is not necessarily continuous either, but rather is often defined

as a series of discontinuous vector relationships to landmarks or self-motion-based ‘checkpoints’ (for example, turning after so many steps). A single route is defined by a series of landmarks and the bearing and self-motion changes an agent takes at each one in order to reach the next. For instance, a step of a route may instruct one to “walk until you see the elevator, then turn right and continue…”. At no point are explicit coordinates defined; instead, space is defined as a series of relationships between landmarks, and the agent is instructed as to how to reach each successive landmark in the chain defining the route. Landmarks are also crucial to the use of a map but for different reasons. As the organism moves, the path integration system accumulates error as described above and the presence of known landmarks serves to correct this error. Thus, both landmark and self-motion cues are fundamental for both systems, but for different reasons.

The discontinuous nature of the route also affects its ability to learn new information, or deal with missing information. Because a route is an ordered set of relations between landmarks (and instructions about what to do at each), a change to the landmarks in the world has catastrophic effects on the utility of the route. For instance, if one is told to “turn right at the tree”, but said tree has been cut down, the user of the route is left with little recourse but to randomly search the environment until the next landmark can be found. By contrast, the spatial component of the map is defined without regard to the landmarks which populate the chart and therefore landmark unreliability does not affect the underlying spatial representation.

Similarly, learned associations between spatial location and cues which are present in the world can be added and deleted at will, subject to the limits of neural plasticity, without affecting space or the representation or stability of neighboring annotations. Lastly, maps are more efficient than routes in two regards. First, a single chart can represent an infinite number of routes passing through it (given a platonic, or idealized, chart – in reality the capacity is limited by the resolution of the map). Because routes are sketches of egocentric relations between landmarks with no common framework, each one is separate and independent even if they contain overlapping allocentric locations. This relates to the second source of efficiency; different trajectories and landmark relations through, and within, a map can directly be compared because there is a metrical allocentric coordinate system subserving all trajectories and landmarks. By contrast, the routes cannot be directly compared because there need not be an absolute metric and therefore no way to compare the distances one travels between two sets of instructions. In summary, for purposes of general navigation and for encoding annotations within a spatial framework, a map is usually superior because it explicitly defines a continuous space with a fixed metric.

Hippocampus and Memory

It is obvious from one's daily experience that there are different types of memories; for example, the birthday of a friend seems like a fundamentally different sort of thing compared to how to ride a bike. This vague notion has been made explicit in the psychological and neurophysiological literature, notably by Squire, who proposed a taxonomy of memory (Squire, 1992). He suggested that all forms of memory can be divided into two classes: declarative and non-

declarative memory. Declarative memory includes episodic memory – memory for events in one's past – and semantic memory – memory about propositions. Non-declarative memory includes all the forms of memory the content of which cannot be declared, such as procedural memory or classical conditioning. (The memories could be declared in the sense of describing them, but that does not transfer the ability to a listener; for example, telling someone how to ride a bike does not, by itself, give them the ability to do so). This taxonomy of memory, while not perfect, has been very influential on the study of the various forms of memory.

The story of the role of the hippocampus in memory begins with the tragic story of patient H.M., identified posthumously as a man named Henry Molaison. In the middle of the 20th century, Mr. Molaison suffered from intractable seizures which prevented him from living a normal life. After other remedies failed, a final attempt at a cure was made by removing the epileptogenic zone, the medial temporal lobe (MTL). The MTL contains a number of regions including the hippocampus and areas within the hippocampal formation. Upon completion of a medial temporal lobectomy, it was found that although the seizures had been abolished, so, too, had the patient's ability to form new memories (Scoville 1954; Scoville and Milner, 1957). Further study shed light on the exact nature of this anterograde amnesia (Milner et al., 1968, Milner, 1972). First, the patient could not form any new declarative memories but could form new non-declarative memories. Second, there was a retrograde amnesic element, too, wherein the patient could not remember facts or events from a time window before his

surgery. This led the clinicians to conclude that the MTL, or a region therein, serves as a temporary storage locale for declarative and episodic memories which are eventually transferred elsewhere for long-term storage. These results, and those from other similar patients, laid the groundwork for the study of various forms of memory in the hippocampus.

Basic Place Cell Physiology

The first physiological evidence that the hippocampus is involved in allocentric spatial representations came from experiments conducted in the early 1970's. In these studies, rats randomly foraged for food in a square box or a three-armed maze while single-unit recordings were taken from CA1 (O'Keefe and Dostrovsky, 1971; O'Keefe, 1976). The authors found units that modulated their firing activity as a function of the animal's location and termed these cells 'place units' (Fig. 1.2). Other units, called 'misplace units', fired when the rat investigated a location where a reward was present where none had been previously, or where one had been present and no longer was. In other words, these misplace units fired when there was a discrepancy between the expectation and present experience of a specific location. However, other firing correlates could have explained these data. For instance, rodents also tend to perform similar behaviors at similar locations; for example, grooming at a preferred location. It was therefore plausible that the apparent spatial firing correlate was an artifact of other variables being spatially co-localized (Ranck, 1975). However, subsequent work eliminated these behavioral confounds as explanations and an increasing number of researchers began studying place cell phenomenology. (This is a good example of the famous distinction between the

'context of discovery' and the 'context of justification' – the difference between when an idea first occurs to someone based on preliminary data (or even conjecture) and when further study supports it conclusively. The relation and progression between these ideas is a fundamental concept in the philosophy of science (Reichenbach, 1938)).

Even if spatial location drives place units, it is not necessarily the case that the firing field truly represents allocentric space. It is possible these units are 'merely' very high-dimensional sensory cells that respond to the full set of cues at a given location. Note, this is different from the earlier criticism that the signal may not be spatial; the question now is whether that spatial signal is a true representation of an allocentric spatial location, or rather is an online representation of the confluence of available cues that, by definition, correlates perfectly with a given location. Studies that removed the available sensory information from a learned location demonstrated convincingly that these are not just sensory cells but neurons with a real representation of space. O'Keefe and Speakman performed an experiment in which a rat navigated to receive food reward on a plus maze (i.e. a four arm

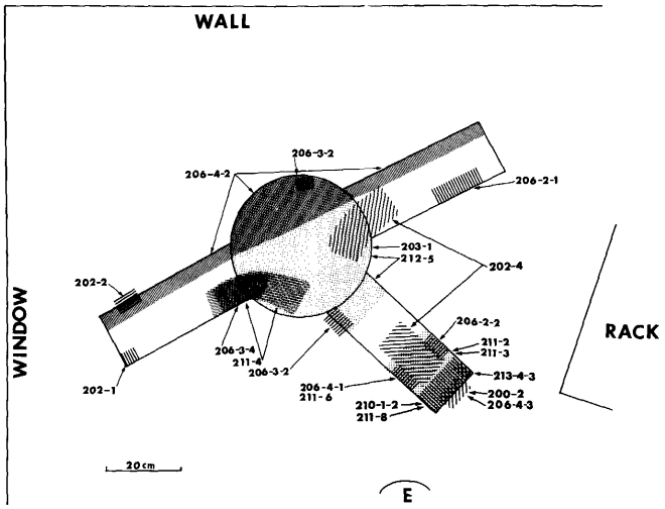

Fig 1.2 Early Place Cell Recordings. Diagram of apparatus used in early place cell recordings. Shaded regions show locations of place fields, annotated with a cell identifier. (O'Keefe, 1976).

maze in the shape of an addition sign) with different configurations. Crucially, salient cues on the walls surrounding the environment, which were present as the animal learned the task, were removed during one condition. Despite the lack of these previously learned cues, place cells continued to fire in the expected location (O'Keefe and Speakman 1987), provided that the rat was able to localize itself on the maze before the cues were removed. Muller and Kubie performed a similar experiment using darkness during a probe condition. Here, too, place cells remained stable in a learned environment when the sensory cues were unavailable (Muller and Kubie 1987). Since the cells continued to fire without visual cues present, the authors concluded that this was evidence in favor of the place hypothesis of hippocampal function. Although these studies have their limitations, they are significant and representative of work showing the presence of a spatial working memory signal in the hippocampus.

Before addressing how place cells encode cues it is important to also address how cues affect place cells in other ways. Cues in the environment still exert a strong effect on place fields, even though these cells are not purely sensory in nature. As mentioned previously, a sense of space is constructed by the nervous system (on both developmental and evolutionary timescales) from the features of an environment and their interrelations. Therefore, changes to cues in the environment would reasonably be expected to alter the place map as the map itself is based, in part, on the cue configuration. In a simple environment with only a polarizing cue card present, rotation of the cue card causes commensurate rotation in the locations of the place fields (Ranck et al, 1983;

Muller and Kubie, 1987). Thus, cues in the environment can help establish the frame of reference which place cells use to set their field locations. Distal cues are more reliable for determining bearing, and less useful for precise location, given that the further away a cue is the less it moves in relation to the animal during locomotion. However, local cues are more useful for determining location at a finer scale given that they move more relative to a moving animal. Therefore, both distal and local cues exert an influence over place fields in complicated ways (O'Keefe, 1976; Bostock et al., 1991; Knierim, 2002). There is a wide literature on cue control of hippocampal place cells; the conclusion here is simply that non-spatial cues in the environment influence the place cell map.

Non-Spatial Cue Representation in the Hippocampus

The cognitive map theory does not simply claim that cues have an influence on the map, but rather claims that cues and items are encoded within the map to support autobiographical memory (as well as being useful for navigation). Early work on non-spatial cue encoding within the hippocampus focused on the neural response to classical conditioning cues. One significant early study showed that hippocampal cells increase their firing rate in response to a conditioned stimulus (CS) after it has been associated with an unconditioned stimulus (US) (Olds et al., 1972). Moita et al. recorded rats as they moved freely in a box under an auditory fear conditioning paradigm. Place fields developed responses to the CS – recapitulating the earlier work – but only when the animal was in the place field (Moita et al., 2003). This provided an important piece of evidence that at least some non-spatial influences on the place map are gated by the place field location. Interestingly, a study using two CS, one associated with

the US and one associated with the lack of a US, failed to find hippocampal complex spike cells that distinguished between the two (Delacour, 1984). However, other neurons (thought to include interneurons) did distinguish between the two suggesting that some cells in the hippocampus can differentiate between multiple non-spatial cues.

These studies demonstrated responses to non-spatial cues but did not address the specificity of potential cue encoding; that is, whether encoding *per se* occurs as opposed to non-specific changes in the arousal state of the neuron. To investigate whether encoding occurs, other studies recorded CA1 responses in more complicated environments with more cues. Some of these studies additionally tested for the presence of conjunctive coding at the CS delivery site of an operant task, that is, encoding of both a spatial and non-spatial cue. Mixed representations of spatial location and cue have been identified with odors (Wiener et al. 1989; Wiebe and Stäubli et al., 1999; but see Eichenbaum et al., 1987 for a lack of conjunctive coding found), textures (Itskov et al., 2011), and internal motivational states (Kennedy and

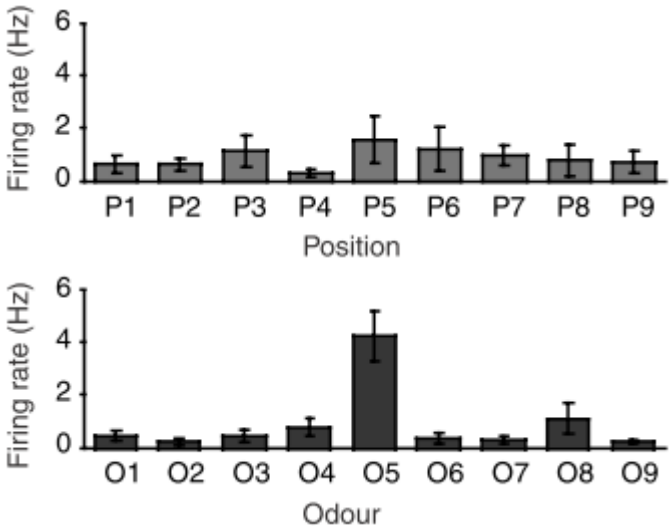

Fig 1.3 Non-spatial Encoding in CA1. An example odor-responsive cell. Each column indicates the average firing rate at each location (top) or in response to each odor (bottom). By inspection it is clear this neuron prefers Odor 5 over the rest and is spatially tuned, albeit broadly and possibly not achieving statistical significance. (Wood et al., 1999)

Shapiro, 2009). In each of these studies, individual hippocampal neurons displayed a preference for one stimulus over the others in a spatially-dependent manner. Others have found conjunctive coding for space and multiple non-spatial categories, specifically stimulus and trial type in a matching task (Wood 1999; Wiebe and Stäubli 1989). There are a number of such papers in the literature and it is worth highlighting two studies to both give a representative sense of what this body of work found and also to discuss data that are directly applicable to the results in Chapter 3.

In the first, Wood and colleagues trained rats to perform a delayed non-match to sample task using odors as they recorded from rat CA1 (Wood et al., 1999).The apparatus consisted of a grid of sand wells within which an odor and reward were buried. The wells were baited with different odors across trials, allowing the authors to dissociate spatial and odor responses. They reported a variety of responses related to odor coding. Some neurons fired predominately in response to one odor, such as the unit shown in Fig 1.3, while other units displayed a more graded response across stimuli. Others distinguished match status, for example firing strongly regardless of the odor identity as long as it was a match. Some cells were active at a small number of reward sites, consistent with a traditional place field response, while others fired at most of the stimulus locations. Although the authors report main effects of position and odor, they lacked the statistical power to investigate the interaction between the two, which would be the analysis needed to show true conjunctive coding of cue and place. However, some examples qualitatively appear as if an interaction would be

present, were more trials run to uncover it. These data demonstrate that the diversity of spatial and non-spatial responses, although complicated and heterogeneous, allow multiple types of task variables to be extracted from the unit responses.

A second study recorded rat CA1 in a more spatially constrained tactile discrimination task (Itskov et al., 2011). On each trial, rats sampled from one of four textured stimuli, two of which indicated reward at a lickport on the left, and the other two reward to the right. The apparatus was placed in two locations to identify spatial fields (although the rat was facing opposite directions between the two, which introduced a directionality confound in the neural response). A subset of neurons (~25%) fired differentially between a pair of textures that both signaled reward on a given side. Some neurons maintained their preferred stimulus as the apparatus moved (and head direction changed), while other neurons switched their preferred stimuli when the apparatus moved. Still other neurons distinguished the reward location through their firing rates. Relevant to the current study, though the authors did not emphasize this observation, the neurons that distinguished different textures did not do so over the entire course of the stimulus sampling. Rather, there was a transient change in firing rate which resulted in a firing rate difference between the two stimuli, while at other time periods during sampling the rates were similar. This presages the results shown in Chapter 3 – that neurons to not exhibit a global change in their firing field but rather a restricted modulation in the firing rate envelope. These studies, and others like them, provide evidence that non-spatial cues from a variety of

internal and external sources are represented in a way that interfaces with the underlying spatial representation.

However, since the experiments described above analyzed non-spatial cues within operant tasks, it is pertinent to ask whether and how items in the environment are encoded if they lack an association with reward. This is important not only to investigate the role of learning and attention on non-spatial encoding, but also because the idea of the hippocampus as a buffer that automatically encodes (attended) experience is an important one. The distinction between these two ideas is whether an item that lacks any task relevance is encoded simply because the animal attended to it. If so, this would support the idea that the hippocampus encodes episodic memory *per se* and not just reinforcement contingencies. This is because the content of attended experience would be encoded and not just the learned associations between cues and outcomes. Morris and Frey suggested that the hippocampus constantly encodes the content of an animal's episodic experience into a short-term buffer (Morris and Frey 1997). This "automatic recording of attended experience", as the authors characterized it, allows experience to be recorded onto the cognitive map within short-term memory. Downstream systems, such as reinforcement learning circuits, decide at a later time what should be stored in long-term memory based on what, if any, associations eventually manifested between the contents of the buffer and adaptive outcomes. This presents a partial solution to the credit assignment problem (Minsky, 1963). Often, the adaptive value of a specific action, or the importance of a specific cue, is not known when the action is

performed or the cue encountered. It is only after some time that the relationships between items and outcomes can properly be examined. Using the cognitive map, in part, as an episodic buffer allows a great wealth of information to be stored for a short period – maybe overnight (Marr, 1971) – and scoured later by the various reinforcement learning circuits to decide what has adaptive value.

A particularly relevant study without an explicit task was that of Manns and Eichenbaum (Manns and Eichenbaum, 2009). CA1 neurons were recorded from rats as they ran blocks of laps around a circular track, receiving reward at random intervals. The track was divided into segments onto each of which an object could be placed for the rat to encounter as it ran. During a single block of laps, a series of four objects were successively placed on different segments of the track, spaced out by three laps. For example, the rat would run three laps with object A on a segment, then three laps with a new object B added to a different segment, and so forth until all four objects had been encountered for at least three laps. Across different blocks of laps, the process would be repeated with different objects at different segments. They found that nearly 17% of CA1 neurons responded significantly to object identity (and a much greater proportion, 60%, to location) via one-way ANOVAs. To explore the population response to the objects, the authors used a k-Nearest Neighbor classifier (k=1) to test whether the distances between population activity vectors in Euclidian space displayed clustering that respected the object label. The classifier successfully predicted a repeated encounter to the same object, pooled across all locations

(~15% performance versus 2.5% chance). However, this obscures the potential role of location; it is not clear whether the population is encoding a conjunctive item-location association or whether the population encodes the item independent of location. To distinguish these possibilities, the authors first decoded the same object at the same location and found that the classifier was able to do so (almost 20% versus 7.7% chance). However, when decoding object identity at different locations the classifier performance was indistinguishable from chance (3.3% versus 2.5% chance, no effect). These data support the cognitive map hypothesis by showing the existence of population-level conjunctive representations of item and location, albeit without illuminating the neural mechanism of the conjunction.

The natural world is far richer than any well-controlled experimental design could be. Still, a number of studies have used multiple types of cues in order to explore encoding within, or cue control of, the place map in more complicated designs. Shapiro et al., used a plus maze with a tactile and odor cue pair associated with each arm (Shapiro et al., 1997). Additionally, there were distal cues on each wall of the experimental room. The authors performed several manipulations which either rotated cues with respect to one another, added/removed cues, or ‘scrambled’ cues of a given modality from their standard configuration. The authors report a range of responses, but of interest here is how the cells respond when cues are scrambled or deleted. Using rotation manipulations to see which cells are controlled by distal or local cues, the authors then either scrambled the cue configuration or deleted cues from the cue

set that controlled the cell's location. They found that scrambling or deletion induces cells controlled by local cues to switch to distal cues, and vice versa. They interpreted this as a "dynamic hierarchical" representation of cues within the CA1 place map. In other words, there is a ranking of preference for the cue sets and if the preferred cue set becomes unstable, the cell will switch to a less preferred, but more stable, cue set. An alternative conclusion is that cells latch onto a different reference frame when their initial one becomes compromised.

A more convincing study regarding hierarchical representations of stimuli and task attributes comes from a contextual discrimination task featuring two scented jars in two rooms (McKenzie et al., 2014). In room A, the jar with scent X was rewarded, while in room B the contingency was reversed. Further, this arrangement was repeated in a different set of rooms with different odors. The authors analyzed the correlation structure within the task by comparing the correlations between population responses divided by task variables (such as room, valence, odor, or odor set). The variables were then sorted in descending order of correlations between the population responses, divided according to that variable. They found a hierarchical structure present within the data, with the context (room) being at the top and the items at the bottom. Although this type of analysis will, by necessity, produce some sort of tree structure, it is of note that it maps onto the hierarchy that the cognitive map theory predicts. Other studies using multiple sets of cues found multiple examples of conjunctive coding, but did not specifically address any hierarchical nature of the data (Anderson and Jeffery, 2003; Wood and Eichenbaum 1999; Wiebe and Stäubli 1999). Still, they

provide additional support to the notion that not only are single cue-location conjunctions possible, but also multiple such associations within the same population, possibly obeying a hierarchical structure.

Splitter Cells

The hippocampus can encode task variables, such as trial type, by a mechanism known as “splitting”. Splitter cells maintain a stable spatial field which is modulated by a task variable that, crucially, is defined by behaviors that occur outside the field. These cells are thought to ‘split’ a task into its constituent trial types, or some other meaningful discretization, by modulating their firing rate between such trial types. Thus, they are very sensitive to variations in task design. The first study to identify this phenomenology recorded CA1 neurons as rats ran a spatial alternation task on a T maze (that is, alternating between right and left turns on subsequent laps), with a modification that the arms linked back to the beginning of the center stem (Wood et al., 2000). The authors examined place fields on the center stem of the maze, because the rat must pass through these fields regardless of the trial type. The authors found, in addition to standard place fields, cells that changed their firing rate based on trial type. For instance, a splitter cell might fire at a high rate when the rat was coming from the left and going to turn right, and be relatively silent in the reverse condition. However, because the previous trial and the next trial are highly correlated (in a well-trained rat, making few errors), it was not possible to determine whether these cells were tuned to where the rat had just visited or where it was about to go.

A similar study published in the same year addressed this concern by recording from CA1 neurons as rats navigated alternating paths between a

center stem and flanking right and left stems (Frank et al., 2000). For example, the rat would run from the center to the right, then back to the center and out to the left, and so forth. Here, it was possible to disambiguate what will be called prospective coding of upcoming trajectories and retrospective coding of recently completed trajectories. The authors found a subpopulation of CA1 neurons that displayed retrospective coding (16%), however only a small number showed prospective coding (3.7%). A follow-up study recorded CA1 as rats completed a spatial memory task on a plus maze (Ferbinteanu and Shapiro, 2003). Rats were trained to remember a rewarded target, and would approach that target from opposing directions across trials, obsoleting the use of a strategy based on what turn to execute. The authors found both retrospective coding (up to 70% of cells at the goal location) and prospective coding (up to 60% of the cells at the start box). The authors suggest these data may be reconciled with the Frank study by considering that in their design the reward location was changed across trial blocks. That manipulation may have promoted prospective remapping in the hippocampus because there was not a habitual response, likely striatal, which could solve the task.

A number of conflicting studies regarding the conditions under which splitting may be observed (Lenck-Santini et al., 2001; Hölscher et al., 2004; Bower et al., 2005) suggest that the origin of the splitting phenomenology may be a conjunction of allocentric spatial information and egocentric motor information, possibly provided by the striatum (Hölscher et al., 2004). Regardless of methodological disputes and the ultimate origins of the signal, the presence of

splitting cells within the hippocampus suggests that place cells are involved in segmenting the environment not only according to cues but also by the set of task contingencies and types of possible behavior. It should be noted that the 'splitting' phenomenon above is a form of rate remapping (described below). It is possible that splitting and rate remapping related to sensory cues are the same phenomenon; however, it is also possible that they are related but distinct based on the different role trajectories and cues play in the cognitive map.

Hippocampal Remapping

The next question is what neural mechanisms support the cue encoding described above. The first study to coin the term 'remapping' used it to refer to changes in the place cell map as the environment is manipulated (Muller and Kubie, 1987). The term reflects that each environment is associated with a map (or piece of a map) and changes to the environment can cause this map to be re-configured, or *re-mapped*. This definition encompasses a variety of related phenomena. Initially, the term 'partial remapping' referred to changes in the place map that were locally restricted, such as in response to a local feature being changed. Cells near the change alter their firing rates, but cells more distal remain unaffected. Conversely, changes to general environmental features like arena shape or wall color induce changes in the firing of cells throughout the map and was originally called 'complex remapping'. However, the use of the terms became muddled and partial remapping became associated with a change to a subset of neurons within the place map, rather than changes to a restricted geographical area of the map. This confusion has led some (Knierim, 2003) to suggest the original term 'partial remapping' be replaced with local remapping

and the current use of partial remapping to remain. Complex remapping, as a term, has fallen out of favor and instead, most of what it originally referred to is captured by the current uses of partial, rate, and global remapping, depending on the specific nature of the data. Rate remapping, a fundamental concept for the work in Chapter 3, refers to changes in the infield firing rate of a neuron in response to a non-spatial environmental manipulation while the cell maintains a stable spatial field. Thus, the set of which neurons represent an environment remains stable, while their firing rates fluctuate – possibly in a manner conducive for use as a communication channel (Shannon, 1948). Rate remapping is hypothesized to be the mechanism by which the binding of the "items and events of experience" (O'Keefe and Nadel, 1978) to the allocentric chart takes place in order to construct the cognitive map.

Another form of remapping is global remapping, which refers to the set of active place fields becoming statistically independent in their spatial tuning. Global remapping typically occurs when the animal moves to a different environment in the larger allocentric world (Leutgeb et al., 2005a; Alme et al., 2014). It is hypothesized that global remapping is used to represent different locations in the wider world with an independent set of place cells. Therefore, different environments would be highly separated from one another in neural space, while different configurations of the same environment would be similar due to the subtler changes induced by rate remapping. Recordings from up to eleven different rooms showed that in each there is an independent, stable set of place fields (in the CA3 region) tiling the environment (Alme et al., 2014). Global

remapping was first referred to as ‘complete remapping’ (Muller et al., 1996) and referred to the entire population of place cells undergoing dramatic and arbitrary change. Many subsequent studies have replicated these findings that different locations of an apparatus will induce global remapping. Non-spatial changes, too, can induce global remapping if the changes are significant enough (though it is unknowable, *a priori*, given the current state of the field just what ‘counts’ as being significant enough by the hippocampus). Changing the wall color, polarizing cue color, wall construction material, and even type of food reward also induced changes in field location in subsets of hippocampal neurons (Bostock et al., 1991; Kentros et al., 1998; Fyhn et al., 2007). However, some changes occurred over time, in contrast with the abrupt global remapping induced by changing the location of the environment. This suggests the changes in field location due to non-spatial changes may be different from those evoked by moving to another environment. It should also be noted that these non-spatial manipulations do not elicit such global remapping with every exposure to every animal. It seems to be the case that global remapping is more reliably induced when the physical location of an environment is different. These data show that the allocentric map afforded by the hippocampal place map uses independent sets of neurons to represent different locations in the larger world.

These forms of remapping manifest in different ways under different conditions. Although they are described categorically, it may be better to conceive of a diverse and complicated set of phenomena to which experimenters have affixed labels. It is important to note, however, that not every change to a

place field should be called remapping. A place field can exhibit a wide variety of changes after a cue manipulation, or simply the passage of time, that do not meet any of the definitions described above. First, some forms of remapping are properties of the population and can only be identified when analyzing the whole population. The loss of a single place field upon moving an apparatus should not lead to a conclusion of global remapping; it is the population of place fields as a whole that change their firing properties after global remapping. Second, a single observation of a field changing is weak evidence of remapping. To be considered remapping, rather than, for example, random noise, the changes should have some measure of reliability or robustness. This may manifest as reliability across stimulus presentations, a subset of neurons responding similarly, or bearing some relation to the cue change. Therefore, all forms of remapping imply a change to at least some of the place fields, but a change to a place field does not necessarily imply remapping has taken place. Remapping is a computation the network performs to register a meaningful change to the environment (or the state of the animal) and update (*remap*) the cognitive map accordingly – it is not simply a catch-all term for heterogeneity in place cell responses. With that said, examining how individual and sets of place cells respond to change – without necessarily adhering to the standard described above – gives insight into the mechanistic underpinnings of remapping.

In one informative study, Anderson and Jeffery recorded CA1 neurons from rats in four different boxes as they randomly foraged for food. Each box had a unique combination of an odor (vanilla/lemon) and color (black/white)

(Anderson and Jeffery, 2003). Rats were recorded in each box twice to see how place fields responded to the change in cues as well as to assess inter-session stability. There were neurons with place fields in all conditions, reflecting a lack of influence of the change in non-spatial cues. It is typically the case that these standard place fields will predominate in most apparatuses. However, other neurons displayed a range of responses in response to non-spatial cue manipulations. Some neurons had place fields in both boxes of a common color, while others had fields in both boxes with a common odor. These cells reflect the sort of sensory and spatial conjunctions discussed above. Other neurons had a field in only one of the boxes, suggesting a requirement for inputs from both modalities to induce activity. This is similar to the multi-conjunctive coding also discussed above. However, some cells showed a more complicated form of remapping. These cells fired in both boxes with a common non-spatial feature, either odor or color, but remapped between these boxes. In other words, one cue had a predominant effect on the cell, causing it to fire in both boxes, but changes in the other modality were sufficient to cause that field to change, for example by changing field location. This extends previous work showing multiple cues can affect a single field to show that multiple cues can change the cell in different ways. Some cells shifted their place field location, while other cells changed their peak firing rate in a box (consistent with a rate remapping effect). These data illustrate the variety of ways that cues cause remapping in CA1 neurons and some of the different ways this remapping can manifest. Remapping can occur immediately after a cue has been changed between sessions, or it can emerge

with learning. In one study, rats trained to randomly forage in an arena with a polarizing cue card initially did not exhibit place field modulations when the cue card color changes; however, over time the place field representation diverged from that recorded in the original environment (Bostock et al., 1991). Further, these changes can persist for up to a month demonstrating that learned hippocampal representations are suitable for long-term memory storage (Lever et al., 2002). Interestingly, the changes that occur over learning appear to be context-dependent. Hayman et al. performed a similar procedure as to Bostock (Hayman et al., 2003). They witnessed the same learned divergence of the representation of the boxes. However, when the color of the walls was changed this effect was abolished and the cells no longer distinguished the two boxes. This suggests that whatever is learned is specific to the circumstances of the learning and is not generalizable across environmental manipulations.

The focus of the experiment in Chapter 3 is rate remapping, and although many of the studies discussed so far involved non-spatial cue manipulation, most did not produce data that directly addresses rate remapping. It should be noted that rate remapping *per se* is a form of remapping, discussed above, while the rate remapping hypothesis is a specific idea about how remapping can multiplex spatial and non-spatial information in support of a cognitive map. In an influential study that coined the term ‘rate remapping’, Leutgeb et al., recorded CA1 as rats foraged in four boxes. Two of these boxes differed in their color and were present in the same location, while the other two were physically identical and present in different locations (and not the same as the location of the first two boxes)

(Leutgeb et al., 2005a). Cells recorded from the two boxes in different locations exhibit global remapping. This was expected, as the boxes were in different parts of world and therefore should draw independent sets of place cells to represent them. However, in the boxes at the same location, the authors observed that many cells were active in both but with dramatically different firing rates – often differing by an order of magnitude. The field location was the same; only the firing rate that was perturbed. Several examples of this rate remapping phenomenology are shown in Fig 1.4. These data provide evidence that stable spatial fields alter their firing rate after cue manipulation, and the authors go further to suggest this as a potential mechanism of encoding non-spatial information onto a cognitive map. However, the results do not fully test the rate remapping hypothesis as it pertains to the cognitive map theory. First, the authors did not observe spatially independent responses to the changes in cue card color. If rate remapping is, in fact, a method of multiplexing spatial and non-spatial information, then place fields need be able to respond

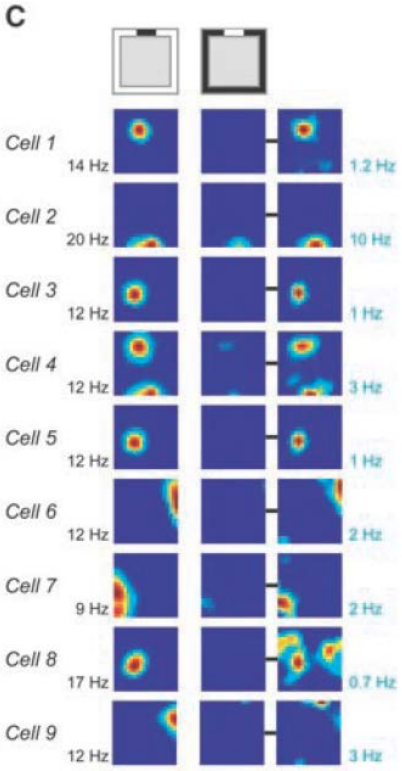

Fig 1.4 Rate Remapping. Comparison of example neuron responses to non-spatial cue manipulation. **Left,** rate maps for each example neuron in the white box. **Middle,** rate map of each example cell in the black box using the rate scale on the left. **Right,** the rate map of each cell in the black box but rescaled to that session's maximum. After switching between white and black boxes – present in the same location – the location of each firing field is stable while the field rate is modulated by up to an order of magnitude. (Leutgeb et al., 2005a.)

independently to cue changes. Second, with only two cues it is impossible to say that the cells were encoding anything, rather than just exhibiting a general change in state, as seen in the early classical conditioning work discussed above (however, see Leutgeb 2005b for an experiment which does provide this type of data, although it was not analyzed in such a way as to draw a conclusion about encoding). Despite these limitations, this study is important for introducing the concept of rate remapping and providing direct, albeit limited, evidence in its support.

Rate remapping is dependent on the subfield being recorded, although the data are conflicting. Leutgeb et al. performed a study in which rats learned to forage in circle and square shaped boxes. They then recorded probe sessions in ambiguous 'morph' polygonal boxes whose shapes progressed from a square to a circle (Leutgeb 2005b). In both CA1 and CA3, many cells exhibited gradual, heterogeneous changes in their firing rates along the morph sequence. For example, a cell may have had a field in box A and not in box B. As the morph sequence progressed A → B, the cell gradually reduced its rate until it was silent. However, Wills et al., performed a similar morph box experiment in rat CA1 (Wills et al., 2005). They observed CA1 neurons that abruptly changed their firing rates part way through the morph sequence, such that the firing became similar to the activity pattern at the further end of the sequence. For instance, a cell with a field in one endpoint box but not the other would abruptly turn off half-way along the morph sequence, rather than gradually turn off as Leutgeb and colleagues observed. These results are in direct conflict with one another; however, Colgin

et al. provide a possible explanation (Colgin et al., 2010). They performed two morph box experiments while recording from CA1, similar to the ones above, but with a key difference: in one experiment the two endpoint boxes were learned at the same location, and in the other they were learned at different locations. In both cases, the morph sequence probe sessions all occurred at the same location. In the first experiment, they observed a gradual change in representations, similar to the rate remapping effect seen by Leutgeb et al., 2005b. In the second experiment, they observed an abrupt global remapping similar to that seen by Wills et al., 2005. The authors concluded that the difference in location where the square and circle boxes are first experienced makes the difference. In the Leutgeb study the boxes were learned at the same location while in the Wills study they were learned at different locations. They theorize that a similar population of place cells was recruited to represent the boxes at the same location because they occurred in the same allocentric location. Any subsequent change to the environment took place on top of a stable place map in allocentric space and manifested as a graded change in rates. Conversely, independent sets of place cells were recruited to represent boxes at different locations. During the progression through the morph sequence, the inputs became more and more similar to the inputs experienced at the other end of the morph sequence. For the boxes learned at the same location, this manifests as a graded change because these populations are overlapping. However, for the boxes learned at different locations the populations are independent and therefore the representation abruptly shifts between the

populations once the inputs became sufficiently similar to the further input. The conclusion is that the underlying allocentric chart exerts a prevailing influence on place cell representations that provide the context for non-spatial representations to be stored.

Attractor Dynamics and Pattern Completion vs. Pattern Separation

These data also relate to the possible role of attractor dynamics in hippocampal function. Attractor dynamics refers to the behavior of stable states within dynamical systems – here, defined by population neural activity (Edwards and Penney, 2008). The population of active place cells defines an activity vector which specifies a point in high-dimensional space. All such possible vectors define a high-dimensional landscape, or manifold, along which the activity moves. Each position along the manifold is associated with an energy, or stability, value. Given the nature of synaptic weights within a network, some states are more stable than others. A state that is particularly stable is known as a basin of attraction, because once the population vector adopts that pattern the nature of the weight matrix favors its maintenance – even in the face of a perturbing input. Therefore, a pattern defining a point on the manifold close to the basin may 'fall into it' because the weight matrix favors changes in direction of the basin more than changes in the direction away from it.

In the previous studies, and many related ones, it is hypothesized that these high-dimensional dynamics explain the physiological results. In the morph box experiments, the endpoints of the sequence in different locations are attractor basins defined by stable patterns of activity created by different sets of

cells. Once the activity pattern in a morph box becomes similar enough to the pattern of one of the learned endpoints, the population activity adopts that pattern due to how the neural dynamics are constrained by the synaptic weights. Conceptualizing information storage in neural networks in terms of attractor basins learned via synaptic plasticity has long been an influential viewpoint (Hopfield, 1984). Attractor dynamics is a popular theory of how the hippocampus may represent information, particularly in CA3 given a unique anatomy suited for such a function (Marr, 1971).

The concept of ambiguous patterns of activity becoming more similar, or not, to learned ones bears a strong relationship to the concept of pattern completion versus separation. If a degraded, or incomplete, version of a stored representation is presented to a system, the system can either recall the stored pattern or provide a different pattern. Pattern completion refers to the process by which a noisy, or incomplete, input still manages to evoke the entire learned representation. This is generally thought to occur via feedback loops within networks containing learned attractor basins. The weight matrix has changed over learning to functionally associate the neurons participating in an ensemble.

When the degraded input is first presented, it activates a subset of the stored pattern. The neurons contributing to this part of the pattern are activated and activate all their functional neighbors, some of which are the other participants in the representation. This cycle will continue, and the positive feedback will eventually activate all members of the ensemble and re-instantiate the memory thanks to the incomplete input serving as a ‘seed’, and the synaptic

weight matrix providing a path for other ensemble members to be recruited. However, if the input is too degraded then not enough of the stored pattern is activated and the positive feedback loop is unable to retrieve the stored pattern. Pattern separation refers to the opposite process, whereby two similar inputs result in output patterns that are more de-correlated than are the input patterns. In the extreme case, similar inputs may be transformed into outputs that are orthogonal. Both of these processes are important, and it is believed CA3 (and specifically, proximal CA3, see (Lee et al., 2015)) and the dentate gyrus (DG) are involved in pattern completion and separation, respectively, thanks to their circuit wiring. CA3 features rich recurrent circuitry which is suitable for the positive feedback process described above. DG is a much larger sub-region, in term of cell number, than CA3 and CA1. Two similar inputs presented to the system have a much larger pool of targets onto which to synapse and therefore the targets are less likely to overlap. Thus, the patterns in DG caused by two similar inputs are likely to be more dissimilar than the difference in inputs would predict. Pattern separation and completion – and the dynamical systems models thought to support them – are key ideas in both computational and psychological literature. They are important, too, for the cognitive map as mechanisms by which a discrepancy in the learned map and the current state of the world may be resolved.

Oscillation-based Subfield Computation

An important novelty of the work in Chapter 3 is the identification of local regions within the place field in which rate remapping takes place; if further corroborated, this would represent a new form of subfield computation. Other

forms of subfield computation have been reported, as well. Arguably the most well-known is theta phase precession (O'Keefe and Recce, 1993; Skaggs and McNaughton, 1996). Hippocampal pyramidal neurons typically burst with a slightly higher frequency than that of theta (which is 4-8 Hz). Thus, as the animal runs through a place field, the bursts occur on increasingly earlier phases of a theta cycle; in other words, the spikes precess through the theta cycle. Subsequent work showed that taking this source of spiking variability into account led to a 40% increase in accuracy of predicting an animal's location (Jensen and Lisman, 2000). Additionally, phase precession may be used to encode non-spatial cues as well (Hirase et al., 1999; Harris et al., 2002). Further, theta cycles can support non-local spiking sequences which have been implication in decision-making behavior (Wikenheiser and Redish, 2015; Gupta et al., 2012).

Another hypothesis for how oscillations may participate in computation is that the theta (4-8 Hz) and gamma (~20-60 Hz) interact to group items in memory (Lisman, 2005; Lisman and Jensen, 2013). Because of the differing frequencies between the two oscillations, several cycles of gamma can elapse in the period of a single theta cycle. The hypothesis above suggests that this could be a mechanism to 'chunk' memory into a sequential buffer. Individual pieces of information are stored within a single gamma cycle, and successive cycles of theta advance these items, such that from cycle-to-cycle the element of memory in the first gamma cycle is removed and replaced with a new item of memory in the last cycle. Thus, gamma organizes items within a working memory buffer,

and theta organizes these items into a constantly-updating sequence of items. More recent evidence has suggested this may, in fact, be the case (Terada et al., 2017).

Place Field Repetition

It has been observed that in environments with repeated spatial motifs, such as multiple rooms or arms, a substantial number of place cells have multiple fields at multiple, or all, examples of the repeated spatial pattern. The first observation of place cells with multiple fields in similar areas of a complex environment came from Skaggs and McNaughton, who recorded CA1 neurons as rats navigated between two compartments arranged in parallel, connected by a short corridor (Skaggs and McNaughton, 1998). They observed place cells with fields in the same relative position in each of the compartments, for instance, in the top right corner of each. A follow up study used a similar apparatus, except that the boxes were initially separated by a wall, which was then later connected via a corridor (Fuhs et al., 2005). The authors found place cells with fields in each box when they were divided, however, upon being explored as a single, connected environment the repetition disappeared.

It is of note that the compartments in the Skaggs study were arranged such that the rat entered from a common direction, whereas in the Fuhs study the rat must turn around to move between boxes. This point relates to the role of heading upon place field repetition and will be expanded upon later.

The first experiment dealing with three or more boxes – and thus providing an opportunity for a clearer expression of repetition – came from Spiers et al., who recorded CA1 neurons as rats foraged among four identical compartments connected by a linear corridor (Spiers et al., 2015). The initial motivation of the study was to address whether place fields would distinguish between multiple identical locations under freely moving behavior, as previous studies had focused on two environments or environments with a restrictive task structure and had provided conflicting sets of data (Skaggs and McNaughton 1998; Singer et al., 2010). The authors found a large number of cells that had place fields in multiple, or even all of the, compartments (Fig 1.5). The authors also noted some slight differences in rates among the different fields, suggesting a possible rate remapping effect between compartments. The repeating field phenomenology did not diminish over time, suggesting that its presence was not due to lack of familiarity with the environment or confusion about the layout. The authors concluded that given the very similar sensory inputs in each of the rooms, it was the path integration signal that was responsible for disambiguating the compartments. Because the rat entered each compartment the same way, the head direction component of self-motion cues

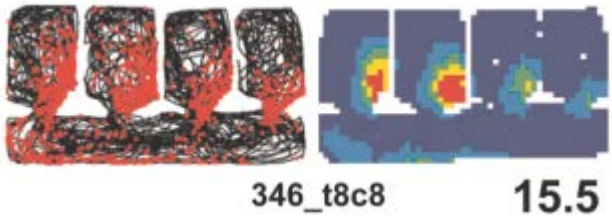

Fig 1.5 Place Field Repetition. Example repeating CA1 place cell from (Spiers et al., 2015). **Left**, spikes (red) overlaid onto the behavioral trajectory (black) as the rat ran a session in the multi-compartment environment. **Right**, rate map of the data on left. The cell has a field in the same relative location in each of the four compartments. Peak rate indicated at bottom right and cell ID shown bottom center. Note the peak rate difference between the subfields. (Spiers et al., 2015)

was uninformative and unable to provide disambiguating information about the different rooms.

A study by Grieves et al., addressed the role of head direction by recording rats performing an odor discrimination task in two versions of a multi-compartment arena (Grieves et al., 2016a). In one version, the four compartments were arranged linearly, as in Spiers et al., while in the other they were arranged radially, such that the entrances to each box were at a 65° angle to one another. They found that animals needed more sessions to reach performance criterion in the linear arrangement compared to the radial one. However, most animals could still learn the task, despite it taking longer to do so. Further, there was a decreased abundance of place field repetition in the radial box condition. Many cells had multiple fields, but very few had fields in three or four of the four boxes and among those that did, the fields were not in the same relative location. These data suggest that an inability to disambiguate environments may drive both repetition and a behavioral deficit.

Another study by Cowen and Nitz provides further evidence that common headings are correlated with the presence of field repetition. The authors recorded from CA1 as rats ran through a spiral maze (Cowen and Nitz, 2014). They observed a subset of neurons that had fields at multiple radial distances from the center at the same angle. As the rat passed through each of these locations it would have been facing the same way. The fields also expanded on segments further from the center, which corresponds to regions with a lower rate of angular change per unit distance, and therefore a longer distance facing the

same general direction. Harland et al., performed a more direct test of the hypothesis that the lack of heading information promotes place field repetition by recording lesioned rats foraging in the radial compartment arena (Harland et al., 2017). The authors lesioned a site known to contain many head direction cells (the lateral mammillary body) and observed the effect on place field repetition (though it should be noted that head direction cells are present in multiple brain regions, notably the anterior dorsal nucleus of the thalamus). The authors found that a lesion to the head direction system increased the prevalence of place field repetition in the radial compartment arena. This provides a direct link between the role of head direction inputs and place field repetition phenomenology; the presence of place field repetition was 'rescued' by head direction lesions in an environment which previously was thought to suppress repetition. This lends further support to the notion that the presence of these field patterns represents a deficiency in the system's ability to disambiguate similar environments.

However, other data suggest that place field repetition may not be a pathological consequence of ambiguous environments. Singer et al. recorded rat CA1 neurons as the rodents ran stereotyped trajectories between a start arm and flanking arms on either side (Singer et al., 2010). This allowed the authors to compare passes through the same location during different trajectories. The purpose of this study was to follow up a previous one (Frank et al., 2000) which found CA1 place cells that distinguished types of trajectories using a single field and entorhinal neurons that did the same across multiple, repeating fields. Singer and co-authors found repetition in CA1, expanding their previous findings. They

also found that repetition occurs over learning; it was not present on the first day of recording, but rather emerged over time. This is inconsistent, though somewhat indirectly, with the results from Grieves. In that study, animals took longer to learn a task in an environment which promoted repetition. However, in that study the animals trained on the task and those from which electrophysiological data were recorded were different populations. Therefore, it is possible repetition was present on the first day of recording in the latter population. The authors conclude that repetition is deleterious to performance and the ability to learn the task suggests some compensatory mechanism. However, if it is the case that place field repetition becomes stronger over time (as in the Singer study), then it is unlikely to be the case that its presence signals a degraded ability of the network to handle ambiguity, if at the same time behavioral performance is increasing. Additionally, the abundance of cells exhibiting place field repetition is usually somewhere between 20-40% of cells. This leaves a majority of neurons still capable of forming standard place fields. Even if environmental ambiguity were to drive repetition, and this repetition were viewed as harmful to behavior, the preponderance of CA1 pyramidal cells still able to form standard place fields should allow, in principle, adequate coverage of the environment.

Repetition in Other Regions

Neurons with repeating spatial fields have been recorded in a variety of regions beyond CA1. As mentioned, Frank et al. found repeating fields in entorhinal cortex, although they referred to the phenomenology as ‘path equivalence’ given that the fields’ rates were strongly modulated by the type of

trajectory being executed (geometry and trajectory are often correlated, as will be discussed further later).

In the subiculum, cells have been recorded with single fields that are modulated by environmental changes such that they maintain relative relationships to geometric features, such as walls (Sharp, 1999). In another subicular study, Stewart et al. found neurons with a single spatial field in a large box, but repeating fields when the box was split into three separate compartments. Significantly, these repeating fields were in the same relative location as was the single field in the large box (Stewart et al., 2014).

While recording from medial entorhinal cortical neurons, Carpenter et al. found repetition in the phase of grid cells between two boxes. Rats were recorded as they foraged between two parallel boxes connected by a corridor, as in Skaggs and McNaughton (Carpenter et al., 2015). Initially, grid cell phases (i.e. the relative position of the hexagonal lattice of a grid pattern with respect to an allocentric reference point) were local and symmetric between each box, possibly due to the similar sensory, geometric, or head direction information between the boxes. However, with experience the grid phases reconciled and became cohesive across the whole apparatus, suggesting that with time some forms of repetition may be abolished. Derdikman and colleagues found a more direct analogue to hippocampal field repetition in grid cells as animals ran through a hairpin maze (a series of parallel corridors connected by 180° turns) (Derdikman et al., 2009). They found grid cells with a normal hexagonal grid on an open platform, but the fields reorganized in the hairpin maze, such that they occurred

at the same relative position along a corridor and skipped every other lap. The presence of a field at multiple instances of the same relative location within the hairpin maze is very similar in principle to hippocampal neurons with fields at multiple analogous locations. Additionally, the fact that the fields occur on alternate corridors suggests a role of head direction – it is only on alternating arms of the maze that the animal is facing the same direction as it runs down the arm. It should be noted that it is not the existence of multiple fields that motivates the comparison to place field repetition – grid cells by definition have multiple fields – but rather that the arrangement of these fields in this study seemed better explained by the environmental similarity than a hexagonal pattern.

Role of Border Signals in Determining Place Field Locations

While a head direction signal is very likely to be important in this context, a large body of work has suggested place field formation is also strongly affected by boundary vector cells (BVCs) or border cells. These cells fire as a function of distance and allocentric bearing to a physical border, such as a wall. Border cells were first identified in the medial entorhinal cortex and neighboring subiculum (Savelli et al., 2008; Solstad et al., 2008). They manifest as cells with a field all along a given wall in an arena. These neurons do not seem to be affected by geometry, as the same cell had a similar firing field in both a square and circular arena. Some border cells express their spatial tuning in the lack of firing along a given wall, while they fire in the rest of the arena. BVCs are hypothesized to be inputs to place cells that help set their field locations within an environment (Hartley et al., 2000, Barry and Burgess, 2007). This model proposes that place cells receive inputs from two or more BVCs and determine their field position by

applying a threshold function to these summed inputs. However, the discovery of grid cells (Hafting et al., 2005) subsequent to this model quickly raised the suggestion that it was, in fact, a summation of grid cell inputs which determines place field location (O'Keefe and Burgess, 2005). The intersection of vertices of cells with different phases will occur at a single location, forming a place field. Despite the conceptual elegance of this model, inhibiting grid cells via medial septum inactivation does not abolish the gross characteristics of place cell physiology; for instance, new place fields still form in a novel environment (Brandon et al., 2014). Still, it is reasonable to maintain the hypothesis that border cells, grid cells, and other spatially-tuned neurons have some influence over place field location, even if it is not as total as was once hypothesized to be. A key experimental finding supporting the role of border cells in setting place field location came from O'Keefe and Burgess who recorded rats foraging in arenas with modular wall configurations (O'Keefe and Burgess, 1996). They used a small square, large square, horizontal rectangle, and vertical rectangle to test what effect, if any, different boundary configurations had on place fields. By comparing place field behavior in these boxes, they found that field location often correlated with a combination of walls, or the relationship between them. For example, one cell fired at a fixed distance from the western wall and halfway between the north and south walls, regardless of what that distance was (and, therefore, the allocentric location defining that midpoint). It was, in fact, this study that inspired the BVC models described above. However, it is not just the walls themselves that seem to control field position, but also cues associated with

them. Fenton and co-authors recorded rats foraging in a cylinder with two different cue cards on the walls (Fenton et al., 200). They made a number of manipulations to the positions of these cards to test any effect on place fields; they rotated the cards together, removed either card, moved them closer to one another, or moved them further away from one another. The place cell map was unaltered under the first two manipulations (rotation and single cue deletion); fields rotated with the cues in the first condition cohesively and were unaffected in the latter. However, in the latter two manipulations place fields moved relative to one another, distorting the map. It would seem as if place fields are controlled differently by different sets of cues, and by manipulating them in a contradictory way the fields, too, shifted in a heterogeneous fashion. These data, and the models investigating network mechanisms supporting them, suggest that place field location is driven in part by distance relationships to borders and landmarks.

Landmark and Object Vector Cells

There is another phenomenology within the hippocampal formation that is relevant to the discussion of how field locations are affected by their distances to different environmental features: landmark/object vector coding (LOV cells). These are cells within the entorhinal cortex and CA1 that fire whenever the animal occupies a position that is at a certain angle and distance from an object; that is, it fires when a preferred vector exists between the animal and the object (Deshmukh et al., 2011; Høydal et al., 2019). In the Deshmukh study, multiple objects were placed within a square arena within which the animal foraged for food. Some CA1 place cells displayed multiple fields that each maintained the same vector relationship to a different object. In other words, the ratemap of such

a cell showed fields that were a rough copy of the cue arrangement with a linear shift applied. In principle, an LOV cell does not need to have multiple fields and maintain a vector relationship to every object. A later study using a single object which moved around a cylindrical arena demonstrated the existence of medial entorhinal cells with vector relationships to the object (Høydal et al., 2019). These data, and unpublished data from this lab (Puliyadi, unpublished), reveal an additional and more detailed way in which the geometry of the environment affects spatial firing fields. While place fields are modulated by a host of factors (as described earlier), the shape of space and the way the animal interacts with it seems to be of vital importance in the location of spatial firing fields.

Border Cells and a Possible Role in Place Field Repetition

The influence of border cells on place field location leads to an explanation for the presence of place field repetition, beyond an inability to resolve separate environments. In an environment with repeating structure, a neuron that happens to be tuned to a confluence of border signals that is part of the repeated geometry will have firing fields at each instance thereof. If this interpretation is correct, then in each of the studies previously discussed, the repeating cell with a field in, for example, the northwest corner of two adjacent compartments, is a cell receiving input from a border cell tuned to the north wall at a given distance and a border cell tuned to the west wall at a given distance. The place cell is stimulated by these inputs at two locations and therefore has two place fields. Absent other disambiguating input, these border cell inputs are left to predominate and drive field formation in multiple locations. Barry and Burgess performed a modeling study, with comparisons to real data, which

support this idea (Barry and Burgess, 2007). They expand on Hartley's more conceptual model of how border cells can affect place field location by instantiating a model border-cell-to-hippocampus network using realistic synaptic plasticity rules. Their simulation results comport with a number of studies, in particular data taken while a rat navigated in a box with a barrier creating two corridors. They found that upon initial exposure to the simulated barrier, the modeled cell had two fields in the same relative positions. However, with experience one of the fields disappeared. Interestingly, this learned loss of repetition only occurred when the barrier was treated by the model to be different from the external walls (to be a removable insert rather than a static feature). When the barrier, instead, was to be treated as a wall like any other, repetition persisted in most cases. These data suggest that repetition occurs when sensory and path integration information do not adequately disambiguate multiple portions of an environment, and the border cell input to a cell then becomes predominant and drives firing in multiple locations. In cases where disambiguating information is present, the repeating spatial field pattern does not occur, or is diminished (Carpenter et al., 2015; Grieves et al., 2016a, though see Singer et al., 2010). Presumably, in these cases the cells are still receiving border cell input at multiple locations, but the differential sensory and head direction inputs are sufficient to keep the cells from firing in multiple locations.

Temporal Representations in the Hippocampus

In Chapter 4, results will be presented related to novel temporal dynamics observed within repeating subfields of a CA1 neuron; therefore, a discussion of temporal representations within CA1 and connected regions is warranted. There

is a wide body of evidence that the hippocampus is involved in the representation of time, ranging from the psychological to neurophysiological levels of data. Damage to the hippocampus is associated with a diminished or abolished ability to remember sequences, the order of items in a sequence, or the delay between stimuli (Fortin et al., 2002; Ergorul and Eichenbaum, 2004; Jacobs et al., 2013). Representations of time can be of two fundamental types, either a representation of the relative order of an item or an explicit metric representation of an interval or a moment therein (Tulving, 1984). Both forms of temporal representation can be found within the hippocampus, presumably to subserve different types of temporal computations. The first physiological data to show temporal coding within the hippocampus came from a study in which hippocampal neurons were recorded for many hours without interruption (Ludvig, 1999). This study, however, lacked proper controls (specifically, controlling for unit stability – a particular concern in a study about changes in unit activity over long periods of time) and so a later study using odor sequence memory is more commonly associated with the first evidence of temporal dynamics within CA1 neurons (Manns et al., 2007). Rats tasked with remembering the relative order of odors did so with a concomitant drift in the CA1 population activity representation. This shift in activity occurred gradually within the delay period and the degree of change tracked behavioral performance. A significant study by Pastalkova and colleagues demonstrated the existence of episode fields, CA1 neurons that fire at given times in a temporal interval (Pastalkova et al., 2008). Rats were trained to run alternating laps on a T-maze with return arms. Between each lap, rats ran on

a running wheel for a period of time. A subset of neurons fired at a certain point during the running wheel period. Despite the fact that the rat was not moving in allocentric space, these cells had fields which appeared similar to place fields, but in the temporal domain. Many such cells tiled the entire running wheel interval. A follow up study recorded CA1 neurons from rats performing an odor-based delayed match to sample task (MacDonald et al., 2011). During the delay period, the authors replicated the finding of time cells tiling the interval. However, upon changing the length of the interval, the authors observed ‘re-timing’ of the time cells – different cells fired during the lengthened interval in a manner reminiscent of spatial remapping. Another study examined a potential confound of the time cell phenomenology as reported by Pastalkova et al. by dissociating time from distance (Kraus et al., 2011). The authors of this study altered the speed of an electronically-controlled treadmill, such that it moved at different speeds across trials but for the same duration (and a well-trained rat ran to keep pace with it). This separates a cell firing at a certain distance in terms of cumulative self-motion from a cell firing at a certain time from the onset of running. The authors replicated the finding of episode cells, showing that they are not simply driven by behavioral covariates, but are representing a segment of a temporal interval. Longer time interval can also be represented within the hippocampus as slowly diverging ensemble representations. Ziv and co-authors reported that mouse CA1 neurons drifted in their activity over the period of a month, while another subset of neurons remained stable (Ziv et al., 2013). Although not definitive evidence of coding per se, this drift could in principle be

used to decode time. Studies of context-dependent memory show CA1 neurons with temporally drifting firing fields that can connect contexts separated in time (Cai et al., 2016). These results suggest that the hippocampus can not only represent short time intervals in an explicit, metric manner (in the form of time cells) but also longer periods by de-correlating neural ensembles.

Further studies have shown the role of time cells in behavior. Optogenetically disrupting the mEC input to CA1 disrupted time cell activity and this disruption correlated with poorer working memory task performance (Robinson et al., 2017). Interestingly, spatial coding and object coding were left intact. A study imaging CA1 neurons during a classical conditioning task revealed cells tuned to the onset, offset, or middle of the CS or US (Modi et al., 2014). Not only do time cells represent intervals but they appear to do so in a context-dependent manner reminiscent of splitter cells. Time cells recorded during a spatial alternation task were organized into different sequences depending on the trial type (Pastalkova et al., 2008). Further, time cells recorded during an odor memory task reflected the current odor in working memory (MacDonald et al., 2011). Taken together, these data demonstrate the existence of CA1 neurons with temporal spatial fields and their role in behavior. Therefore, the temporal dynamics observed within repeating place fields fit into a larger literature of temporal intervals being represented within CA1 and used during adaptive behavior.

General Methods

Animal handling and pre-training

Long-Evans rats were acquired when the rodents were between 3-6 months old and weighing between 325-350g. Upon arrival, animals were given *ad libitum* food and water for one week to allow their weight and stress levels to stabilize after transportation. After this period, animals were subjected to a food deprivation schedule to reduce their weight to 80% of their *ad libitum* weight with the goal of improving motivation during the task. This process was achieved by gradually reducing the number of food pellets they received per day. In parallel with food deprivation, animals were handled for roughly 15-30 minutes per day to habituate them to human touch and handling.

Pre-training began once the animal's weight was near the target weight and its behavior was calm in response to handling. Animals were trained once a day for approximately one hour to run clockwise laps around the perimeter of Ratterdam, receiving liquid reward (~50uL 1:1 water:Ensure). Rewards were dispensed pseudo-randomly with a 15% probability of a reward at one alley, a 15% probability of a reward at three alleys, and a 70% probability of a reward at two alleys. No floor stimuli were present during pre-training. Over the course of pre-training the number of laps and time spent in the start box were increased to match those of a real recording session. When the animal reached a performance criterion of 30-60 laps of consistent, motivated behavior, the animal was deemed ready for hyperdrive implantation.

Hyperdrive construction

Design and Mechanism

Custom hyperdrives were built to be implanted in each experimental animal, allowing simultaneous recording of hippocampal ensembles from a number of independently adjustable tetrodes (Wilson and McNaughton 1993). A tetrode is a single recording unit consisting of four wires twisted together. The reason for having multiple wires record the same signal is that an electrical source will be recorded slightly differently by each wire, owing primarily to their different precise locations and impedances. Therefore, by comparing the signal across multiple wires, it may be better resolved, akin to having multiple microphones in a crowded, noisy room to better triangulate the speakers. Although the design of the hyperdrive underwent substantial revision over the course of the project, the underlying design consists of a custom 3D printed body containing a number of openings for the mechanisms of the hyperdrive to be constructed. The hyperdrive consists of eighteen independent microdrives, each of which contains a moveable assembly containing a tetrode that can be lowered or raised along seven millimeters of travel. Several microdrives are visible in Fig 2.1A, visible at this stage of construction as a screw with a shuttle attached (front of the shuttle is facing the interior of the drive, away from the viewer). The tetrode is glued to the inside of a 33 gauge cannula which provides support. This tetrode/cannula component is then glued to the innermost hole of an aluminum shuttle. This shuttle is the key piece of the microdrive that joins the tetrode/cannula with two 25 gauge support posts and a ¾ inch 0-80 screw with a socket cap. Crucially, the bottom of the screw extends into a section of the plastic drive body that has been

reamed to be exactly the diameter of the screw and a nut/washer combination is glued to the bottom of the screw. Fig 2.1A shows the screws of several microdrives extending between the top and bottom plates of the drive body. The consequence of this exact fit is that when the screw is turned counter-clockwise the rotational momentum is transferred to the shuttle, moving it down along the support posts instead of causing the screw to dig deeper into the drive body. A serious issue with any design of this type is the problem of backlash. In brief (and discussed further in Construction), when the direction of travel is reversed some amount of turning of the screw is needed before the tetrode actually starts moving in the opposite direction. A variety of factors contribute to the degree of backlash, including a small gap between the screw and the drive, friction between the different steel cannulae walls, or lack of alignment between the microdrive parts.

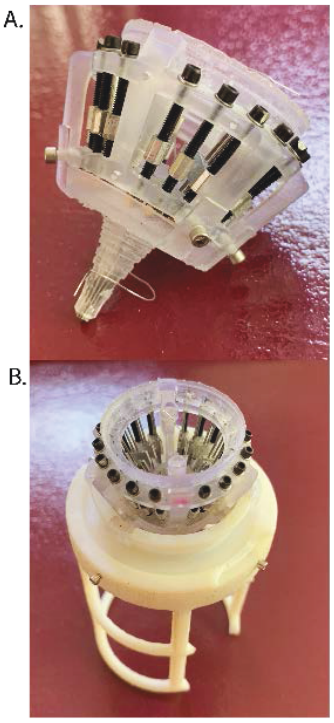

Fig 2.1 Tetrode hyperdrive. **A.** Hyperdrive lying on its side. Narrow section on bottom left contains the bundle of tetrode cannulae. The tetrodes emerge from the tip of the bundle. The wider section of the hyperdrive contains each microdrive. This drive is in the midst of construction, before outer shells and EiB board (see below for definitions) have been added). **B.** Hyperdrive at same stage of construction as in A, but sitting in a stand. The screws of most of the microdrives are visible as is the interior chamber of the hyperdrive. *(Images courtesy of Brian Li, JHU undergrad).*

As the tetrode is lowered, it (and its 33G support cannula) fit into a larger 29G guide cannula which extends to the base of the drive. Each 29G cannula curves at a shallow angle so that all the tetrodes converge into a bundle that is

approximately 3mm across. In this way, each microdrive allows independent targeting of neural tissue that sits within 7 millimeters of the bundle (although variant designs allow the bundle to be split to target different regions which are not co-linear with one another along the dorsal-ventral axis of the brain).

Construction

The body of the drive, as stated above, is 3D printed as a single component or two components which are then cemented and glued together, depending on the design version being used. Once printed the drive body is then cleaned, washed, and the various holes are reamed to their correct sizes with drill bits or reamers of appropriate diameter. Next, the cannulae are made by cutting them to approximately the correct length and then electrolytically etching the ends to bring them to the correct length and to provide a smooth and uniform aperture on either end. The cannulae, shuttles, screws, nuts, and washers are then assembled into each microdrive and glued into place where necessary with cyanoacrylate glue. At the base of the drive, the 29 gauge cannulae are cut horizontally, reamed, and electrolytically etched to provide as flat a surface as possible. This is important so that the tetrodes extending out of them are all aligned and travel in the same direction vertically. At this point, the ground wire is threaded into the interior of the drive such that it is accessible from the top to be crimped to the interface board (see below) and accessible from the bottom exterior of the drive to be attached to the ground screw during surgery (see Hyperdrive implantation for details). Once the ground wire is inserted, two part dental cement is mixed and used to fill the interior of the drive. The rationale behind this step is to create, once the drive is implanted, a contiguous mass of

dental cement from the skull up to and including the hyperdrive. Next, at least eighteen tetrodes are made from 0.0017'' nichrome wire that has been treated with special reagents that assist in the subsequent melting/bonding steps. Sixteen of these tetrodes will be used as recording tetrodes while the remaining two will be used as references (by connecting all the wires together to serve, effectively, as a single wire). Each tetrode is made by cutting a length of this wire approximately 37cm long, folding it back on itself twice, and cutting the bottom to create the four wires of the tetrode. The wires are then spun 65 turns clockwise and 22 turns counter-clockwise (to alleviate some of the rotational tension) and heated for 36 seconds in six, six-second passes along the length of the tetrode with a heat gun set to 380 degrees Fahrenheit. These tetrodes (recording and reference) are loaded into the 33 gauge cannulae manually and glued in place. Next, the electrode interface board (EiB) is attached via screws to the top of the drive. This board connects the tetrodes to a tether cable that itself connects to the recording system (see Electrophysiological Recording for details). With the board screwed in half way, each of the four individual tetrode wires (and each of the two single reference wires) are crimped to conductive holes in the board with gold pins. The ground wire is crimped to a dedicated conductive ground pad. Then the board is lowered all the way. Penultimately, the tetrodes are lowered and cut to their final length of approximately seven millimeters. Care is taken that the cut be quick and smooth so that the exposed wire surface is as flat and clean as possible. Lastly, the tips of each wire are cleaned by applying a one second pulse of +0.117uA current and gold plated with repeated bursts of one second –

0.117uA current. The gold plating is performed with a series of decreasing target impedances (of 1000kOhm, 750kOhm, 500kOhm, 250kOhm, and final target 130kOhm) with 10 attempts of a one second –0.117uA pulse used to reach each target impedance before moving on (NanoZ system, Multi Channel Systems, Reutlingen, Germany). At some point during the different steps involving lowering and raising the tetrodes, the bundle is mapped so that the correspondence between each microdrive and where it exits the bundle is known. Once the tetrodes are raised for the final time before sterilization, the tetrodes are only raised as far as needed to have them just aligned with the ending of the bundle. Additionally, protective 3D printed shells are glued to the sides of the drive, which until this point had been exposed so the inner mechanisms were accessible and visible during construction. The drive is gas sterilized (12 hour ethylene oxide, 24 hours cool off) before surgery (see below).

Hyperdrive implantation surgery and pre/post-operative procedures

Pre-operative procedure

Three or four days before surgery, rats are taken off the food deprivation protocol and put on *ad libitum* food and water to increase their weight and physical vigor before the stress of anesthesia and surgery. Three days before surgery, the completed hyperdrive is gas sterilized using ethylene oxide. This process takes 36 hours – 12 hours for the sterilization process and 24 hours for the toxic gas to dissipate, particularly from the plastic components. Along with the hyperdrive, a number of other tools are gas sterilized that cannot safely be autoclaved. At some point before surgery a ground screw (and replacements) is created by

taking a 1/8 inch 0-80 screw and soldering a small length of wire at the end of which is a small segment of 29 gauge cannula. One end of the cannula segment is crimped to the wire of the ground screw while the other is left open to be crimped to the ground wire of the hyperdrive during surgery. The day prior to surgery, or the morning of if necessary, the remaining tools are sterilized by autoclaving along with consumables such as paper towels, swabs, etc. At the same time, the surgical room is prepped for surgery. The primary surgical station is set up with a stereotax with electronic coordinate tracking, actuating lamp, heating pad, glass bead sterilizer, vacuum suction tube station, and electric drill. Two auxiliary stations are set up; one station is for shaving the rat's head and the other is for overflow surgical supplies, in particular consumables such as saline or extra swabs. Approximately 15 minutes before the surgery, the entire room is cleaned with Novalsan. Particular care is taken to wipe down with Novalsan at this time every handle, surface, lever, or other object that the surgeon may reasonably be expected to touch or otherwise come into contact with. At the same time the heating pad is turned on so that is has reached its operating temperature by the time the rat, poorly able to regulate its temperature under general anesthesia, is placed on the operating table. Measurements are made of the amount of oxygen left in the tank, isoflurane present in the vaporizer, and charcoal present in the gas exhaust collection canisters to make sure the quantity of these reagents is sufficient for a surgery expected to last several hours. At this point each drug to be injected is drawn into a separate, labelled syringe. Ketamine (80mg/kg males, 40mg/kg females) and xylazine (10mg/kg

males, 5mg/kg females) are used as an injectable anesthetic cocktail (delivered via an intraperitoneal injection) while Marcaine (0.15cc, alternative drug: Ropivicaine 0.15cc, subcutaneous in both cases) is used as a local analgesic, epinephrine (0.20cc, applied directly to skull) as a pro-coagulant, and meloxicam (2mg/kg, oral or IP post-op) as an analgesic.

Surgery

Rodents are initially anesthetized using gaseous isoflurane (1L O2/min, 4% isoflurane or as needed) and injected with the ketamine-xylazine cocktail. The animal's head is shaved from between the eyes to the base of the skull in the anterior-posterior (A-P) dimension and just beyond the lateral skull ridge in the medial-lateral (M-L) dimension. The rat's eyes are covered with artificial tears to avoid desiccation and this reagent is reapplied periodically during surgery. The scalp is sterilized with Novalsan and the animal's plane of anesthesia is monitored via response to a tail pinch, retracted leg pinch, and corneal reflex test. Once these tests, and in particular the corneal reflex test, elicit no response the animal is ready to be placed in the stereotax. From the point of initial injection until the animal has fully recovered (or succumbed to the surgical process) the plane of anesthesia is monitored (typically by tail pinch) every 30 minutes and logged.

The animal is placed into the stereotax and the snout is placed into a nosecone receiving a constant flow of isoflurane (1L O2/min, variable iso. percentage, ideally 0.25%-1%). The animal is held in place with two ear bars, which attach to the sterotax and fit firmly into the interaural canals, and the

nosecone. A rectal thermometer is inserted and its reading included in the half-hourly animal status check (along with current isoflurane and oxygen level). Marcaine (or Ropivicaine) is injected subcutaneously where the incision will be made. The rationale of applying proactive analgesic is the theory that it is more effective to apply an analgesic before an insult and after, rather than just before. A sterile field is placed over the rat with a section for the skull exposed to isolate it from the non-sterile body as well as to aid in trapping body heat for thermoregulation. If the animal continues to lack a response to the wakefulness tests described, an incision is made along the midline beginning right around the inter-ocular region and extending back to the end of the cerebellar plate. The incision and all subsequent surgical steps are performed under a binocular surgical microscope on an articulating arm.

Once the incision has been made, the skin and attached muscles are pulled to the side with skin hooks (small fishing weights attached to hooks on a wire). The fascia is then retracted and the skull is cleaned. The skull must be totally clean, free of fascia, blood, or any other detritus. Additionally, care must be taken to clear the fascia from the lateral skull ridges or else the strands attached here will moisten and clutter the skull surface. Epinephrine is then applied to the skull to help stop bleeding and let sit for a few minutes before being aspirated. Next, the skull is leveled and the coordinates of the implant are found and physically marked on the skull. Two prominent landmarks formed from the junction of different sets of skull sutures, termed lambda and Bregma, have historically been used as reference points for implantation coordinates. The

distance between them along both the A-P and M-L axes are recorded and the angle of the skull is adjusted until the vertical distance between them (the dorsal-ventral axis, D-V) does not exceed 200 micrometers. Then the coordinates for the hyperdrive implantation are found, relative to the more anterior Bregma landmark. The standard target coordinates for CA1 are roughly -2.5mm A-P and +2.3mm M-L, although the size of the drive, age of the animal, and other variables may cause this to be adjusted. The center of the eventual craniotomy is marked and a circle is traced around it to admit the diameter of the bundle. Care must be taken that the circle is not lopsided due to parallax caused by performing this step under a microscope, in which case the hole will need to be made bigger later on in the surgery.

Next comes the drilling of the anchor (and ground) screws as well as the craniotomy. Several anchor screw holes are drilled with a large (#12) drill bit in a manner wherein the drill excavates a single uninterrupted channel of bone. By convention, four are placed in the frontal plate, three in the cerebellar plate, and one in the parietal plate contralateral to the hemisphere where the drive will be implanted (typically the drive is implanted in right hippocampus). One of these screws is the ground screw (which also provides anchor support), with the exact location being variable. Note that the screws in the cerebellar plate should be added after the craniotomy (the holes themselves may be drilled at this point) so that the screws do not obstruct one's ability to perform the craniotomy and clean the skull surface before the dental acrylic is applied. A 1/8 inch 0-80 screw is then screwed in four revolutions. The purpose of the anchor screws is to create a

complex, three-dimensional contact surface between the dental cement (added later) and the skull, rather than having a flat, smooth bone-cement interface that may shear and lose its adhesive power. The craniotomy is performed by taking a smaller drill bit and tracing a groove along the circular markings made before. This indentation is made gradually deeper until the center piece of bone can be removed using forceps. Next, the duraectomy is performed by using small needles to tease the dura from the surface of the brain and lifting it up and removing it. This step is often challenging as the dura may be confused for the surface of the brain causing confusion as to whether the dura has in fact been removed or if more gentle scraping is needed. The surface of the brain is much whiter than the dura, although if damage is caused the brain will appear ‘bruised’. The craniotomy is then cleared of any bone fragments, dura remnants, and blood.

Once the craniotomy is completed, the hyperdrive is placed into the stereotax and the drive is maneuvered to the coordinates defined above. A tetrode in the center of the drive is lowered (using the bundle mapping described above) to confirm that the bundle will fit in the craniotomy. This tetrode is then raised (note: keep track of how much this tetrode is lowered so it can be retracted the same amount to be flush with the bundle ending) and the whole bundle is lowered just until it presses against the surface of the brain. The air-brain interface caused by the fact that the bundle will never perfectly fit inside the craniotomy is sealed with a special reagent, Kwik-sil in the present work (WPI, Sarasota, FL). At this point the ground wire is placed inside the segment of

cannula of the ground screw and crimped. Next, the dental cement is added in roughly three stages. First, a special, stronger form of cement (Osteobond, Zimmer Biomet, Warsaw, IN; or Palacos, Heraeus Medical, St. Paul, MN) is applied to the entire surface of the skull that is designed to adhere strongly to bone. Next, a less specialized version of dental cement is used in larger quantities to build up the mass of the implant. Finally, any gaps or exposed regions of skull or ground wire are filled in with the second form of cement. Each step consists of multiple rounds of cement application and must be paced such that the cement has time to dry. When the process is completed the drive is gently removed from the stereotax holder and covered with a protective cap.

The last steps in the surgery involve first swabbing the exposed region of tissue around the base of the drive with antibiotic ointment. If the skin cut during the incision at the beginning of the surgery is too loose, a suture is placed in at this point and removed some days later once the skin has healed (see below). Five cc's of saline are injected subcutaneously under each shoulder blade (half the volume for a female rat). The thermometer is removed and the isoflurane is stopped. The animal is removed from the stereotax and placed on pure oxygen in a new cage on a heating pad.

Post-operative procedure

The animal is monitored on pure oxygen until it is awake and responsive to stimulus. At this point it may be returned to the animal room. From this point through the lifetime of the experiment the animal will be given food in a mash form rather than dried pellets (i.e. pellets mixed with water to soften them). On

the day of surgery and the following day meloxicam is added to the food in liquid form. Additionally, 0.15 cc Baytril and 30 mg tetracycline are added to the mash with every meal for the lifetime of the experiment. The animal is allowed to recover for several days during which time the sutures, if sewn in, are removed and the health of the animal is monitored. Meloxicam may be administered beyond the 48 hour point if necessary, although if the animal appears in persistent distress the veterinarians must be informed and a discussion had as to whether to continue the experiment or euthanize the animal on humanitarian grounds. If the animal recovers successfully after this period the next stage of the experiment may begin.

Tetrode Adjustment

As noted above, each microdrive contains an independently adjustable tetrode and the multi-wire design of the tetrodes allows for a better isolation of electronic sources compared to a single recording wire. During this phase of the experiment, each tetrode is slowly lowered over the course of many days to reach the target region (here, CA1) and allowed time to settle in order to achieve stable recordings of large neural ensembles. Tetrodes are lowered, as noted above, by turning the screw associated with a microdrive counterclockwise (and turned clockwise to retract the tetrode). The design of the microdrive is such that each revolution of the screw lowers the shuttle by 317.25 micrometers (emphasis on the shuttling being what moves – the tetrode is not guaranteed to move if, for example, it gets stuck in the tissue or comes loose from the microdrive). The target region of this project is CA1, which sits at a nominal depth of

approximately 2.5 mm below the surface of the brain. A typical experiment will involve one to three weeks of daily tetrode turning in order to each CA1.

Each tetrode is adjusted incrementally according to a flexible schedule of how much to advance the tetrode based on the history of movement, present conditions, and estimation of remaining distance to CA1 (as well as considerations such as whether the animal's post-op behavioral performance is sufficient). There are (in this lab, currently) two primary techniques by which tetrodes are advanced. First, there is a linear method in which the tetrodes are advanced each day, at first by a large amount and then by a decreasing amount until the smallest adjustment is needed to place the tetrodes in the CA1 pyramidal cell layer. A hypothetical yet realistic schedule would be to advance a complete turn for two or three days to get clear of the cortex, spend a variable number of days turning between ¼ and 1/8 of a turn, and finally turn 1/16 or 1/32 of a turn for a day or two to make the final, slight adjustment needed to enter the cell layer. The second strategy is an oscillatory approach, termed 'chirp' turning after the digital signal processing term of the same name. In this method, tetrodes are advanced by a turn or two to clear the cortex as in the linear method but then the tetrodes are advanced over the course of a single day to the CA1 layer, then retracted

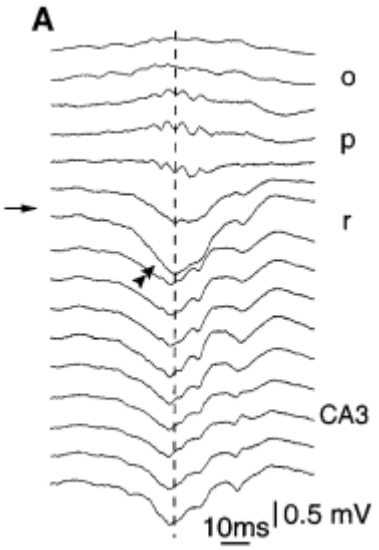

Fig 2.2 Sharp-wave ripple. Sharp-wave ripple (SWR) relationship to depth. Each trace is EEG filtered 100-200 Hz at a specific depth; depth into hippocampus organized vertically. Single arrow shows likely site of reversal, double arrow shows EEG segment with maximum deflection. O – stratum oriens; p – stratum pyramidale; r – stratum oriens. (Csicsvari et a.,1999)

back half the distance. On the following day the process is repeated, but in theory the new distance is half of what it was the day prior. This decaying oscillatory turning approach (which resembles the chirp function if distance traveled per day were plotted against time) is repeated for several days until the tetrodes are close enough to the layer that slight adjustments, as in the linear method, bring them into the layer. Tetrodes are given time to stabilize in the layer regardless of the turning method.

In either case, any retraction of the tetrode (whether done as part of a strategy or as a reaction to, e.g., believing one has passed below the layer) will induce backlash and obfuscate the estimation of the tetrode's current position as described in Construction. Backlash is a serious problem during tetrode turning as it adds a great deal of uncertainty as to how much of a given rotation of the microdrive screw actually translates into downward motion of the tetrode. During tetrode turning, detailed logs are kept of each turn made, the cumulative depth of the tetrode, and any resulting change in the detected signal. The experimenter uses these logs (along with the real-time signals described below) to estimate the position of the tetrode and therefore plan future adjustments. Backlash causes these nominal depths to deviate from reality because some of the turns were "wasted" in overcoming the backlash. Thus keeping backlash and tetrode retraction to a minimum is of high concern in this step (for the chirp method, although backlash occurs by design, the large amount of adjustments made per day in opposite directions causes it to cancel out on average).

In addition to the depth logs, knowledge about each tetrode's current position is gained from monitoring the real-time EEG signal. Detailed discussion of the EEG and how it is acquired will be described below, but in brief an EEG signal associated with each tetrode gives information about the ambient electrical environment around that tetrode. Patterns within the EEG vary across brain regions and, in the case of the column of tissue from cortex to CA1, there is a robust and predictable set of patterns that indicate the distance to CA1. Further details about the spatial patterns in the EEG, as they relate to hippocampus, can be found in (O'Keefe, in Andersen et al., 2007; Buzsáki, 1986; Csicsvari et al., 1999). There are four EEG patterns relevant to finding CA1. For each EEG signal, there is a distinction between seeing the signal on the recording screen and hearing it in the audio. As a general rule, signals that can be heard in the audio are closer than those that can only be seen onscreen (this is not some physical limitation but rather reflects that the audio and visual signals are filtered differently). The first signal, sleep spindles, is a low frequency (4-8Hz) oscillation originating in the cortex. The waveform appears as a narrow deflection of high amplitude in either direction of polarity. Spindles occur when the animal is sleeping or at rest and most often occur in bouts lasting for a fraction of a second up to several seconds in duration consisting of many cycles of individual spindle waveforms. Presence of the characteristic 'syncopated' sound of spindling in the audio is a clear sign that the tetrode in question is in the cortex, far from the hippocampus (although, anecdotally, a similar signal may be heard very deep in the hippocampus possibly near the fornix output bundles). The second oscillation

of interest is theta (4-12Hz), which is a lower amplitude signal than the spindle and appears roughly sinusoidal in shape. The theta rhythm is very important in the physiological and computational properties of the hippocampus but here its usefulness rests in the fact that it emerges as a tetrode approaches the hippocampus. First the signal may appear in the visual EEG, then when the tetrode is very close to the cell layer some of the cells will be theta-modulated in the audible firing rate activity.

The last two oscillations co-occur and for the present purposes can be thought of as two aspects of the same signal called a sharp-wave ripple. The first component is the sharp-wave which is a deflection in the EEG that can occur as a single event, or in a short train of events (doublet, triplet, etc.). The origin of the sharp-wave is within CA1 (specifically, the synaptic drive from CA3 to CA1 in the stratum radiatum) and therefore the polarity of the signal reverses depending on whether the tetrode is above or below the CA1 layer (Fig 2.2). This property makes it very useful in determining whether a tetrode is above the layer or has drifted below it, e.g. overnight or after a gap in tetrode turning. Additionally, because the origin of the signal is in CA1, the observed EEG follows the following pattern: a small sharp-wave develops and increases in positive amplitude (defined as downward deflecting by convention) as the tetrode gets closer. However, as the tetrode gets even closer to the CA1 pyramidal layer, the amplitude attenuates until it disappears in the cell layer. The pattern reverses as the tetrode leaves CA1 and continues deeper into brain (Fig 2.2). The second component is the ripple, which is a high-frequency (150-200 Hz) oscillation of

smaller amplitude than the sharp-wave component and appears like a ‘ripple’ in the EEG. The amplitude of the ripple component increases monotonically as the tetrode approaches the CA1 layer, beginning with the emergence of a small ripple far from the layer and increasing until a distinct, large amplitude signal is present in or near the layer. Additionally, because the ripple is generated from the population activity of CA1 neurons, the cells themselves will sound entrained to the ripple (though of course that interpretation reverses the causation – it is the cells themselves that generate the ripple, unlike the theta rhythm which is exogenous to CA1 and modulates certain cells’ activity).

Using the changing patterns in the EEG, along with the depth logs, the tetrodes are guided into the cell layer over the course of a couple of weeks. Once the tetrodes are picking up single units the experimenter must decide whether to make additional small adjustments in the hope of getting a better yield or to allow the tetrodes to stabilize where they are over a couple of days and then begin the experiment. The EEG signals may be difficult to interpret or seemingly be in conflict with one another or the estimated depth. Tetrode turning can therefore be a very difficult process and requires experience to be successful. Once an adequate cell yield is found and the tetrodes have stabilized, the experiment can begin.

During tetrode turning the references are also moved into position. Typically, one reference will be placed above the hippocampus and one below as different oscillations can be picked up with more fidelity at different depths. Because the references are not targeting a specific depth they may be moved

more aggressively into position and then allowed to sit. Making very slight adjustments every day or so, or even simply vibrating the screw with the tetrode turning screw driver, can often help mitigate this problem.

Behavioral tasks and overview of Ratterdam control

Apparatus ("Ratterdam")

The overall project consists of two aims that have been investigated using two different tasks that make use of the same apparatus. The commonalities between the two tasks and how the apparatus functions are discussed here while specifics related to each task are discussed in Chapters 3 and 4. The apparatus, Ratterdam, is a 0.9 m x 0.6 m platform enclosed by 15.24 cm walls. Six pyramidal blocks (18.4 cm x 18.4 cm x 15.24 cm) are arranged in a 2 x 3 grid on the platform (Fig 2.3A). The blocks are pyramidal, with the edges chamfered, to avoid the recording cable catching on a wall or having the walls occlude the head LEDs from being tracked. The outer walls and interior blocks define a series of seventeen alleys arranged in a city-block design (Fig 2.3A). Each alley is a possible reward location and has a lickport embedded in the side of one wall, above which

A.

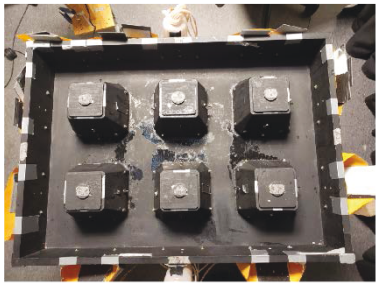

B.

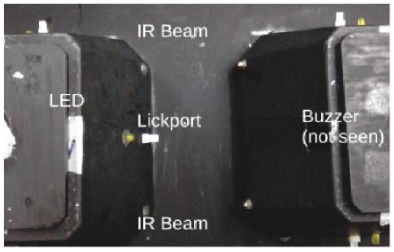

Fig 2.3 Apparatus design. A Top-down view of Ratterdam showing all seventeen alleys Reward reservoirs can be seen attached to top and bottom walls; additionally, texture floorplates for Beltway task seen stored in attached pockets around sides of track. **B.** Single alley, annotated with key features. Pair of IR emitter-detectors on affixed to both sides of entry. In the center of the alley is a lickport with a visible lick LED shown. Below the alley (not visible) is a buzzer. Buzzer and visible light LED used as feedback signals.

there is a visible-light LED as a reward feedback signal. An IR beam emitter–detector pair is present at either end of the alley to detect entry (Fig 2.3B). As the rat navigates through whatever section of the maze is available given the current task, its entry into each alley is detected. When the rat enters a given alley the task program determines whether a reward should be given at that alley and, if so, a small liquid reward is dispensed and a light and tone signal are provided as feedback. The rat then consumes the reward and continues navigating through the maze. The control software records the history of reward delivery and alley entry, using this history to guide future rewards. The exact way reward selection is done depends on the task and will be discussed in the relevant sections.

Software Task Control

The control program is divided into two parts, the hardware and software controlling the apparatus itself, and the behavioral task software that controls the task. The apparatus's hardware design is modular with each alley being associated with an Arduino Uno (Arduino is a trademark of Arduino AG and is used under a Creative Commons ShareAlike 3.0 License). Each Arduino in turn is connected to the IR detectors, visible light LED, buzzer, and peristaltic pump for reward delivery. Additionally, each Arduino is connected to a common power and communications line connecting all the Arduinos. Each alley Arduino is programmed to receive an input from a single controller Arduino instructing it to dispense a reward the next time it detects an entry into its alley. Absent such an instruction the Arduino does nothing upon alley entry. After a reward is dispensed, the alley Arduino transmits this information to the controller Arduino and resets to the default state (do nothing) until further instruction. The controller

Arduino is constantly polling all of the alley Arduinos, reading any state changes from the alley Arduino and giving any new instructions if necessary. Communication between the controller and alley Arduinos is managed via the I2C protocol (Phillips Semiconductor (now NXP Semiconductor), 1982; https://www.nxp.com/docs/en/application-note/AN10216.pdf). This protocol uses two wires, a data wire and clock wire, to define the controller as such and give an address to each alley Arduino. The protocol allows sending and receiving information between the controller and a single alley at a time. A series of codes was defined that correspond to, e.g. “Give Reward”, “No Reward”, “Reward Received”, etc. In addition, the controller Arduino receives input from a user-controlled keypad that controls the overall task status. The controller Arduino transmits any new information, from the alleys or the user, further upstream to the second component of the control program, the behavioral task software. Thus, the hardware and software controlling the apparatus itself has no knowledge of the task or memory about past events. The components simply

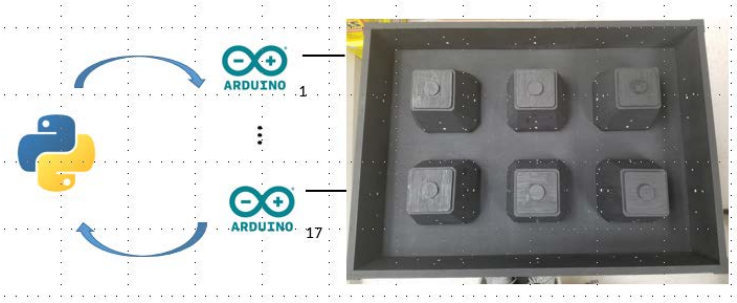

Fig 2.4 Schematic of software task flow control. Each of the seventeen alleys is controlled by an Arduino Uno. The Arduino controls the hardware described above and initiates actions based on input further up the command chain. A single Arduino Mega serves as a relay between the alley Arduinos and the Python controller (not shown). The Python controller implements the task, receives input from the alley Arduinos, and decides future actions the alleys should take based on these inputs and the task program parameters. Arduino is a trademark of Arduino AG and is used under a Creative Commons ShareAlike 3.0 License.

pass reward information to each alley and transmit feedback about reward delivery.

It is within the behavioral task program that the task is defined, the status tracked, and all information saved. The program is in constant communication with the controller Arduino as it in turn constantly polls all of the alleys (Fig 2.4). The communication between the program and the controller Arduino uses the Serial protocol which provides a single one-to-one channel between devices (Arduino Serial end is built in, Python support for Serial provided by PySerial, https://pypi.org/project/pyserial/). As with the hardware, a set of simple codes was defined that correspond to events the program is sending to the controller or that the controller is sending to the program. Communication between the behavioral software and the apparatus occurs one alley at a time using the I2C protocol. The program loads the information to send, the controller receives it, addresses the alley in question, and sends the information. The same process is repeated with the controller asking the alley Arduino for any new information. Each poll cycle of the program consists of reading from an alley, writing to an alley, and seeing if there is new information from the keypad. Then the program instructs the controller to move on to the next alley. Each poll cycle is very slow by computer standards, taking 17ms to complete. However because the alleys store a memory of their state this in practice is not an issue. The task program has the rules of the task stored, as well as functionality to decide which alleys should be rewarded next along with statistical counterbalancing of these rewards. As the rat navigates, the task program is constantly being updated with any

information and deciding how to update the reward policies for each alley appropriately. As this occurs, all information is then saved to a file.

Electrophysiological recording

Recording schedule (across and within days)

The number of recording days needed for a rat varies based on the quality of the units recorded and the behavior of the rat, among other factors. For a well-trained rat with a sufficient and stable cell yield, 3-5 days would be recorded on the Beltway task and 5-7 days recorded on the Ratterdam Open task. Although the number of cells needed for a dataset varies based on many factors such as the effect size and cell quality, a yield of 30 or more cells active during the experiment for Beltway and 20 for Ratterdam Open was used as a rough heuristic. The Beltway recording days were performed first, followed by the Ratterdam Open recordings. This was to avoid the potential confound of the repeating cell dynamics appearing in the Ratterdam Open task and persisting in, or at least affecting the results of, the Beltway task.

Within a recording day there are three recording periods: sleep 1, task, and sleep 2. The sleep sessions are roughly 20-30 min periods of recording the rat while it rests, ideally sleeps, on the pedestal. The task length is variable but is roughly 90 min for Beltway and 60 min for Ratterdam Open. There are two rationales for the sleep sessions. First, they give a measure of stability of the cells active during the task. During the task cells may exhibit various changes in their activity level that reflect task-relevant processing or something unrelated to biology such as the tetrode drifting away from the cell. Comparing the stability of a cell between sleep sessions before and after the behavioral task allows one to

disambiguate these possibilities. Second, the cell yield in the sleep sessions gives an overall cell yield as some cells recorded during sleep may be inactive during the task simply because they do not have a place field on the apparatus.

Recording system and setup

The recording system used is a 64-channel Neuralynx Digital SX box with the associated Cheetah acquisition software (Neuralynx, Bozeman, MT). Each wire of the tetrode, as well as the two references wires, are assigned a channel number. The electrical signal from each wire follows a route through various pieces of equipment from the brain to the recording system. The signal from the wire is routed through the EiB board implanted on the rat to a terminal connector. A removable headstage is attached to this connector. The headstage provides an interface between the implanted EiB and the tethers. The headstage divides the channels into two banks of 32 channels, with a tether plugging into each bank. These tethers are routed from the animal up into the ceiling where they plug into a commutator. The weight of these tethers, as well as the weight of the drive, can be significant for an animal's neck muscles and so an elastic cord is attached between the tethers and the commutator to support the weight of the drive/tethers. The commutator is a device that rotates the tether along with the animal's head rotations so that the tether does not tangle as the rat moves throughout the maze. From the commutator, two MDR-50 cables carry the signal to the Neuralynx box. From there the signals are amplified and filtered (see 2.6.4 for filtering and other acquisition parameters).

Video tracking setup

To track the animal's position, a removable component with red and green LEDs was attached to the headstage. Care is taken before an experiment to ensure that the LEDs are of sufficient brightness and that the tether configuration does not cause occlusions between the LEDs and the camera. A camera in the ceiling is connected to the recording system via a frame grabber which processes the incoming frames from the camera and arranges them in a queue for the recording system to access. The recording system tracks position by thresholding the image's red, blue, and overall luminance content and then identifying the center of mass of the surviving pixels. Each of these thresholds must be set before the experiment and checked daily to ensure high-quality video tracking.

Spike and EEG channel setup

The raw voltage signal is passed into the recording system as described in 2.6.2. The signal from a single, user-defined wire from each tetrode is then copied to a separate input bank to be filtered separately and serve as the EEG signal for that tetrode. Thus, each tetrode has five inputs associated with it: four tetrode signals and one EEG signal. The tetrode and EEG signals are then amplified, converted from analog to digital, and filtered. The analog-to-digital conversion results in a signal sampled at 32,000 Hz. The filtering is achieved via a FIR filter with a 600-600Hz range for the tetrodes and 1-300 Hz for the EEG. The filter is defined chiefly by the number of taps used, here low-cut 32 and high-cut 64 (spikes) and low-cut 0 and high-cut 128 (EEG), which specify the narrowness and specificity of the filter.

Once the signal has been processed, the spike detection parameters are set. The two most important parameters are the voltage deflection threshold, above which a spike event will be said to have begun, and the input gain, which determines the range of voltages that can be detected. Once a spike is detected, 32 samples are taken from the input signal, seven before the detection event and 24 samples after (with the 32nd sample being the one during which the voltage threshold was crossed). This waveform is saved to a file for further processing.

Referencing

Because voltage is a form of potential energy, it is an inherently relative concept. There are a number of ways to reference the recorded signal depending on the situation and even the stage of the experiment. As mentioned above, there are pros and cons to having the references either above or below CA1 and the choice depends on the experimental question (specifically how important is a high-quality theta oscillation recoding) and the quality/status of the drive. In addition to the reference wires, the tetrodes may be referenced to Animal Ground, which is the ground screw. Referencing to animal ground is not ideal for experiments, as multiple noise sources can be picked up owing to how far away the ground screw is from the recording site (additionally, if a cerebellar ground screw is used, then strong and prevalent muscle contraction artifacts will be picked up as the neck muscles are very close by). However, during tetrode turning, using animal ground is common because there is no chance of picking up a hippocampal-related signal on your wire that is actually present on the reference. Changing references can also be helpful to better identify signals in the EEG. If one is recording from a tetrode referenced to, e.g. animal ground,

and the signal is noisy, an option is to reference that wire to a nearby tetrode which is known not to have the same EEG signal present. Two nearby wires share much of the electrical background and so the target signal will become much flatter allowing any small EEG signal to be detected. Care must be taken to ensure the reference tetrode does not share the same signal. Afterwards, the target wire is then re-referenced to the original reference.

De-noising

Given the small size of the target signals, tetrode recordings are very sensitive to ambient noise. This is usually caused by other equipment, lights, differential grounding, or even the way the various tethers and cables are bundled. In the United States, electronics operate at 60Hz and so a strong, highly consistent signal of that frequency is a sign there is electrical noise present (there are biological signals at that range, e.g. the gamma oscillation, but they are not nearly as strong and consistent as an artificial source). To avoid noise, first one should check that all the equipment shares a common ground. This means each piece of equipment is plugged into the same outlet (or the outlets share a building ground). Even electronics that are not part of the experiment but are plugged in – such as a charging cellphone – can be an issue. Next, check the cables to make sure they do not form loops or ‘figure-eights’. If so, this can pick up noise. These steps should solve most noise issues but if not further testing may be required.

Spike sorting and data pre-processing

Spike sorting

Once data have been collected, the individual waveforms must be assigned to a neuron (or identified as noise). Although modern advances in automatic spike sorting have made great improvements, they still do not work as well as manual sorting which is done here. Spike sorting exploits two facts: first, that the same signal will be picked up slightly differently on two tetrode wires and, second, that there are multiple parameters of a waveform that can potentially identify a neuron. A neuron will have characteristic spike waveform parameters that differ from those of its neighbors. Because the waveforms of different neurons are different from one another, when any two waveform parameters are plotted against each other, each neuron will appear as a two-dimensional Gaussian on this plot, also called a projection (Fig. 2.5). The reason the neuron appears as a Gaussian is that there is variability in the spike waveform around some characteristic value for that cell. The user then defines a polygon around this cluster which ideally admits all the points belonging to this cluster and none that do not. The spacing or overlap between each cluster is a

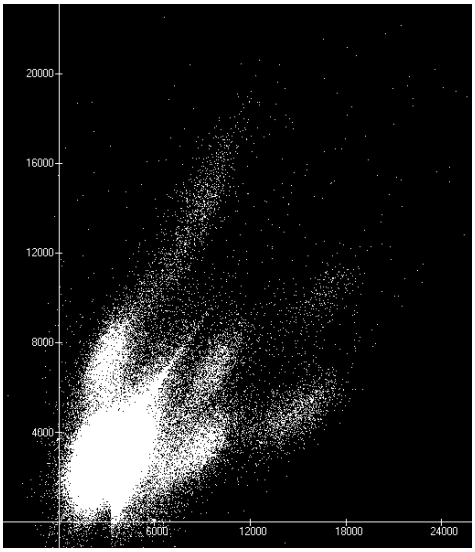

Fig 2.5 Example of spike sorting. Data from a single tetrode is shown. Each dot is an event that crossed threshold (outside of a refractory period). The axes are parameters of the spike waveform, here the peak value recorded across two different wires. Events from different units appear as Gaussian-like 'clouds' of points that the user then encloses with a border. This can be done for multiple choices of axis parameters (multiple 'projections'). All the points lying within the intersection of border definitions across projections are defined as the spikes for the corresponding unit.

function of how similar the neurons are to one another and how good the recording is. If, for example, the tips of the tetrodes are not clean and have high-impedance then the signal impinging on each wire will appear similar – and the clusters overlapping – simply because subtle differences between them appear attenuated due to the low-quality recording. Further, there will always be a ‘noise cluster’ near the origin reflecting all the events that appear the same across wires. These are the events from neurons so far away that the signal seems virtually identical across wires (but note the signals are neural and the term ‘noise’ refers to the inability to isolate not that they are artificial). Two neurons may differ from each other only in a subset of their waveform parameters, therefore multiple combinations of different parameter pairs are visualized to identify the pair that best isolates any one neuron from the rest. Different choices of parameters may be required to isolate a given neuron from different neighbors and therefore a single cluster is defined by the intersection (in the set theoretic sense) of boundaries drawn on each relevant projection. Typically, the waveform peak on each wire is the most informative parameter although the energy (a quantity proportional to the area under the curve) is also informative in some cases. The isolation quality of each cluster is noted and used to segregate the data set. Cells are labeled with the quality of the isolation (both from other units and the ‘noise cluster’) on a five-point scale. Neurons with a score above some threshold, typically 3 or above, are considered well-isolated for further analysis.

Data preprocessing

Once the clusters have been defined, the data must be preprocessed before it can be analyzed. There are two major forms of preprocessing: speed filtering and occupancy normalization.

Velocity filtering removes spikes that occur during periods of motion less than a threshold, typically between 1-3 cm/s. Note, the motion is that of the headstage LEDs which move not only during locomotion but also during behaviors that would not seem to count as 'motion' such as grooming or head scanning. Further analysis is needed to remove these suprathreshold non-movement epochs but is often not performed. The velocity filter is applied because it serves as a rough proxy for the real variable of interest which is neural state. The hippocampal place map is active when the animal is in a theta-dominated state which correlates with attentional behavior and movement. Hippocampal activity during other oscillatory regimes, e.g. LIA, SWR, SIA, are related to functions other than instantiating the place map and are undesirable for the analyses in question (but of course are of great interest for different types of questions).

Occupancy normalization adjusts the observed firing rate at a position by the time spent at that position to standardize the rate across locations which the rat visited more or less often. The result expresses activity as spikes per second (unit: Hertz). First the environment is binned into two two-dimensional histograms, one for spikes and another for occupancy samples. The former is divided by the latter and the result is scaled by the camera frame rate and

smoothed to yield a map of firing rate for each bin. The bin size must be chosen to be small enough to capture meaningful firing rate changes across space but not so small that the bins can be frequently empty due to, e.g. camera occlusions or a lack of sampling. Once these (and any other) preprocessing steps are done, the data may be used to address specific questions to address the hypothesis at hand.

Perfusion

Once the experiment is finished the animal is perfused. To prepare, 100mL distilled water, 100mL saline and 300mL formalin (3.7% formaldehyde in 0.9% saline) are drawn and the peristaltic perfusion system flushed with the water. Then the perfusion system is primed with the saline. The animal is then anesthetized using 4% isoflurane. Once there is no longer a response to veterinary checks, specifically the corneal reflex response, the animal is injected with a euthanizing agent (Euthasol, 1cc, Virbac Inc, Westlake TX) and monitored to ensure the plane of anesthesia is deep enough that the animal will not recover. However, the procedure must not be delayed so long that the heart stops beating. Next, the animal is placed on a rack with its sternum exposed. A midline incision is made, the skin is separated from the musculature, and the musculature separated to expose the internal cavity. The xiphoid process, at the base of the sternum, is located and a lateral incision made directly below it. The internal organs and tissues caudal to this are moved aside to reveal the diaphragm, which is then sliced open. With the upper chest cavity exposed through this window, the rest of the cavity is exposed by cutting and removing the ribcage laterally from the diaphragm to the neck. The lungs and heart are rolled

to the side to allow the descending aorta to be clamped. Clamping these vessels restricts the blood flow to the anterior half of the body and maximizes the fixative agent concentration per unit volume in the upper half of the body. The left ventricle is punctured with the perfusion outlet line, careful not to pierce the inner cardiac walls, and the right atrium is pierced. This creates an open loop that allows solution to flow through the circulatory system through the brain and then out of the body. Next, the 100mL saline is pumped into the animal. Once the liquid coming out of the right atrium is clear, or the 100mL have been used, the 300mL formalin are added to the perfusion system while making sure no air gaps are present in the tubes at the transition point between saline and formalin. The formalin perfusion will take roughly 20 minutes after which the upper body of the animal should be rigid. After the perfusion is completed the head is decapitated and the skull is cleaned of all skin and tissue. Further, the foramen magnum in the rear of the skull is removed to allow an entry point for the next fixative. The skull (with brain inside and drive attached, tetrodes in place) is placed in 4% sucrose formalin solution for at least 24 hours with the tetrodes left in place. After the soaking, the tetrodes are retracted and the brain is removed and placed back into a 4% sucrose formalin solution until the histology is performed.

Histology

Once the brain has been fixed, it is sliced and slices corresponding to regions of interest (i.e. around the tetrode tracks) are mounted. The purpose of this step is to confirm where the tetrodes were implanted by visualizing the tracks tetrodes made as they traveled through tissue. First, the brain is sectioned in the coronal plane. The general region of interest can be identified by looking for a

depression in the dorsal surface of the brain where the hyperdrive was implanted. Slices are then cut using a microtome (chilled via dried ice), with a slice thickness of 40μm. These slices are placed on slides (typically, six to a slide) and labeled with the slice number. Next, the slides are subbed, which refers to embedding them in a gelatin matrix so that the slides remain adhered to the slide during subsequent steps. The subbing process utilizes deionized water, gelatin, and chromium potassium sulfate (the last reagent positively charges the embedding matrix so that it will adhere to the negatively charged tissue). Slides are then stained via a standard Nissl stain (http://www.ihcworld.com/_protocols/special_stains/nissl.htm). Finally, slides are visualized to identify where tetrode tracks occur (see Appendix for histology).

Chapter 3 – Rate Remapping and the Beltway Task

Introduction

Background

The cognitive map theory described in the General Introduction became more influential as an increasing volume of data challenged the predominant Skinnerian model that all animal behavior can be reduced to stimulus-response chains (Tolman, 1948). This alternative theory posited that the brains of at least some animals contain a Euclidian, metric-based topographical map that allows for flexible navigation (O'Keefe and Nadel, 1978). Further, learned associations between locations on the map and the items that exist there allow for 'annotations' to the map useful for navigation, decision-making, and other cognitive processes. The spatial and non-spatial information present within a cognitive map are in principle independent; over time the same item may move about in space and the same location may harbor different items. Therefore, mechanistically, some form of multiplexing must take place, if the cognitive map theory is correct, to allow these independent types of information to be interrelated (Leutgeb et al., 2005a).

Given that the hippocampal cognitive map is composed of place cells, the question of how to multiplex spatial and non-spatial information becomes one of how to combine these signals within the parameters of place cell physiology. Place cells, by definition, fire action potentials as a function of the animal's position. A downstream readout neuron (or network) must be able to distinguish between the in-field and out-field firing rate, but the actual magnitude of the rates

involved is less important (so long as they are large enough to overcome issues such as, e.g., the stochastic nature of synaptic transmission). This suggests the possibility that the presence of firing above some threshold can indicate the animal's position within an environment and that the magnitude of supra-threshold firing can encode other variables, specifically the sensory cues present within the vicinity of the field. The rate remapping hypothesis advances that this is the case: the relative firing of the place cell is used to indicate the animal's allocentric position, while the actual amount of firing is modulated to encode, at the unit level or as part of a distributed population code, the non-spatial items present in, or nearby, that place field. Thus, the spatial map is kept stable because the place field positions do not change, while the distribution of place field firing rates (over and above that which is needed to indicate presence in a place field) encode the presence or even identity of non-spatial cues at that location.

However, the rate remapping hypothesis did not propose a specific pattern of rate changes. Different models are consistent with the notion of stimulus-induced rate change. For instance, a gain modulation in which the entire field is affected, or a local modulation, in which the rate is altered within a spatial fraction of the field, are both consistent with the rate remapping hypothesis. In other words, the hypothesis stipulates *that* the rate changes, it does not specify *how.* The actual pattern of rate changes the map employs would have significant implications for the nature of the representations computed by the cognitive map.

A separate question concerns the role of attention in the processing of experiential information. It has been suggested that the hippocampus automatically encodes attended episodic information into a short-term memory buffer, to support later computations in other regions (Morris and Frey, 1997). Whether the attended aspect of experience is behaviorally relevant is, under this proposal, irrelevant; anything that receives the 'spotlight' gets stored into a short-term buffer. A key question addressed in the present work is whether this is the case, and if so whether irrelevant stimuli will be represented in CA1, presumably for storage into this episodic buffer.

Previous Work and Limitations

A number of studies have addressed the rate remapping hypothesis, however, open questions remain. Leutgeb et al. showed that sensory cues can cause a significant change in neural firing rate while keeping the center of mass of the firing fairly constant (Leutgeb et al., 2005a). Rats were recorded as they randomly foraged in a cylindrical arena with a prominent cue card. Across sessions the color of the cue card changed but the environment remained in the same spatial location. CA1 place cells displayed robust firing rate changes, up to an order of magnitude difference, between each recording session. However, when the firing rates in each session were rescaled to their own session-based maximum, the place fields looked quite similar. The authors interpreted this as a sensory-driven change in place field firing rate that did not affect the spatial position of the place field, in line with the rate remapping hypothesis. However, the authors were unable to test whether cells responded independently to different cues, as the there was only a single non-spatial cue (wall color) that was

perceptible at all locations within the box. The rate remapping hypothesis makes a strong prediction that place cells are able to encode cues independently of one another; cues in a certain location would likely be encoded by place cells with fields at that location. However, such a fine-grained analysis was not possible in that design.

An earlier study by Moita et al. explored how any sensory-driven change in place cell firing rate was affected by the rat's location. The authors found that an auditory cue could affect the firing rate, but only when the animal was present in the place field. This suggests a gating mechanism, in line with the rate remapping hypothesis, that restricts any non-spatial rate modulation to the location at which the non-spatial stimulus is present (Moita et al., 2003). This is significant as, *a priori*, hippocampal pyramidal neurons that respond to non-spatial cues need not be place cells. It was conceivable that some cells would respond to a given cue regardless of its location, with a resulting loss of spatial tuning.

A limitation of the design of the Moita study is that it did not distinguish between cue response and encoding. Not every response to a cue reflects the encoding of its identity; a cell may respond to a cue in a non-specific manner indicating a differential arousal level based on the cue present. To encode a cue, however, requires a more specific pattern of results. There must be a reliable and differential response to at least one cue versus multiple other ones. Earlier studies (e.g. Delacour, 1984) demonstrated that hippocampal neurons can respond to the CS in a classical conditioning paradigm. Moita and colleagues

extended this to show this response can occur in a spatially-selective manner; in other words, at least some of the cells that respond to non-spatial cues are place cells, as opposed to a functionally distinct population. However, it remained to be shown whether cue encoding could occur in such a spatially-gated manner, which is a computationally more demanding task than a differential cue response.

Another study by Wood et al. examined CA1 firing rate responses to a set of odors at different locations (Wood et al., 1999). They found examples of units with significantly different firing rates based on odor and firing in predominantly one reward location. However, the presence of rate modulation within a spatially stable field was not addressed. The authors examined average firing rate at each stimulus location, and showed cells that responded to cues differently at different locations. However, the authors only examined the main effects of position or stimulus as they lacked the power to test the interaction between them. Some example units seemed consistent with such an interaction, encouraging subsequent experiments to test a stimulus-position interaction in a more rigorous manner. Regardless, the presence of rate modulations within a spatial field was not addressed at all and, as discussed below, an open question from these data is what form the rate changes may take.

An important work by Manns and Eichenbaum showed the ability of CA1 neurons to encode cue identity in a spatially-dependent manner but, like the Wood study, did not address how this occurs (Manns and Eichenbaum, 2009). As mentioned above, there are multiple, specific patterns the rate changes could

adopt which would be consistent with the conclusions from this study. Rats ran laps around a circular track, periodically encountering objects as they did so. By examining the firing rate response to repeated presentations of the same cue in the same, or different, locations, they were able to provide direct evidence that cue encoding takes place in a spatially dependent manner.

A more recent work, and arguably the most related to the present study came from Herzog et al. who recorded CA1 neurons as rats foraged in a box. Different types of tastants were delivered to the rat via a cannula inserted in the mouth, allowing for the authors to compare the responses to each tastant at different locations (Herzog et al., 2019). They found single unit responses that seemed to distinguish between some subset of the tastants, or between one versus the others, when firing rate was plotted against stimulus onset. Given that these stimuli were presented across the track, this result provides arguably the first direct evidence that multiple cues can be encoded at multiple locations independently. It is of note that the authors also noticed firing rate fluctuations restricted in time – the firing did not tonically increase or decrease in response to a given stimulus, but rather the rate exhibited a temporally localized modulation. Itskov and colleagues reported CA1 responses to textures that also looked similar to the data of Herzog and colleagues, with localized regions of modulation; however, the animal only encountered the cues in a single fixed position so the independence of cue encoding could not be established (Itskov et al., 2011). Given that these studies examined CA1 responses over time, it is unclear whether and how the fields changed as a function of space. Because the

cognitive map is fundamentally spatial in nature, an intriguing open question from these data is how the rates changed in the spatial dimension.

Another phenomenon that can be described as rate remapping is 'splitting'. Splitting refers to a cell (a "splitter cell") that alters its firing rate in response to a turn choice (or other task-variable) made outside of its field. First reports showed cells that significantly depressed or potentiated their firing depending on the type of path the rat executed (Wood et al., 2000; Frank et al., 2000). Further studies showed that some cells respond to upcoming choices ("prospective coding"), while others respond to recently made choices ("retrospective coding") (Ferbinteanu and Shapiro, 2003). Given that the location of the fields remain stable and it is a non-spatial (here, movement- or choice-related) variable that affects the firing, splitter cells are considered another example of the broader rate remapping phenomena (though not specifically implicated in the original rate remapping hypothesis).

Experimental Questions

Previous studies provided a wealth of information about the role of the hippocampus in episodic memory, but a number of important open questions remain.

First, it is unknown what form rate changes take to encode non-spatial information. *A priori*, it is possible that the entire field is altered in a consistent manner; an additive or multiplicative gain model would allow the field envelope to change in a stimulus-dependent manner, while subjecting each small piece of the field to the same computation. Alternatively, there could be local changes to the field; possibly a rate modulation manifests at salient locations in the environment,

such as texture onset or at the lickport. Still further complex patterns of rate changes are possible, yet have not been explored. Herzog and Itskov, in separate studies, examined the change in firing rate over time from stimulus onset (Herzog et al., 2019; Itskov et al., 2011). Responses occurred not only at stimulus onset (or after some short delay to account for transmission to CA1) but throughout a ~2.5 s window post-delivery. These data did not look at how the spatial fields were affected as they both examined time windows (and in the Itskov study the rats were not freely moving). However, it is crucial to understand how temporally restricted changes in the firing rate envelope interact with the spatial map. Knowing, for instance, that a cell responds during a 0.5 s window from stimulus onset does not specify how the spatial field responds. Depending on the behavior of the animal, it is possible that 0.5 s elapses as the animal runs through the field, possibly resulting in a gain modulation. However, it is also possible that the animal tends not to traverse the entire field in that window and, therefore, the rate change is restricted to a small portion of the field. It is also possible that the apparent temporal modulations these authors observed were, in fact, spatial modulations within the firing field envelope. Analogous to the example discussed above, vagaries of behavior could make a spatial modulation appear to be a temporal one. Only examining the time window of the response does not distinguish between the gain modulation and fluctuation models. The rate remapping hypothesis, and the cognitive map theory it supports, gives the spatial map primacy in the encoding of episodic information; the items of experience are encoded in terms of their spatial location. Therefore, it is

important to understand how specific patterns of rate change interact with the underlying spatial map.

Second, it is unknown whether and how rate remapping, as a mechanism of multiplexing, occurs in the absence of an association between the cues being represented and a reward. Rate remapping has been observed in conditions where the cues have no relationship to rewards (Leutgeb et al., 2005a, Anderson and Jeffery, 2003; Shapiro et al., 1997). However, in the studies which examined rate remapping as a way of encoding non-spatial information, the cues had a salience that may have affected how they were encoded (Wood et al., 1999; Herzog et al., 2019; Itskov et al., 2011; McKenzie et al., 2014). It is unclear whether cues would be encoded if they lacked any relevance to the task design. As discussed in the General Introduction, it has been proposed that there is a distinction between information encoded because it is relevant for behavior, and information encoded automatically because the animal chooses to attend to it (Morris and Frey, 1997). The distinction is subtle, but important; in the latter case, any and all episodic information is encoded into a short-term buffer if the animal attends to it. This more permissive form of encoding may populate a so-called 'episodic buffer' with information that can be used offline by other neural systems to extract information about the world that was not behaviorally relevant at the time of encoding. It is an open question whether rate remapping can support encoding of 'attended experience'. Demonstrating that this is the case would not only support the existence of an episodic buffer, but also would support the idea that the cognitive map encodes episodic memory *per se*, and is not just a

spatially-based look-up table of reinforcement contingencies the animal has learned.

Aim 1 Methods

Data set

Data were recorded from the right CA1 of four rats, two male and two female, as they completed the Beltway task. The number of days recorded and cell yield per day are listed in Table 3.1

Table 3.1 Data sets used in Beltway Task

Rat	Day	Yield (overall/included)
R781 (M)	3	32 / 26
R781 (M)	4	33 / 18
R808 (F)	4	12 / 9
R808 (F)	6	17 / 11
R808 (F)	7	28 / 10
R859 (F)	1	24 / 7
R859 (F)	3	23 / 17
R859 (F)	5	41 / 31
R886 (M)	1	22/21
R886 (M)	2	29/23

Table 3.1 Data sets used in the Beltway task. Left, rats used and their sex. Middle, data used across rats. Right, total yield recorded per day and the number of cells included based on the criteria described below.

Task Design

The task used for Aim 1, termed ‘Beltway’, makes use of the apparatus described in the General Methods chapter. The inner alleys are blocked off leaving the outer perimeter available for the rat to navigate, consisting of nine alleys and a start box. The rat runs clockwise laps around the track, receiving reward at an average of two alleys per lap according to the schedule: 15% chance 1 reward, 70% chance 2 rewards, and 15% chance 3 rewards. Floorplates are placed on the floor of each alley and are interchanged between

each lap. The stimuli are interchanged such that on each lap there is a different pseudorandom pattern of stimuli present across the alleys and that across the course of a session each stimulus will be present at each alley multiple times. Additionally, the association between alley and reward is counterbalanced.

Data Inclusion Criteria and Filtering

Single units were processed as described in the General Methods. Although the qualitative texture response properties are analyzed for each unit, quantitative analyses are only performed on units that pass inclusion criteria based on lap-by-lap activity within alleys as well as spatial cohesiveness of the average field. For each alley, the cell must fire on at least 12 trials with a minimum threshold of 1 Hz in at least one spatial bin. Additionally, when the activity within an alley is trial-averaged, at least three contiguous bins must have a minimum rate of 0.5 Hz (out of 12 roughly 1.2 cm long bins). Any cell that has at least one alley meeting these criteria is included for analysis.

Permutation Tests

The first quantitative analysis performed for Aim 1 was a permutation test, following closely the procedure performed in Fujisawa et al., 2008. Permutation tests are designed to approximate the null distribution of a test statistic based on the observed data. The labels for each trial corresponding to the variable of interest are shuffled between the trials, thus destroying any structure within the data that is dependent on the variable of interest, while preserving other statistical patterns within the data. Here, the test statistic is the bin-wise difference in firing rate between the trial-averaged linear rate maps of two given stimuli. There are three observed test statistics: the difference vectors for

stimulus A vs B, B vs C, and A vs C. The permutation test consists of many shuffling iterations, during each of which the stimulus labels are shuffled between trials, the trial averaged linear rate maps computed, and the (null) test statistics found. The distribution of these null test statistics is compared to the observed test statistics to quantify which spatial bins, if any, of the observed test statistics are statistically significant. For each spatial bin, an upper and a lower firing rate threshold is found which only allows a certain percentage of the null firing rates to be above or below the threshold, respectively. This threshold is equivalent to half of the bin-wise p-value, here 2.5%. There are three types of multiple comparisons used here; first, there are the number of alleys tested, second, there are the number of comparisons being made within an alley, and third, there are the number of bins within an alley. To adjust for the number of test statistic comparisons and the number of alleys tested, the p-value is defined to be $\frac{0.05}{3*n}$, where n is the number of alleys being tested. To adjust for the number of spatial bins, a more stringent threshold is defined such that only 5% of the nulls (Bonferroni corrected) may be more extreme than the thresholds (upper or lower) at any spatial bin. If the real test statistic for a given condition exceeds this heighted threshold, the comparison is deemed significant. The spatial extent of the effect is found by finding the region of contiguous bins, within each of which the real test statistic value is more extreme than 5% (Bonferroni-corrected) of the nulls. Binomial tests are used to determine if the abundance of cells which pass a permutation test is greater than one would expect by chance.

Linear Mixed Effects Models

Linear mixed effects models (LMER models) are a family of models that extend the concept of linear regression to more complicated situations (Hastie et al., 2009). LMERs were run in R (version 4.0.3) using the lme4 package (version 1.1-23). LMER models support multiple regression, allowing the effect of multiple covariates on the dependent variable to be analyzed. Further, these covariates are "mixed" in that they can be divided into primary variables of interest (fixed effects) and other variables which contribute to variability but are not being analyzed directly (random effects). A curve is fit to each covariate which, here, is a spline in order to capture non-linear relationships between the independent and dependent variables. A number of degrees of freedom and order of the spline are defined. These parameters set how many inflection points are used, and the amount of curvature that can be captured, respectively. Additionally, the random effects can vary in their intercept, slope, or both depending on the nature of the question. It should be noted that the complexity of the model – in terms of number of terms, interactions, and complexity of the random effects – affect the ability of the model to converge (which means the output approaches a certain, presumably optimal, value).

Coefficients are estimated for each fixed effect. The coefficient reflects the percent change in the dependent variable caused by the independent variable (compared to a reference variable, typically the first level of the factor in question). The significance of each fixed effect is found by computing a Wald confidence interval around the estimate; if the interval does not include zero then the variable is determined to exert a significant effect on the shape of the curve

that relates the variable to the dependent variable. Further, confidence intervals can be fit to the curves as well, allowing comparison of different curves to one another.

An LMER model was created for each alley with the following formula:

$$rate \sim texture * spatialBin + reward + (1|trial)$$

which is read as “the dependent variable of firing rate is a function of the stimulus crossed with the spatial bin (yielding main effects of both and their interaction) and reward; trial is a random effect with a random intercept for each trial”. For each model, only the interaction terms between texture and location (as defined by the degrees of freedom of the natural spline) were assessed for significance. This results in nine comparisons per alley and n alleys per cell, where n is the number of alleys that passed the inclusion criteria. Therefore, the nominal p = 0.05 was adjusted by *9*n* to yield the familywise error rate (FWER) corrected alpha. This was used to find the confidence interval level appropriate for that alley.

Results

Overview of Data

To examine qualitative texture-dependent changes in place field activity, a set of standard plots was created for each alley for a given cell. The summary plot for one alley for one cell is shown in Figure 3.1. The session ratemap for the cell shows three or four firing fields, with the most prominent in Alley 1 (southwest corner of the track, next to the start box) (Fig 3.1A). Firing is indicated by heat of color, with locations of no firing (but occupancy sampling, i.e. the rat visited that spatial bin) shown in blue; the 95th percentile firing rate is indicated on

top. The 95th percentile of the firing rate is used as a variant of the maximum firing rate that excludes outlier values of firing in a spatial bin. Note that the large, ovoid area of sampling in the south of the track overlies the start box, where it was common for the rat to scan and rear extensively. Trials were grouped according to the texture present and one-dimensional rate maps were created along the long axis of the alley with ~1.2 cm bins. These were stacked into three matrices, with texture and rate cutoff indicated above each (Fig. 3.1B). These matrices are averaged along their rows to yield trial-averaged traces, which are visualized plus/minus the standard error in Fig 3.1C. The place field within this alley is located towards the eastern end of the alley, likely being cut off by the end of the alley, and does not show any significant texture modulation.

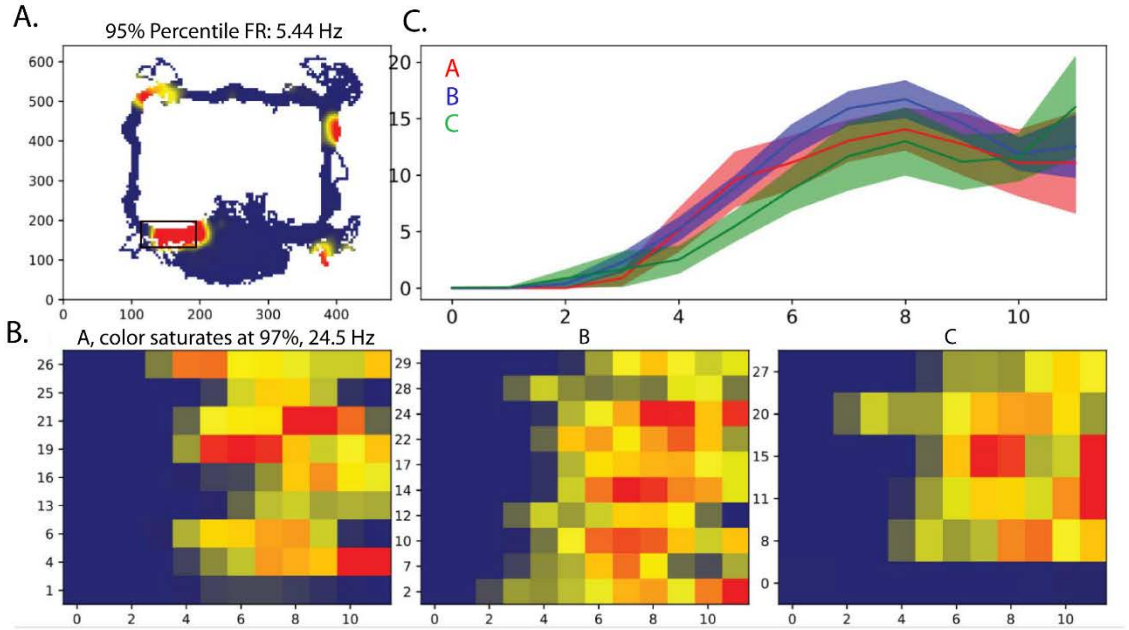

Fig 3.1. Example place field on Beltway task. A. Overall session ratemap. Color corresponds to firing rate at each pixel. Blue indicates occupancy without firing while white indicates pixels without any occupancy. Rate within each bin is calculated by the number of spikes occurring within that bin normalized by the number of occupancy samples and adjusted by the camera frame rate to result in spikes/second (Hz). Further, data are speed filtered such that periods of >1cm/s of head LED motion are excluded from the analysis. This is done to remove periods of low velocity movement or stationarity that are not associated with place field activity. Segments of off-track occupancy, for instance in the north east corner of the track, correspond to exploratory head scanning behavior. Field analyzed in **B** and **C** is indicated by box. The cell has multiple firing fields on the track, although one dominates in size. This field is situated on the eastern half of the first alley, next to the start box. **B.** Each matrix corresponds to the trials under which texture A (left), B (middle), or C (right) was present. Rows are trials and columns are spatial bins. The data have been linearized along the longer dimension of an alley to turn a two-dimensional rate map, as in **A**, into a one-dimensional one. The linear rate maps are oriented such that 0 is the south or west end of the rate map, depending on the orientation of the alley. The matrices share a common scale with the 97th percentile indicated as the saturation point. 95th percentile also used in some cases. The bins were smoothed with a step-wise kernel such that the value of bin n is equal to $((0.5*bin_{n-1})+bin_n+(0.5*bin_{n+1}))/3$. Rewarded trials have been removed. **C.** The matrices in **B** are averaged and plotted +/- one SEM. Texture A in red, texture B in blue, texture C in green.

Quantitative Analysis of Rate Modulation via Permutation Tests

Permutation tests were applied to the recording days in Table 3.1 to test whether firing fields located within alleys were sensitive to the texture stimuli. These days were selected based on the quality of cell yield as well as behavioral performance of the animal. Within each recording day, each cell that passed the inclusion criteria was run with the permutation test. The test for a single unit considers each alley separately and sets a significance threshold based on the number of alleys being tested.

Multiple units across days passed the permutation test, although (as discussed below) the significance of the yield is highly dependent on the manner of data pooling. Example units that pass the test are shown in Fig 3.2. In each case, the rate changes did not manifest as a global change across the field, for instance via a multiplicative or additive gain modulation. By contrast, local regions within the field displayed a potentiation or de-potentiation under one stimulus versus the others. In no case were all three textures mutually distinguishable; each case showed an “odd-man-out” configuration of rate patterns.

Examining the trial-averaged firing rate trace for each example shows the unique pattern of rate mapping present in each neuron. For instance, the field in the first row exhibited a peak in activity in the center of the alley when texture C was present versus the others (Fig 3.2A). Similarly, in the third example there was a brief spike in activity as the rat re-entered the start box when texture A was present, but fired with a more modest firing rate otherwise (Fig 3.2B). In other cases, however, the rate change was not a simple de-/potentiation of firing at a

single location. In the third example, a Gaussian-like field (cutoff by the end of the alley) decayed more slowly when texture A was present compared to the other stimuli (Fig 3.2B). This resulted in an expansion of the firing rate envelope when that stimulus was present. In another case, there appears to be a shift in the firing rate peak under one texture versus the other (Fig 3.2D). The shift in the centers of mass between the two sets of trials increases the effective signal, because the peak rates are not very different and so any signal would have to manifest in a shift of the distributions of firing, as is seen.

Beyond the differences in firing seen from the trial-averaged firing envelopes, the trial-by-trial linear rate maps also provide insight into the nature of rate remapping in these data. In some cases, the cell fired on each trial regardless of what texture was present, though the firing given a certain texture was greater. This was the case in the first and second examples (Fig 3.2A, B). In other cases, the cell did not fire on every lap at the alley, but the variability was correlated with one of the stimuli. For instance, in the last row, the cell did not fire

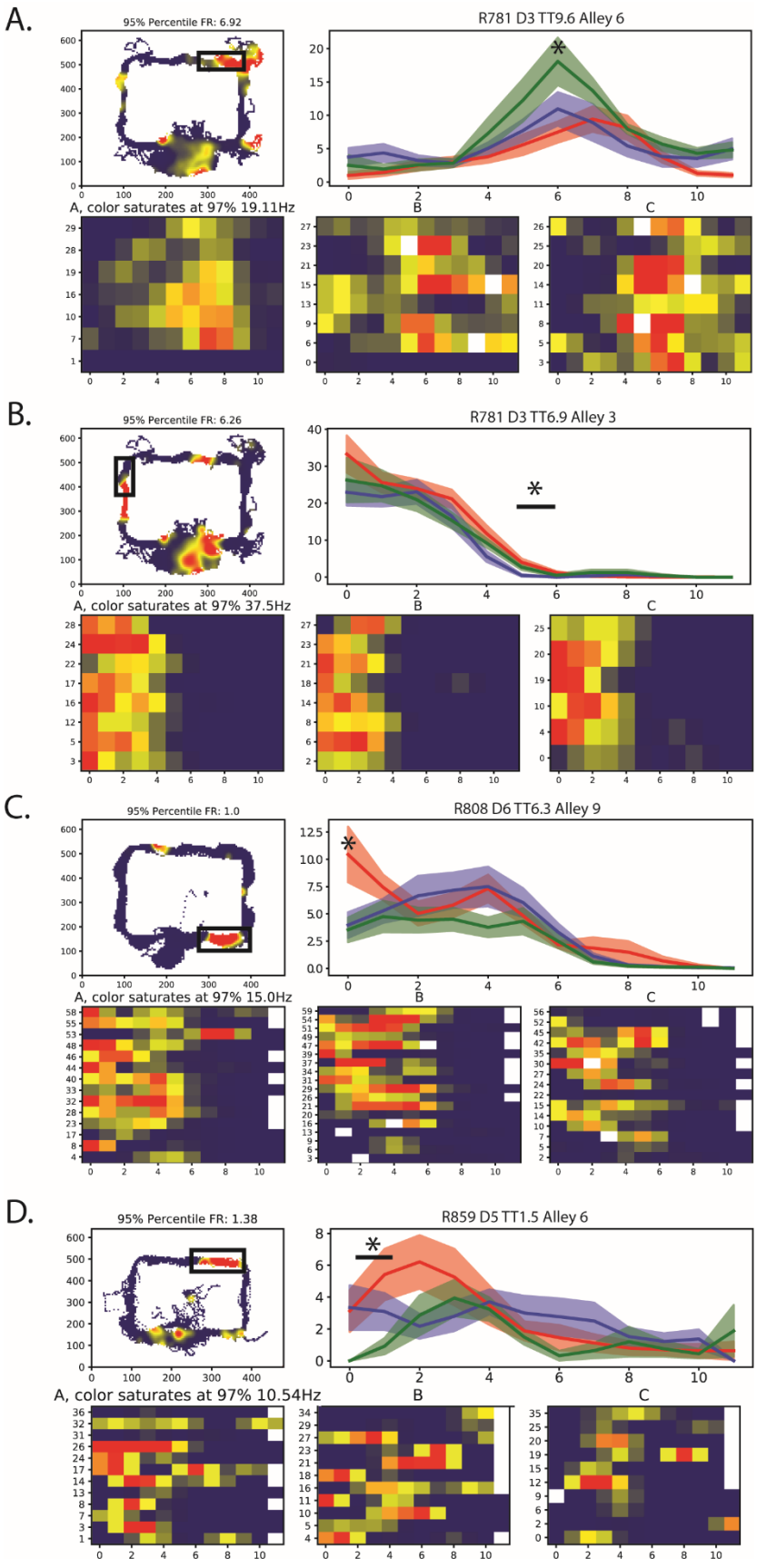
A.
95% Percentile FR: 6.92
R781 D3 TT9.6 Alley 6
A, color saturates at 97% 19.11Hz
B
C
B.
95% Percentile FR: 6.26
R781 D3 TT6.9 Alley 3
A, color saturates at 97% 37.5Hz
B
C
C.
95% Percentile FR: 1.0
R808 D6 TT6.3 Alley 9
A, color saturates at 97% 15.0Hz
B
C
D.
95% Percentile FR: 1.38
R859 D5 TT1.5 Alley 6
A, color saturates at 97% 10.54Hz
B
C

Fig 3.2 Example units that passed the permutation test. Top, Session rate map, with 95th percentile firing indicated above. Alley under analysis indicated by box. **Bottom,** Trial matrices for each stimulus, as in Fig. 3.1. Rewarded trials are not included, trial number shown on y-axis and spatial bin on x-axis. **Top right,** Trial-averaged trace for each texture with standard error of mean shown shaded. Zero is either end of alley closer to origin of video frame. Stars/bars indicate region of significance; star without bar represents single bin that passes test, while bar indicates the extent of region that passed test. **A.** Neuron which doubled its firing rate in the center of the alley when texture C was present versus texture A. Inspection of linearized rate maps shows all but three trials with C were greater than every trial with A. Texture B elicited intermediate firing rate with respect to A and C. **B.** Alley 3 cuts off roughly half of what the session rate map shows is a Gaussian-like place field. The field decayed more slowly under texture B than the others. Linear rate maps show that both textures reliably elicited firing, but firing rate persisted longer for A. Note, the field extends into Alley 2 which did not maintain the same (or any) visible texture selectivity (not shown). **C.** A Gaussian-like field in Alley 9 which exhibited a pulse of activity at the end of the alley closest to the start box when texture A is present. Rate maps show firing was more reliable, and of higher magnitude, when A was present than the rate given the other stimuli. **D.** Place field with irregular rate profile across alley. Firing increased when entering Alley 6, though with some variability.

– or fired with a low rate – on multiple trials (Fig 3.2D). However, there were more 'miss' trials (lower or a lack of firing) when texture C was present compared to A. It should be noted that the peak firing under A was also greater than that of C. It is possible that the parameters of firing – such as peak rate, variability, or peak shift – can interact to mediate gross changes in the firing rate.

There are multiple ways to pool data to determine whether the number of units with a detectable texture response is significant (Fig. 3.3). Two will be reported here, only one of which provided evidence in favor of the rate remapping hypothesis in this dataset. The first way is to pool all cells across days and animals. This resulted in a small, but significant, number of units with texture-related information in their firing rates (12.5% (22/176 units), $p < 7.7*10^{-5}$, one-sided binomial test, alpha = 0.05). However, when considering the number of days which contained a significant number of texture-responsive cells (assessed

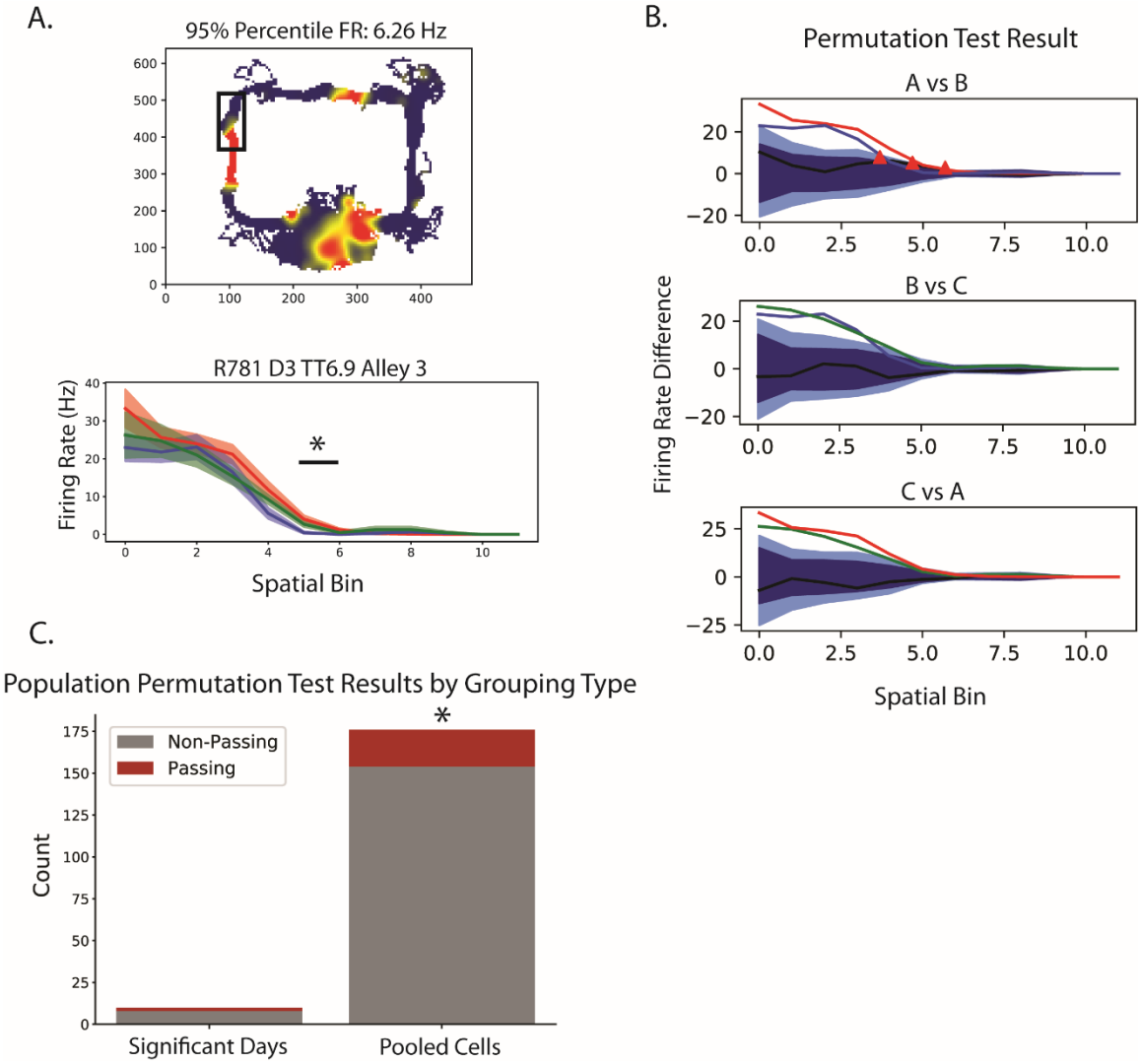

by a binomial test within each day, alpha = 0.05, one-sided), the results were not significant (20%, 2/10 days, p = 0.086, one-sided binomial test, alpha = 0.05). The two days came from two rats out of the four tested.

The data from the permutation test suggest that CA1 neurons are able to encode stimulus identity in their firing rate modulations, even in the absence of an operant task. Despite this positive result, there are reasons to believe the

Fig 3.3 Overview of permutation test and results. A. Top, Rate map for example unit which passed permutation test. Permutation tests were run on each alley separately, alley under consideration marked by box. Firing field is centered on intersection and extends into Alley 3. **Bottom,** Average linearized rate maps under each texture stimulus (A, red; B, blue; C, green). One-dimensional rate maps of each trial along the long dimension of the alley are averaged and shown +/- standard error. Field extends further into alley when texture A was present, owing to a slower rate of decay. **B.** Permutation results for the example unit. Each row shows the results of a single pair-wise comparison of two textures; the permutation test consists of running each of three pair-wise comparisons between stimuli. Within each comparison, the real trial-averaged rate trace is shown, colored as in the lower panel of A. Black trace is the bin-wise difference in firing rate. Shaded regions correspond to null distributions, point-wise in dark blue and FWER-corrected in light blue. These significance bands are found by shuffling trial labels, generating null trial-averaged rate traces, and computing how many null traces are allowed to exceed the real one to satisfy the alpha level. (see Methods). Firing rate under A is significantly different from that of B as the field ends. Triangles indicate bins which exceed the point-wise alpha threshold (and at least one of them, by definition, passes the global threshold as well). **C.** Results of permutation test across days. Each bar shows the absolute number of data units, indicated on the abscissa, that pass the test (red) stacked on those that do not (blue). The number of cells that pass the test pooled across days is significant (12.5% (22/176 cell), $p < 7.7e-5$, one-sided binomial test, alpha = 0.05).

permutation test is not the ideal test for these data and a more principled approach would be beneficial. First, the permutation test does not explicitly take into account the shape of the firing rate envelope. The test looks for local changes within each alley, but each spatial bin is independent and there is no model created that relates the firing in each bin together into a single, cohesive representation of a field. Further, there are multiple sources of variability in the data that the permutation test cannot take into account, or result in a loss of power. The reward-status of a trial cannot be taken into account by the permutation test (at least as implemented here), and so rewarded trials are removed at a loss of statistical power. The cell may respond differentially to reward and there are cases of cells exhibiting strong temporal dynamics in their firing over time. The temporal dynamics are a significant source of variability which has affected this analysis to a great degree (as well as earlier analyses not

reported here). It is well-known now that CA1 neurons exhibit time dynamics beyond simple trial-to-trial variability (see General Introduction). A proportion of cells are seen in these data which turn on or off over the course of the session, resulting in periods of activity that last some significant fraction of the session but not the entire course. This adversely affects methods such as a permutation test that treat all trials identically. Lastly, although the general approach of randomization is a standard one, the specific implementation used here was an *ad hoc* approach used in a study with a very different design and experimental question (Fujisawa et al., 2008). A more appropriate statistical tool in this situation is a linear mixed effects model, an extension of linear regression that can account for these complications.

Linear Mixed Effects Models with Spline Interpolation

For the reasons discussed above, a linear mixed effects regression model was used with spline interpolation (LMER model). The model defined fixed effects of texture and position on firing rate within alley, as well as their interaction, and reward. Trial number was modeled as a random effect with random intercept to account for the temporal variability of cells described above. The curves of firing rate under each texture were fit to a natural spline with three degrees of freedom. Confidence intervals (Wald method) around the coefficient estimates determine what parameters had a significant effect on the shape of the curve. Confidence intervals around the fitted curves were also used to assess the significance of a given interaction.

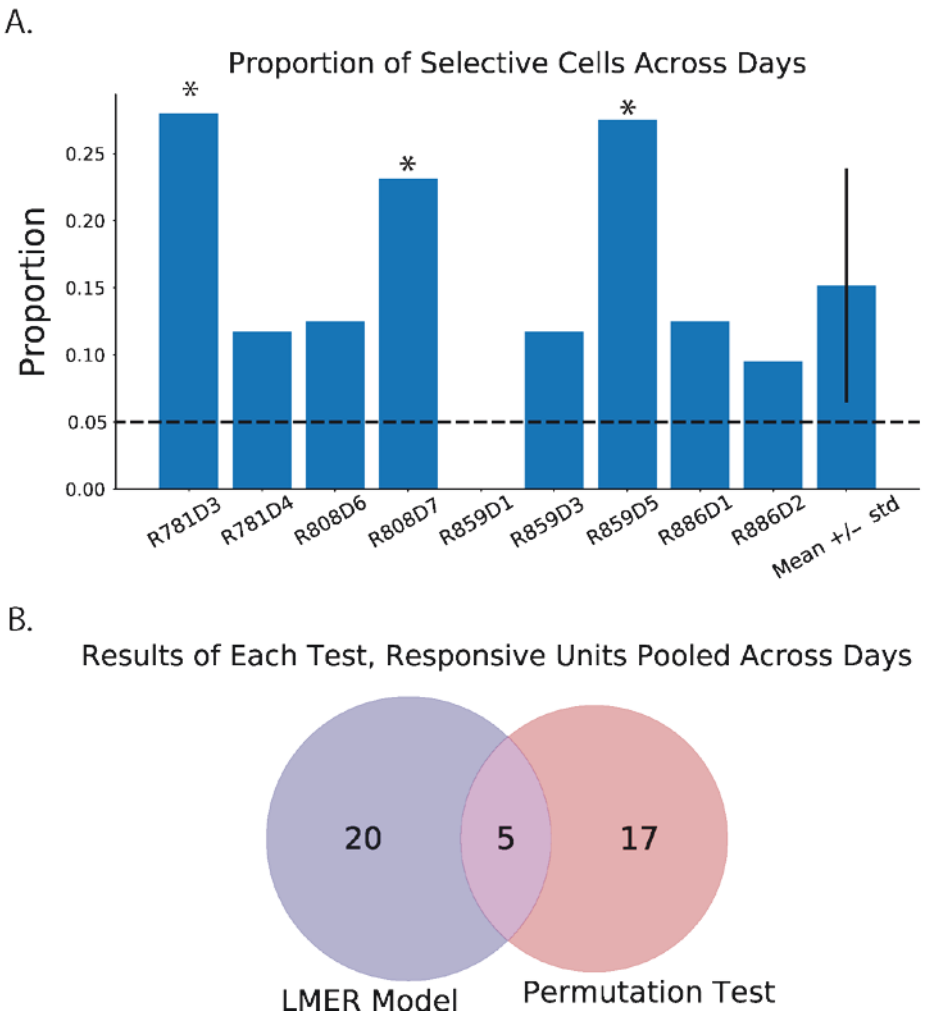

Fig 3.4 Results of LMER analysis across days. A. Nine recording days from four animals, each bar (save for the right-most) shows the proportion of cells on that day that had detectable texture information. Nine parameters, per cell and alley, are tested for significance: each stimulus interacting with each of three degrees of freedom of the spline fit. A cell is defined to contain significant texture information if at least one of the nine parameters at an alley is judged significant by the Wald test and the confidence intervals of the fitted curves for at least one pairwise texture comparison do not overlap. Significance stars indicate days that contain a significant number of texture-responsive cells by a binomial test (R781D3, 7/25 cells, p = 0.002; R808D7, 3/13, p = 0.024; R859D5, 8/29, $p=6*10^{-5}$, one-sided binomial test alpha = 0.05 in all cases). Note, most days have more texture-responsive cells than expected by chance (even if the abundance does not meet the significance threshold of a binomial test, 8/9 days). Dashed line corresponds to alpha = 0.05. Last bar is mean proportion of texture-responsive cells across days, with one standard deviation shown above and below mean. **B.** Venn diagram showing the number of single units that passed each, or both, of the tests used.

The linear mixed effects models were more sensitive than the permutation tests to the rate remapping phenomena, possibly for the reasons outlined above. Models were fit to all cells that passed the inclusion criteria and nine of the model parameters were tested for significance using a corrected Wald test: the three degrees of freedom of the natural spline crossed with the three stimuli. Confidence intervals around the coefficients and fitted curves were between the 99.4^{th} and 99.9^{th} percentile, depending on the number of active alleys for a cell. A cell was determined to have significant texture information at a given alley if it passed two criteria: (1) one of the nine coefficients passed a Wald test and (2) the pairwise comparison of the corresponding fitted curves had non-overlapping confidence intervals somewhere along the alley. Summary data across days is shown in Fig 3.4. The proportion of texture-responsive neurons according to Wald tests and fitted curve confidence intervals of the LMER model are shown for nine days of recording from four rats (Fig. 3.4A). Three of the nine days had a significant number of texture-responsive neurons, more than expected by chance (3/9 days, $p = 0.008$, one-sided binomial test, alpha = 0.05). Additionally, three of the four rats had one significant day of recording. Pooled across days and rats, roughly 15.2% of neurons were texture selective according to this analysis (15/172 cells, $p = 5.2*10^{-7}$ one-sided binomial test, alpha = 0.05). These data suggest that there are a significant number of texture-responsive neurons across days, as detected by a LMER model.

It is useful to compare the results of the LMER model to the permutation test. Fig 3.4B shows a comparison of pooled cells across days that pass one of the tests, or both. It can be seen that they are largely sensitive to different populations of neurons. This may not be unexpected given the different ways the tests analyze the data (see Discussion for details). This further justifies the approach of using complementary approaches in uncovering a signal.

Example units with detectable texture coding are shown in Fig 3.5. The left of each shows the raw data as described above; overall ratemap with alley under analysis indicated by box (top left), linearized trial rate maps (bottom), and trial-averaged rate maps with S.E.M (top right). The right shows the results of the LMER model, with fitted spline curves plotted by texture. Each example shows a field in which the rate and/or reliability of firing was changed depending on the stimulus present. In the first example, both the rate and the robustness of firing were modulated such that the firing was maximal when texture A was present compared to the other two (Fig 3.5A). The cell fired intermediately for C and very little in response to B. In the second example, the cell fired with a similar rate and reliability of firing when textures A or B were present and only on a few trials, with a reduced rate, when C was present (Fig 3.5B). In the third example, a place field is centered on a corner of the track such that it encroaches into one of the alleys.

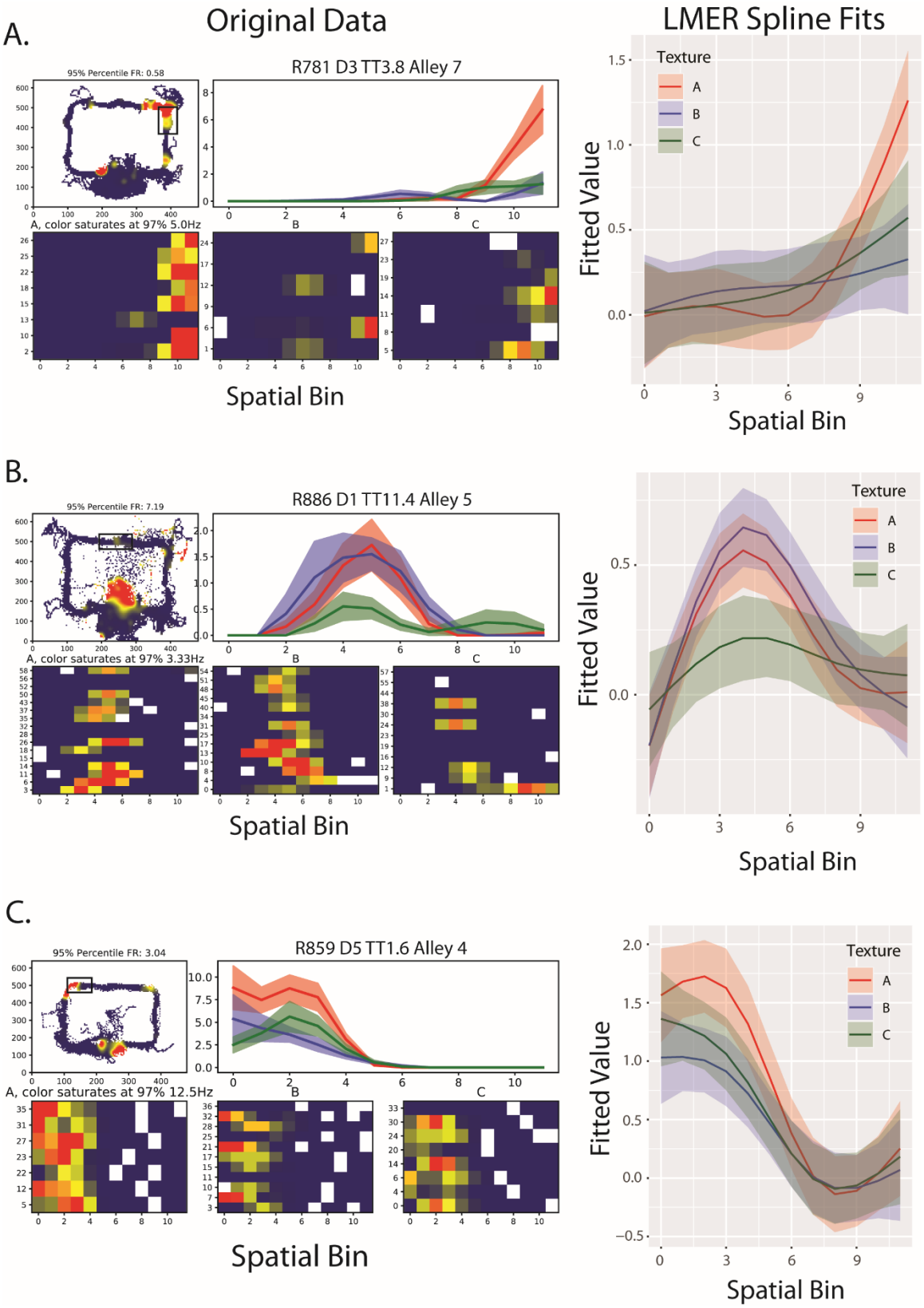
A.
Original Data
LMER Spline Fits
95% Percentile FR: 0.58
R781 D3 TT3.8 Alley 7
A, color saturates at 97% 5.0Hz
B
C
Spatial Bin
Texture
A
B
C
Fitted Value
Spatial Bin
B.
95% Percentile FR: 7.19
R886 D1 TT11.4 Alley 5
A, color saturates at 97% 3.33Hz
B
C
Spatial Bin
Texture
A
B
C
Fitted Value
Spatial Bin
C.
95% Percentile FR: 3.04
R859 D5 TT1.6 Alley 4
A, color saturates at 97% 12.5Hz
B
C
Spatial Bin
Texture
A
B
C
Fitted Value
Spatial Bin

Fig 3.5. Example LMER Data. Example units with detectable texture information based on a LMER analysis. **Left, each.** Session rate map (top left) with alley under consideration boxed, trial-by-trial linearized rate maps by texture (bottom) and trial-averaged linear rate maps +/- S.E.M. (top right) as described previously. **Right, each.** Fitted linear mixed effects model of the interaction between stimulus and spatial bin, with no reward (model includes same interaction with reward present, not shown here). Abscissa is spatial bin, as in left-hand plot. Ordinate is predicted rate value of the LMER spline model. Note, negative values exist because the model fit, given d.f. = 3, is constrained by cubic polynomial dynamics and can spuriously enter invalid ranges due to fitting the data faithfully elsewhere. **A.** Unit with field wrapping around corner in northeast corner of the track, which extends into alley. Linearized trial rate maps show consistent, and relatively high rate, firing occurs on northern end of alley when A was present. Texture C was associated with variable firing, while cell is significantly quieter when texture B was present. **B.** Cell with field in start box and Alley 5 (top center of track). Cell fires reliably and with relatively high rate when texture A and B were present. Conversely, cell was active on fewer trials with a lower rate when texture C was present. **C.** Neuron with primary field around corner of northwest corner of the track. Trial rate maps show higher and more reliable firing under texture A versus other two textures.

The cell fired more when texture A was present, with both an increased rate and higher reliability, compared to the firing under the other conditions (Fig 3.6C).

In the context of the models used in this study, the Wald test of the interactions assessed any differences in the shape of the firing rate curves elicited by the presence of the three textures. This is not the same as examining a change in rate, as the permutation test did. Two firing rate curves could have a similar magnitude but very different shapes; the Wald test may be sensitive to a difference in this situation whereas confidence intervals of the fitted curves may still overlap. As mentioned above, we have adopted a conservative method to assess statistical significance by requiring that a cell pass both the Wald test and a test of non-overlapping error bars. Whether it is permissible to rely on the Wald tests alone, while the confidence intervals of the fitted curves overlap, is the subject of further analysis and consultation. However, it is still useful to examine the results of the Wald tests alone. 63% of cells across days had at least one

significant coefficient of the interaction terms. Fig 3.6 shows the result of the Wald tests for one example day of recording. In Fig 3.6A, all unsigned Wald coefficients are divided into those that were non-overlapping with zero (colored red) and those that were overlapping zero (colored grey). In panels A and C the histograms of significant and non-significant Wald coefficients are displayed as a frequency density, which is frequency/class size. This normalizes each and makes them appear the same size. This was done for visualization purposes as relatively few Wald coefficients were significant and raw histograms were difficult to compare. Panel 3.6B shows the absolute difference in non/significant Wald coefficients for each of the comparisons tested. In this panel it is clear that most coefficients are not significant; however, most cells had at least one significant coefficient. These results are not inconsistent because each cell is tested nine times, contributing a data point for each test (again, with an alpha corrected for these comparisons). In Fig 3.6C, it can be seen that the unsigned Wald distributions are skewed, with the distribution of significant intervals more right-shifted than the non-significant coefficients (by definition). The Wald coefficient indicates the percent change in the dependent variable by the independent variable under consideration, compared to a reference variable. These panels show that there was between a 50% and 300% change in firing rate among the different interaction types. There are qualitative differences in the distributions of the significant coefficients between parameter types; however, this effect has not been statistically analyzed here. These data show the range of influences of

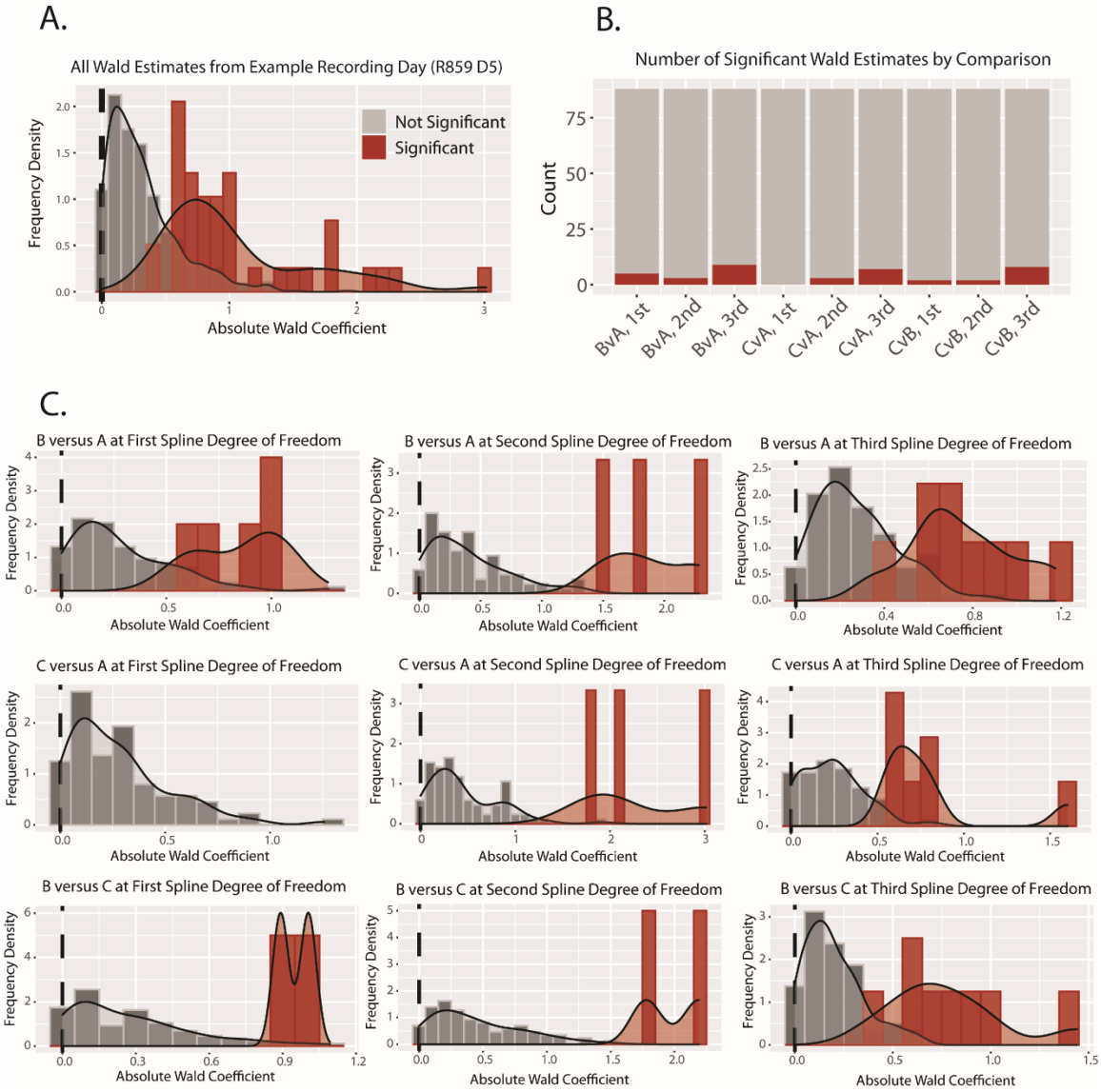

Fig 3.6 Distribution of Model Coefficients for an Example Recording Day. A. Histograms of model coefficients for each cell and each alley. Coefficients for the nine model parameters under analysis are included (three stimuli crossed with three spline degrees of freedom). Distribution of coefficients which do not pass a Wald test (i.e. fail to reject the null that coefficient is 0) shown in grey; those that do pass shown in red. Y-axis indicates the frequency density of the distribution, which is the frequency divided by bin width. Kernel density estimate for each histogram overlaid as a smoothed curve. The value of the coefficient is interpreted as the percent change in the dependent variable between the two conditions; e.g. a coefficient of 0.5 in a B v A parameter indicates a 50% increase in firing when B is present compared to A. **B.** Number of significant coefficients broken down by parameter type. Note a single cell may have multiple significant coefficients at a single alley. Each column corresponds to a model parameter; for instance, "BVA, 1st" refers to interaction of texture B versus A at the first degree of freedom of the spline. Total number of coefficients is the height of the bar with the grey component being the non-significant estimates and the red component being the significant estimates. **C.** Histograms, as in A, divided by each parameter type.

stimulus / spatial bin interactions on the shape of the firing rate curve and give a sense of the magnitude of the effect size.

The LMER models were able to detect changes in firing rate in cases of non-stationary firing across time. These cells were only active for a portion of the session and were difficult to analyze using methods that treated all trials equivalently (such as the permutation test). Fig 3.7 shows examples of detected rate remapping effects in temporally unstable neurons. In some cases, the cell was silent for parts of the session and only had a place field during a limited number of laps. In the first two examples the cell was virtually silent for portions of the session. In the first example, the neuron stopped firing roughly three-quarters of the way into the session (between trials 43-44). During the time it was active, it displayed a preference for texture A in terms of the rate of firing as well as the reliability of firing (Fig 3.7A). The cell fired when B or C were present for three or five trials, respectively, over the entire session. The cell fired for nine trials when A was present and these were typically higher rate than those of the other textures. In the second example, the cell is mostly silent for the first half of the session (Fig 3.7B). During the second half of the session, the cell was active, however there was an effect of stimulus on the firing rate in this period. Similarly to the first example, there was a difference in both the reliability of firing and the rate of firing when the field was present. The cell fired on more trials when B was present versus the others; additionally, the firing rate was higher on these trials versus those on which the cell fired for the other textures. This is shown in the fitted LMER spline curves at the eastern end of the alley. In the third example,

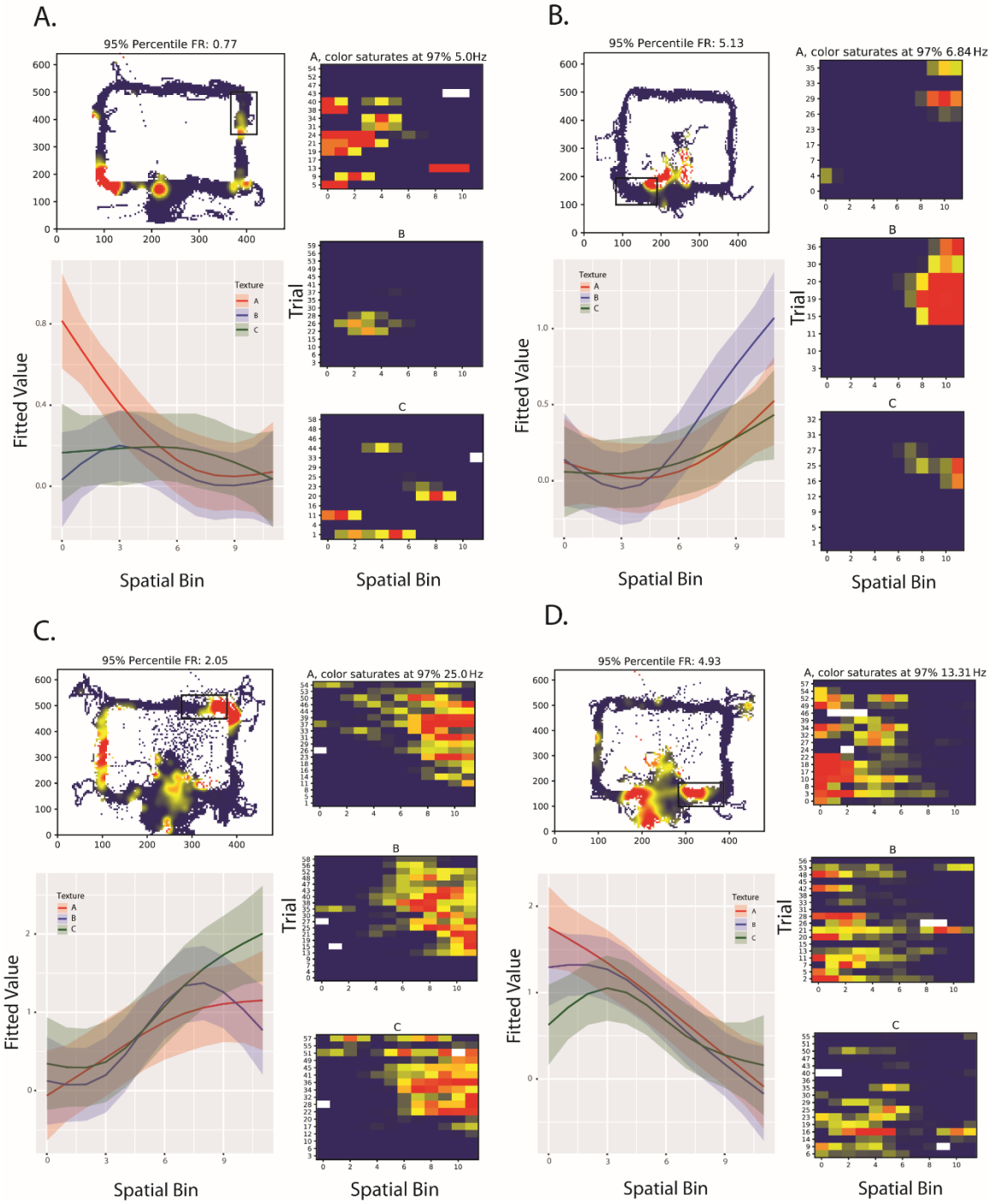
A.
95% Percentile FR: 0.77
A, color saturates at 97% 5.0Hz
B
C
Texture
A
B
C
Fitted Value
Trial
Spatial Bin
Spatial Bin
B.
95% Percentile FR: 5.13
A, color saturates at 97% 6.84 Hz
B
C
Texture
A
B
C
Fitted Value
Trial
Spatial Bin
Spatial Bin
C.
95% Percentile FR: 2.05
A, color saturates at 97% 25.0 Hz
B
C
Texture
A
B
C
Fitted Value
Trial
Spatial Bin
Spatial Bin
D.
95% Percentile FR: 4.93
A, color saturates at 97% 13.31 Hz
B
C
Texture
A
B
C
Fitted Value
Trial
Spatial Bin
Spatial Bin

Fig. 3.7. Examples of rate remapping in temporally unstable neurons. Top left, each. Overall session ratemap. Alley under analysis indicated by box. **Right.** Linearized trial rate maps. Rewards have been excluded. 97th percentile firing indicated on top. **Bottom left,** Fitted spline with Bonferroni-corrected confidence interval showing interaction between spatial bins within alley and firing rate under a given texture. **A.** Cell with firing field on the northeast section of the track. The cell was active until the last quarter of the session (trial 44), after which it was silent. During the period in which it was active, cell fired with a higher rate for texture A. **B.** Cell with firing field near the start box. Cell is active during approximately the second half of the session third of the session and is virtually silent before that point. Consistent firing is associated with texture B and much less so for the other stimuli. **C.** Cell with fields on the west arm and northeast corner of the track, with the latter under analysis here. Cell is active during most of the session, though is mostly silent towards the beginning. However, the field location shifts over time. When taking into account how the firing evolves over time, an increase in firing for texture C is detectable versus B at the east end of the alley. **D.** Cell with firing field in the last alley. Cell was active during the entire session, however at trial 35 it mostly shut off when texture C was present. The cell had fired when that stimulus was present before that point in time, and continued to fire for the other two textures; this is evidence of stimulus-dependent temporal dynamics.

the cell was silent for the first 10 trials and then became active (Fig 3.7C). While the cell was active, the cell fired with equal reliability for each of the three textures. However, over time the field shifted westward, beginning at about the second half of the session. After the field began to shift, the shift occurred more when texture A was present, compared to when the other textures were present. However, the LMER spline curve shows a significant interaction of texture B versus C at the east end of the alley; this can be corroborated by observing in the trial rate maps that the cell fires with a higher rate when texture C was present versus B. Finally, the last example shows a different pattern of temporal non-stationarity, namely one that is gated by stimulus (Fig. 3.7D). The cell fired throughout the session, with some trial-to-trial variability. However, the cell did not fire consistently when texture C was present; rather, the cell fired in response to that texture until about trial 35, after which it gradually shut off when that stimulus was present (with two exceptions). This raises the intriguing possibility

that the temporal epochs of firing CA1 neurons display could be stimulus gated in some cases (which would be consistent with other work showing time dynamics of CA1 linked to context or stimulus (Pastalkova et al., 2008; Taxidis et al., 2020).

Extended Results

There were two simplifying assumptions made in the LMER results presented above. First, the data were assumed to satisfy the assumptions of the model, and in particular the normality assumptions of linear models. Given that many bins in the trial rate maps had no spikes, the distribution was skewed and therefore did not satisfy normality assumptions. However, the LMER model was still thought to be appropriate based on consultations with Dr. Scott Zeger, Professor of Biostatistics at the Johns Hopkins University Bloomberg School of Public Health. Nonetheless, it was important to perform an analysis with a model that does not rely on such assumptions, such as the generalized version of linear models (GLMER models). The two main differences between the LMER and GLMER models are that 1) a distribution is specified which matches the empirical distribution and 2) a link function is specified which transforms samples from the data distribution to be appropriate for use in linear models. A GLMER model was used with a Gamma distribution as the data distribution and an inverse link function using the lme4 package in R, as cited above.

Second, all recorded units were analyzed in the LMER model described above, and units were only excluded if they did not have sufficient on-track activity. However, as discussed in Chapter 2 General Methods, units also differ in their isolation quality. To ensure that only high-quality units were included, only units with a score of 3 or higher (out of 5) were included here.

The results of the GLMER model analysis on high-quality units only are shown in Figure 3-E1. A pooled subpopulation of texture-selective CA1 neurons was identified (Fig 3-E1A; 13.8%, 13/94 neurons, $p = 0.0008$, one-sided binomial test, alpha = 0.05). The pattern across days was qualitatively similar to that of the LMER model results (Fig 3-E1B). Two days, instead of three days under the LMER model, had enough selective cells to pass a binomial test, although the decreased number of cells due to the quality filter may account for this.

Overall, the results under the GLMER model comported with those under the LMER model. A similar proportion of texture-selective cells was identified with a similar pattern across days and rats. These extended data suggest that violations of normality or cluster contamination do not account for the results reported in the main text.

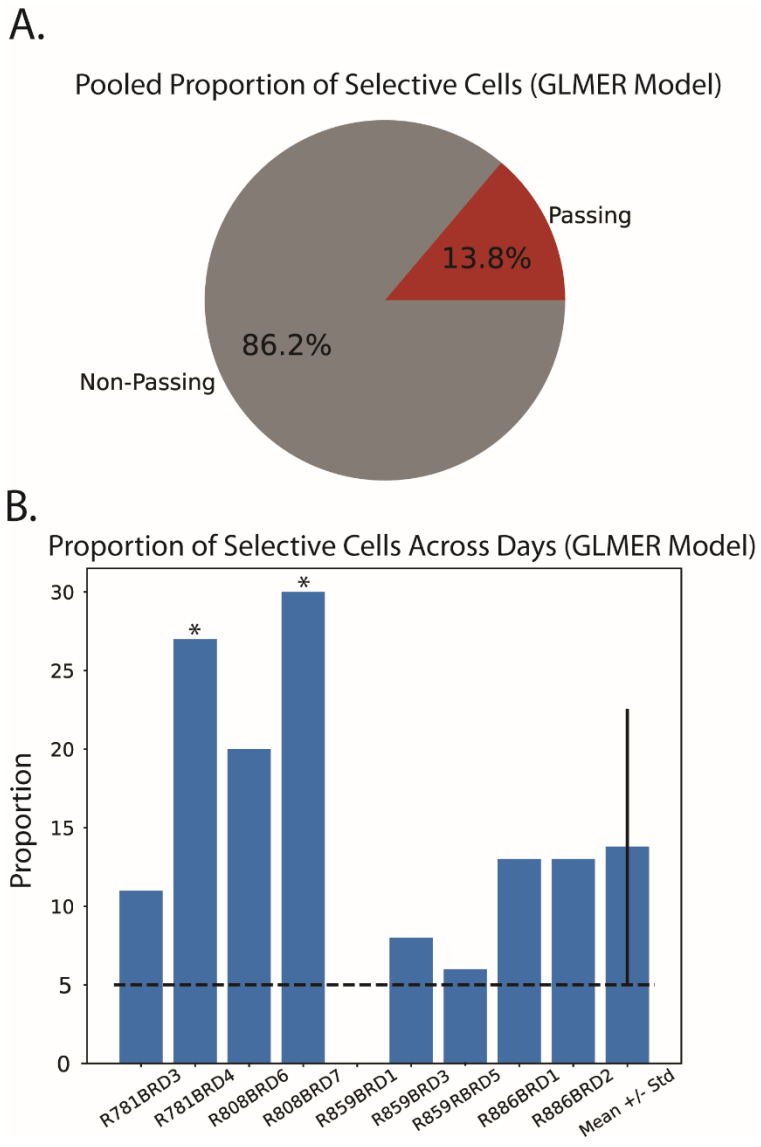

Fig 3-E1 GLMER Model Results with High-Quality Units. The data set used in the LMER model results was re-run using a generalized linear mixed effects (GLMER) model. Additionally, only units with a quality score of 3 or higher (out of 5) were included. A. Pooled cells across days and rats that were texture-selective according to the GLMER model (13.8%; 13/94 units; p = 0.0008; one-sided binomial test, alpha = 0.05). B. Pattern of GLMER results across days. 8/9 days had more selective neurons than the 5% chance level would predict. Two days had enough selective neurons to pass a binomial test within the day (R781BRD4, 3/11 units, p = 0.015; R808BRD7, 3/10 units, p = 0.011; one-sided binomial test, p = 0.05 in both cases).

Discussion

The data in this chapter support and expand the rate remapping hypothesis. Permutation tests and linear mixed-effects models (LMER models) revealed a subset of hippocampal CA1 neurons that modulated their firing rate fields in a stimulus-dependent manner. The stimuli were not associated with a reward or other contingency, which extends the rate remapping hypothesis into cases where there is no learning. Further, these analyses showed that rate modulations were localized within the firing rate envelope; this raises the possibility of a new form of fine-scale computation within a place field.

Limitations

Before discussing the implications of the data, it is important to discuss their limitations. First, there is the discrepancy between the permutation tests and the LMER models. The differences between the tests themselves will be discussed below, but it is potentially problematic that the sets of texture-responsive cells found by each test are so different. One might expect that two different tests would identify the same signal (for the most part), just using different means to do so. Here, it seems as if the tests are differentially sensitive to the way a rate remapping effect can manifest. At minimum, this suggests further work is needed to investigate the different ways neurons can encode the cue identity. More consequentially, this discrepancy could mean that neither test buttresses the results of the other, thus weakening the finding overall. While this is an important consideration, a possible resolution is to identify the features that each test is sensitive towards and show that in the cases where a given test did not identify a texture-selective neuron, the type of feature the test was looking for

was not present. In other words, if it is possible to explain why the tests did or did not find a signal where they did, the discrepancy between them may be less concerning.

LMER models versus permutation tests

The results of the permutation test and linear mixed effects models (LMER models) differ in several aspects. First, they reveal different populations of texture responsive neurons in terms of both size and cell identity (Fig 3.4B). Their mechanisms of action are also different, which may explain in part the difference in results. The LMER model identified a subset of CA1 neurons which was roughly twice as large as the population identified by the permutation test. This raises the question of whether the LMER model was more sensitive, or appropriate, in this analysis, or whether it was more prone to Type I errors.

There are reasons to believe the LMER models are a more appropriate analysis to use on these data. First, the LMER model created an explicit model of the firing rate, while the permutation test did not. The LMER model fit a spline to the data which related the spatial bins to one another. A spline is composed of multiple polynomials which are fit to different sections of the data, linked together at junctions called ‘knots’. Therefore, the estimate of firing rate at a particular spatial bin was not independent of the estimate at neighboring bins. By contrast, the permutation test statistic applied to each bin (pairwise trial-averaged rate difference) was done independently for each bin; it is only the global familywise error rate-corrected alpha that considers all bins together and this does not affect the test statistic, just the significance threshold. Firing rate envelopes under different stimuli could have a similar rate at a given bin but a much different local

curvature around that bin – the permutation test is insensitive to this. Therefore, a significant difference between the approaches is that the LMER test can examine the curvature of the firing field and assess both the difference in scale of firing as well as the shape of the curve, while the permutation test can only look at differences in magnitude at a single spatial bin at a time. Relatedly, the firing rates at adjacent bins are correlated with one another – a significant difference in firing rate at one bin increases the likelihood of there being a significant difference at the adjacent bins. The LMER model respects this given the smooth nature of the fitted spline curve. Again, however, the permutation test has no knowledge of significance of the test statistic at neighboring bins and cannot use that information as prior information when considering other bins.

Second, there are multiple potential sources of variability in the data beyond the effect of texture. Firing rate could be affected by variables such as reward or trial number. The latter, in particular, is an important source of variability given that many cells exhibited non-stationary firing rates over the session. Some cells were only active during a portion of the session while others were active over the duration of the session but greatly modulated their firing rate over time. This adversely affects the permutation test because trials with a putative texture signal are averaged with silent trials and, therefore, the overall signal is attenuated.

Another source of variability is the temporal non-stationarity in the firing. Cells may fire differently given the presence of reward, and therefore the firing envelope of a given texture could be distorted by conflating rewarded and non-

rewarded trials. The permutation test treats each trial identically, which makes it vulnerable to the temporal confound. Although rewarded trials were removed, which mitigates the second issue, it resulted in a smaller data set with lower power. By contrast, a major feature of the LMER model is that these types of variables can be taken into account as either random effects or fixed effects, depending on the nature of the variable.

These considerations support the notion that the LMER model was a more suitable method for these data. These data were complicated by the effects of multiple spatial bins, the reward, and time in a way that the LMER model was better suited to accommodate.

Rate remapping and place field modulations

The design of this experiment allows the rate remapping hypothesis to be directly tested in a way that has not been done previously. Only three experiments to date have examined the coding of multiple cues across an environment (Wood et al., 1999; Manns and Eichenbaum et al., 2009; Herzog et al., 2019) and only one (Herzog et al., 2019) examined how CA1 neurons responded to different cues across space at a fine scale. That study addressed how neurons respond over time (~2.5 s from stimulus onset) to a variety of tastants. This was an important result as it not only confirmed that neurons within the CA1 place map could independently encode cues across the environment, as the cognitive map theory would predict, but also that the fields respond on fine timescales to the non-spatial cues. A natural question to ask, given that CA1 serves as a place map, is how the neurons respond to cues on a fine spatial scale in addition to a temporal scale. By linearizing alleys, the fine-grained spatial

response properties could be studied. Although the two tests used in this study had significant differences, both were sensitive to local changes in firing rate on a scale finer than a typical place field.

These data support the hypothesis that place cells do not encode non-spatial cues via global changes to their place fields, but rather though localized rate fluctuations in the firing rate envelope. Shifts in the overall field magnitude were not observed; instead, cells displayed changes in firing rate at certain locations within the field. In some cases, this manifested as a consistent burst of activity at a specific location, but in others it was the shape of the firing rate envelope that changed under a given texture. In some cases, the rising or falling phase of the field was altered such that it occurred more or less slowly under a given texture. This not only results in a local change in the firing rate, but also a shift in the field location when a given texture was present. In other words, texture-induced changes to the place field not only affected the rate locally within the field, but in so doing also affected shape parameters such as skewness and center of mass. Taken to an extreme, this could challenge the rate remapping hypothesis in that the hypothesis asserts the place field location is unaffected by rate changes. However, the changes in skewness and center of mass observed here may not be severe enough to cause a meaningful change in the spatial receptive field.

There are a number of computational reasons why rate changes would be spatially restricted within the place field. Local changes within the firing field could be associated with salient locations in the environment. Place cells could

respond to a cue at a task-relevant location in the environment that happens to be positioned within the cell's place field. There are at least three salient locations in the apparatus: the alley entrance, the lickport, and the alley exit. Interestingly, multiple examples of rate remapping occurred at the beginning or end of the alley. This is consistent with encoding at salient locations, but it also could be due to some fields being cut off by the alley boundaries. However, if cells really do respond to non-spatial cues at salient locations in the environment, it could be a result of computational efficiency. Rather than tonically responding to a cue throughout the duration of the animal's encounter with it, the neuron might respond only at a location of cue change, such as at the alley entrance or exit. This could allow efficient coding of the non-spatial features of an environment by only encoding changes, or differences, in the cue configurations across trials. Rather than encode an explicit representation of the cues within an environment, a sparser map of changes in cue could be created, which can be interpolated later to restore the full map. For example, rather than encode the entire spatial extent of a given texture, the onset and end of the texture could be encoded (along with its identity) and the space between the two could be interpolated later to recapitulate its full extent.

Automatic recording of attended experience

An important feature of this experimental design was that there was no relationship between the stimuli and reward. Even with irrelevant stimuli, there was evidence of cue encoding within single CA1 neurons. This is significant as most studies that investigated rate remapping used some operant task structure, or cues that were inherently relevant (tastants), in order to increase the chances

of observing a stimulus response. However, there are important theoretical reasons to study what the CA1 place map does when the cues encountered are incidental to the ongoing behavior. Encoding episodic information absent a salience signal could be, as discussed in the introduction, an adaptive way to store information in a buffer that can be used later by other systems for various computational purposes.

There are (at least) two problems which an automatic, episodic buffer could help solve. First, there is the credit assignment problem (Minsky, 1961), which refers to the situation in which the adaptive value of an action or cue is not known at the time of its execution or encounter. The putative CA1 episodic buffer is a proposed solution to this. Information about the world is encoded into the buffer as it is experienced and the contents of the buffer are then processed offline, by various other systems, to establish causal links between action/cues and future outcomes. These associations can then be used to guide future behavior.

However, supporting reinforcement computations is not the only rationale for maintaining an episodic buffer. For one, humans are capable of remembering episodic information far more remote than what would be stored in a short term buffer. Furthermore, the utility of this information is sometimes questionable. What is the adaptive value of remembering the flavor of cake one had at an early birthday? One possible explanation is that the storage of large amounts of memory (episodic, declarative, procedural, etc.) serves as the raw material for flexible cognition. One of the most valuable and inimitable qualities of human

cognition is the ability to extrapolate, create new ideas, and otherwise think ‘creatively’. While the last word is vague enough to defy a strict operational definition, any plausible one would include the ability to take pieces (of ideas, concepts, etc.) and combine them into a new, and useful, whole. The ability to do this rests on having a reservoir of knowledge from which to draw, combine, and recombine facts and ideas in adaptive ways. The individual pieces of information in this reservoir may be of low importance, but it is the cumulative store of such knowledge that becomes valuable. Therefore, the automatic attending to experience (and any analogous process for other forms of memory) may be useful in filling long-term memory with a variety of information that can be used later to respond to novel circumstances.

Temporal dynamics and rate remapping

As discussed in the introduction, it has become clear in recent years that CA1 activity is often strongly modulated over time. In some cases this may be to explicitly encode time, while in others the role of temporal dynamics is less understood. Many cells were recorded which were only active during a period of the session. Other recorded cells remained active throughout the session, but displayed marked differences in their baseline firing across time. The LMER model was able to recover a rate remapping signal in some of these cases. This raises the question of whether these temporal epochs are related to rate remapping, and are beneficial in some way, or whether it is an unrelated phenomenon in which CA1 neurons participate in addition to rate remapping.

Any neural circuit that is involved in encoding information has to balance the need of having enough computational capacity to do the job properly against

the cost of spending precious computational resources to maintain this capacity. A decision has to be made (possibly on evolutionary timescales) about how to optimally allocate storage space. In the case of CA1, the amount of information that needs to be encoded varies across time and environments. Neurons with transient activity could form a flexible pool of 'dynamically recruited' neurons which participate, briefly, in an ensemble representing information before detaching and becoming involved in other computations. In other words, a core population of CA1 neurons would exhibit stable spatial tuning across time. However, a penumbral population would join the ensemble briefly, participate in encoding, and then leave to perform other computations. This high turnover could mean that at any given point in time there is a large number of neurons participating in the ensemble representing an environment, but each neuron outside the core set of place cells is only active for a short while. The difficulty in a downstream system in reading out such a dynamic signal (in terms of which inputs it is receiving having non-spatial information) could be solved through oscillatory coupling; the downstream 'listens' to signals occurring at certain phases of theta, for example, regardless of the identity of the upstream CA1 neuron.

What benefit might this confer? First, it may assist is maintaining a flexible ensemble size that can be adapted to the computational needs at the moment. If a neuron participates in an ensemble for an extended period of time it would, due to synaptic plasticity rules, become more strongly associated with that ensemble. Removing the neuron from that ensemble, so that it might participate in other

tasks, becomes more energetically expensive. This difficultly comes from the fact that neurons in an ensemble undergo physical changes, such as additional AMPA receptors inserted into the surface membrane, that more strongly couple the neurons. For a system with a predictable computational load this may not be a problem. For a system like CA1, with a changing computational load across environments and time, this is disadvantageous; sometimes more or fewer neurons are needed, and constantly altering strongly wired ensembles becomes prohibitively expensive. However, neurons which only fleetingly participate in the ensemble would provide the additional computational capacity, when needed, but not stay involved so long that they become too strongly wired into an ensemble. Therefore, temporal dynamics may be a mechanism of supporting flexibility in ensemble size and dynamically allocating computational resources.

Chapter 4 Place Field Repetition and the Ratterdam Open Task

Introduction

Place field Repetition, Path Equivalence, and Geometric Similarity

It is well established that if CA1 neurons are recorded from a rat navigating a maze in which a high degree of symmetry or repeating structural motifs are present, a substantial proportion of place cells may exhibit multiple fields at occurrences of one of these repeating features (Spiers et al., 2015; Grieves et al., 2016a; Singer et al., 2010). Qualitatively similar patterns of data have been observed from rats navigating a series of identical rooms along a corridor (Spiers et al., 2015; Grieves et al., 2016a), a spiral maze ((3D) Hayman et al., 2011; (2D) Cowen and Nitz, 2014), an M-shaped or comb-shaped maze (Frank et al., 2000; Singer et al., 2010), and a hairpin maze (Derdikman et al., 2009) (although these latter data were recorded from grid cells in layer II of medial entorhinal cortex, not place cells).

Despite the phenomenology often being visually striking, it remains unclear what environmental features are treated as the hippocampal system (or other regions in which repetition has been observed). Some studies have attributed the repeating fields to geometric similarities between each location (e.g. Spiers et al., 2015; Grieves et al., 2016a). This suggestion is supported, first, by observing that fields seem to be arranged in the same relative locations with respect to boundaries. For example, in the present work there are examples

of cells with fields in multiple vertical or horizontal alleys. These alleys share common geometric features in an allocentric space; for instance, the vertical alleys all have walls on the East and West side of the rat. Second, previous work has observed spatial signals within the hippocampal network related to quantities such as the distance and bearing to a border or the vector relationship between the animal and a salient object (O'Keefe and Burgess 2006; Deshmukh and Knierim, 2016; Høydal et al., 2019). The presence of these signals demonstrates that the types of inputs necessary for a geometrically-tuned repeating place cell are present within the hippocampal formation. However, observing these signals is indirect evidence in favor of the geometric similarity hypothesis; it is possible that despite the existence of these signals, they are not inputs to repeating place cells and, rather, synapse onto other hippocampal neurons.

Other studies have suggested that repeating place cells are driven based on inputs related to the route an animal takes through the field. Data collected as rats shuttled between arms of an M-maze (Frank et al., 2000), and expanded upon with a larger comb maze (Singer et al., 2010), show repeating fields that occur as an animal runs through locations with certain, repeated geometric features, but only from a given direction. For example, fields may occur at each junction between the arm and the main corridor. However, these fields are only present when the animal runs through them in an east-to-west direction. This led the authors to conclude that the 'path equivalence' between the trajectories was the real variable that drove the repeating fields. Under this hypothesis, it is the fact the rat is making a particular trajectory, e.g. an eastbound right turn, that

drives the cell to fire, rather than the similar configuration of the environment at each location. However, the wall configuration in these experiments is correlated with the types of trajectories that an animal can make at a given location; indeed, in the Frank et al. study they are perfectly correlated. Therefore, these data do not provide compelling evidence to distinguish the two phenomena and it is in fact not clear that the hippocampus even makes such a distinction – it is possible the trajectory and the environmental geometry around it are integrated into a 'geometric-behavioral context'.

Place field repetition and head direction

Head direction has been proposed to be a crucial variable which affects the expression of place field repetition. In the experimental designs in which place field repetition has been observed, the animal is facing the same direction in each of the regions containing a repeating place field. If repeating fields are driven by inputs that are similar at different locations in the environment – whether those signals are geometrical or behavioral in nature – then the lack of a disambiguating head direction signal may be sufficient to produce multiple, repeating firing fields. Conversely, in environments in which the similar locations are not facing the same direction place field repetition would be less common or abolished.

Grieves and co-authors performed such a study by recording from two apparatuses in which rats were trained to perform a spatial memory task, one with rooms in a linear arrangement along a corridor and another with identical rooms oriented at 60° from one another along a curved corridor. (Grieves et al., 2016a). Rats took longer to reach performance criterion in a spatial learning task

in the linear corridor maze compared to the radial corridor design, providing indirect evidence that the environmental geometry made the compartments in the former harder to distinguish. Single units recorded in the linear corridor environment displayed place field repetition as had been observed previously. However, few units in the radial compartment design exhibited repetition. Among those that did, the fields tended to be in two of the four boxes, whereas repeating cells in the original design usually had fields in all four boxes. Crucially, the multiple fields in the radial compartments were not in the same relative position in the different boxes. It is worth noting that cells with multiple fields in different compartments but in different relative locations have been reported before and were interpreted as a form of remapping (Anderson and Jeffery, 2003) and not place field repetition. Those authors concluded that the different heading of the rat into each radial compartment allowed the system to disambiguate the rooms and this led to both quicker learning and less, if any, repetition.

A more direct study lesioned a region in the head direction system (although it should be noted head direction cells are present in a variety of regions) and reported reduced place field repetition (Harland et al., 2017). Rats were recorded in the radial compartment maze and those with the lesion had reinstated place field repetition. Thus, differential head direction signals seem sufficient to block the expression of place field repetition. The authors of these studies conclude that repetition is a pathological case experienced in contrived environments, however this is not necessarily the case (see Discussion).

Splitting, Prospective and Retrospective Coding

Another body of work has studied cells that modulate their firing rate as a function of task variables such as trial type (Wood et al., 2000). These 'splitter' cells fire differently, but in the same location, based on attributes of the trajectory through the field, such as future turn direction. Thus, these cells are said to split the representation of the environments into separate representations of the kinds of behaviors possible within it. The original paper to define the phenomenology utilized a sequential alternation task and so the trial type was synonymous with the type of trajectory that the rat performed.

Further investigation revealed that some cells distinguished between the types of upcoming trajectories the rat was about to make while others preferred certain types of trajectories the rat had just completed, which was termed prospective and retrospective coding, respectively (Ferbinteanu and Shapiro, 2003). Some splitter cells also segment behaviors in tasks with multiple, sequential decisions to make within the same trial (Ainge et al., 2007). Thus, in tasks where the animal can take different paths through the apparatus, splitter cells seem to indicate, via their firing rate, salient differences in the types of trajectories executed by the animal. This is a form of remapping characterized by rate modulations in a spatially stable field, based on changes that occur outside of this field. Splitting, then, is related but possibly distinct from the rate remapping discussed in Chapter 3, as that remapping is thought to include changes that occur within the field, such as cue manipulation. This is relevant to the discussion of place field repetition because, although splitter cells have a single field canonically, both they and repeating place fields are thought, at least by some

(Frank et al., 2000; Singer et al., 2010), to reflect types of turns and motions through the field(s).

Time cells and other neural representations of time

It is well known that the hippocampus is involved in the representation of time or the use of temporal intervals to guide decisions (see Introduction). CA1 neurons have been shown to encode time, or at least display temporally modulated dynamics, across a range of time scales. Neurons can encode a specific period of multiple seconds within a window of tens of seconds (Pastalkova et al., 2008; MacDonald et al., 2011) and population dynamics can reflect temporal changes on the order of hours to many days (Manns and Eichenbaum, 2007; Cai et al., 2016; Ziv et al., 2003). Cells encoding time on the order of a second do so in a manner that tiles the entire interval, in a manner qualitatively similar to place fields on a one-dimensional track. For longer durations, the set of which neurons are active can drift such that knowledge of which neurons are generally active or inactive can be used to decode time on a coarse timescale of hours or days.

Temporal dynamics have also been reported in other regions of the hippocampal formation. Tsao and colleagues reported the existence of cells within the lateral entorhinal cortex (LEC) whose activity could be used to decode the passage of time (Tsao et al., 2018). Rats completed multiple sessions of random foraging during a single day of recording; activity of LEC neurons could be used to decode which epoch of foraging the activity was taken from. These data are consistent with the hypothesis that the hippocampal formation is involved in encoding episodic memory because time has been proposed to be

one aspect of part of a tripartite conception of episodic memory (Tulving, 1984). Time, place, and content ("when", "where", "what") are the components comprising a memory about one's experience. Further, damage to the hippocampus is associated with an impaired ability to use temporal intervals or sequences in task behavior (See Introduction). Multiple animals – rodents, humans, and non-human primates – have demonstrated deficits in temporal reasoning after damage to the hippocampal formation.

Experimental Questions

Previous experimental designs limited the types of trajectories that the rat could perform. For instance, all the arms on the M-maze (Frank et al., 2000) and the boxes in the corridor design (e.g. Spiers et al., 2015) were collinear and were only accessible from one direction. Therefore, different combinations of directions, turns, headings, and boundaries could not be distinguished from one another. To properly investigate the roles of these variables, and their interactions, in place field repetition a task design is needed that allowed for a more comprehensive set of trajectories.

The design of Ratterdam offers an opportunity to disambiguate the role of these environmental and behavioral variables on place field repetition. The city-block structure of the arena allows the rat to make any right-angled turn while facing in any cardinal direction. Thus, all permutations of turns and headings may be compared against one another to more precisely identify any preferred movement variable. Further, because the arena comprises a series of linear passageways, the animal's behavior is more constrained than on an open track which could reduce the effect of other behavioral correlates to activity.

Additionally, the entire track comprises repeating features (alleys and intersections), which means the animal's path through self-similar regions is uninterrupted. In other designs, this was not the case. This is important to note as breaks in a trajectory can serve as boundaries within the hippocampus and a temporal signal could be affected by this, e.g. by resetting the rate of a subfield to a mean value rather than allowing the mean to drift and eventually shift as it can in Ratterdam.

The second goal was to explore the intriguing temporal dynamics observed in pilot data – many repeating cells had fields which modulated their firing rates over time, both in an absolute sense and relative to one another. It should be stressed that the analysis of these temporal changes is preliminary. Self-guided motion, without the interruptions that an operant task usually imposes and with the ability to control for movement variables such as direction, allows for exploratory analysis into the origin and utility of these temporal dynamics. The results provided here argue against the hypothesis that these dynamics are not simply due to chance variation when observing so many concurrently recorded signals. Rather, the preliminary data support the hypothesis that the temporal interactions of these fields generate a decodable signal of time. Present and future work will explore the role of this signal in hippocampal dynamics.

Methods

Task design

The task for Aim 2 consists of one hour of random foraging on the Ratterdam apparatus with all alleys available for traversal. There are no textured floorplates

present, although a black curtain on the western wall of the recording room serves as a polarizing cue. Liquid reward is available pseudo-randomly from alleys as the rat traverses the arena. Two alleys are rewarded at any one time; once the rat visits a rewarded alley and receives the reward, a new alley is selected that is at least two alleys removed from the current one. Rats are not disoriented before the recording session and are placed in the arena at the northwest corner at the beginning of the session.

Place field detection algorithm

A custom place field detection algorithm was designed by a rotation student and expanded by the author. First, two-dimensional rate maps are created with a bin size of 2.1 cm (10 pixels) and a Gaussian smoothing kernel of 1.5 pixels. Local firing rate maxima are found with a minimum distance of 40 pixels between them. These are the seeds of potential place field peaks and the borders around each are expanded until the firing rate dips below 20% of the peak rate for each bin of the expanding border. These regions are then passed through two thresholding steps. First, the area must be at least 1% of the walkable track area. Second, the peak firing rate found earlier must be at least 1 Hz. Any region that passes these inclusion criteria is a place field, although it may be split into smaller fields in the next step and removed in another pre-processing step (see Data Filtering and Pre-processing, below).

Each field is then iteratively split into smaller fields using a watershed algorithm and recombined back into a single field if the split does not produce two acceptable, albeit smaller, fields. The scikit-image package was used with the segementation.watershed function (scikit-image version 0.17.2 https://scikit-

image.org/docs/dev/api/skimage.segmentation.html#skimage.segmentation.watershed). This splitting process begins by identifying all local maxima within the field. For each pair of in-field local maxima, the watershed algorithm expands the regions around each peak until they collide. This results in two potential place fields and the boundary between them. The mechanism works by a geological analogy to water filling basins that are divided by a ridgeline, hence the name. Here the 'water level' is a firing rate threshold which is steadily increased around each peak and considers all bins that fall under the 'water level' as belonging to that peak. The threshold stops increasing when it reaches the expansion zone of another peak – as if two water basins were filled until they meet at a ridgeline. These smaller fields are considered to be real if they not only pass the size and activity thresholds described before but if the firing rate of the boundary between them (the height of the ridgeline, in the analogy) is not more than 75% of the firing rate of the larger peak. In other words, if the basin between two fields is steep enough then they are considered to be independent fields, otherwise they are recombined into the original field. When the iteration process has exhausted all possible subfields the algorithm concludes (see Data Filtering for another processing step for false positive fields).

Place Field Repetition Detection

To assess which CA1 place cells had repeating place fields, the output from place field detection program was tested for the presence of place field repetition. For each neuron, each detected field was assigned to three possible types of locations: a vertical alley, a horizontal alley, or an intersection. Assignment was determined based on overlap between the area of the field and

the area of the track region; if the field overlapped with at least 75% of the area of the track region, then the field was said to be present in that region (among possibly other regions as well). If the field overlapped with multiple locations, for instance extending from an alley into an intersection, then each overlap location was tested to see if the section of field in that location contained at least 25% of the field's overall firing rate. This was computed by summing all the firing rate values in the bins of the rate map in the region and dividing by the summed rate for the whole field. The field was labeled as being present in any and all locations that passed this measure. Finally, any cell with labels from two or more common types of locations, e.g. two horizontal alleys, was said to be a repeating unit. Note that this definition is based on pattern matching and does not take into account any pattern violations. For instance, a cell may have two fields in horizontal alleys and one in an intersection and still be judged to be a repeating cell. The justification for this relative permissiveness is that many units have a complicated pattern of repetition. It is unclear, from both these data and previous literature, what degree of spatial periodicity should be classified as repetition. Examples of clear repetition in addition to other fields may still be functionally part of the same phenomenology. Further, considering the possible influence of other variables besides geometry, it could be expected to see fields that break a geometric repeating pattern because they are instead obeying, say, an egocentric prospective coding pattern.

Data Filtering and Pre-processing

The rate maps described in the place field detection section were created with data that were filtered by running speed with a threshold of 3 cm/s. To be

included in the data set, the firing rate distribution of two-dimensional rate map bins must have a 95th percentile of ≥ 1 Hz. The place field detection algorithm sometimes provided false positives that were removed with a post-processing step. Specifically, due to the 'greedy' nature of the algorithm, the last fields to be processed were often large, amorphous regions on the track that, while satisfying the recursive definition of fields used in the algorithm, were clearly not real place fields. To remedy this, fields were discarded if bins ≤ 0.2 Hz made up more than 10% of the total number of bins. To examine the role of directionality on occupancy or firing, the point-to-point vector between subsequent (speed-filtered) occupancy points was computed and defined as facing either North, South, East, or West in an allocentric frame. A 90° cone centered on each cardinal direction ensured each point was classified as facing in a certain orientation. These points were then separated into four categories and the rate/occupancy maps constructed as usual.

Qualitative Analysis of Place Field Dynamics

To visualize repeating place field dynamics over time, the overall firing rate of a visit was plotted as a function of visit number. The overall firing rate is the number of spikes emitted divided by the duration of the visit. The visits are defined as periods of occupancy within a place field that are more than 1s long and separated by at least 3s. The vector of firing rates across visits was Gaussian smoothed with a kernel of +/- 1 visits.

Inter-field Rate Difference Plots (IFD plots)

It was observed that the repeating field dynamics within a cell seemed to bear a relation to one another. For example, two fields may periodically modulate

their firing in anti-phase, or a field may turn off as another turns on. Other fields exhibited strong temporal dynamics in complicated relationships to other fields. To further explore this, the pattern of rate changes between fields was analyzed over time. First the firing rate vectors from above were adjusted to be time-varying instead of visit-varying and broken into 5 minute sliding windows with a 1 minute offset. Within each window, the average firing rate of each subfield was found by averaging all of the visits within that window. To ensure that the data from different fields were evenly sampled, and to account for the case in which there were no visits in a particular window, a spline interpolation was used. A 1-D PCHIP (Piecewise Cubic Hermite Interpolating Polynomial) monotonic spline fit was used from the scipy.interpolate.PchipInterpolator function in python (Scipy version 1.4.1; https://docs.scipy.org/doc/scipy/reference/generated/scipy.interpolate.PchipInterpolator.html). This type of spline mitigates the over/undershooting of spline fits that can often be seen. Next, the absolute difference between each pair of in-window subfield firing rate averages was computed and the entries stored in a (symmetric) matrix. Thus, a single sliding time window is associated with a single matrix with entries corresponding to the pairwise absolute average firing rate differences in that window. These matrices, in practice, often take on a ‘checkerboard’ or ‘flag’ style pattern. Visually, it often seemed that the inter-field rate patterns remained stable over time before switching, often abruptly, to a new pattern. To quantify this, an autocorrelation of each IFD matrix against all others was performed. Stable patterns of inter-field rate differences appear as blocks

along the diagonal, while transitions between patterns appeared as ‘pinch-points’ between blocks along the diagonal.

k-Nearest Neighbor Decoding Algorithm and Shuffling Methods

A k-Nearest Neighbors (k-NN) cluster-based decoding algorithm was used to decode time from each neuron’s inter-field firing rate patterns. The function used was from the sci-kit learn function sklearn.neighbors.KNeighborsClassifier (sci-kit learn version 0.23.1). The session was divided into temporal epochs, typically (see Discussion). The inputs to the classifier are vectors of inter-field firing rate difference within a sliding window. Each vector is labeled with its ordinal position in the session and what epoch it is within. The input data are separated with, typically, 70% of data used as training data and the remaining used as a test.

The k-NN algorithm computes the Euclidian distance between a test vector and all training vectors. The training vector with the minimum Euclidian distance to the test vector is the nearest neighbor to the test vector. If the actual epoch label of the nearest neighbor matches the test vector then the comparison is a match, otherwise it is a non-match. Performance is computed as the proportion of matches versus the number of test samples used. Because the algorithm functions by making distance comparisons, rather than explicitly defining a model, the terms ‘test’ and ‘train’ are technically misnomers as there is no model to train but are used here, and in the general literature, as they serve an analogous purpose.

To determine whether the decoding performance was significantly greater than chance, the train/test process described above was repeated multiple times on the real data and the average computed. This repeated decoding was to

account for the variability caused by choosing different samples to be in the training and testing set. The mean of these values was the real decoding performance. To compute the null distribution, the input labels (corresponding to the order of the IFD vectors in the session) were shuffled, then the k-NN decoder was run the same number of times as for the real data and the mean returned as a single point in the null distribution. Thus, the real decoder performance could be appropriately compared to the null distribution as they were computed in identical ways, save for the shuffling manipulation. If the observed data passed a one-tail test against a 95th percentile of the null then that cell was determined to have some form of temporal information. Further, the number of cells passing this test was tested with a binomial test, described below, to determine if the number of cells with significant temporal information was higher than expected by chance.

Results

Dataset Sizes

Data were recorded from CA1 of the right hemisphere of five rats as they randomly foraged throughout Ratterdam. Four of these rats performed the task with no floor stimuli after completing several days of the Beltway task while the fifth rat (the first to be recorded) foraged with changing floor stimuli and completed no other tasks. Table 4.3.1 tabulates the datasets recorded. It should be noted again that place field repetition takes 1-3 days to emerge and therefore the number of days exhibiting the phenomenology will differ between rats.

Table 4.1 Data Sets for Ratterdam Open Paradigm

Rat (Sex)	No. Recording Days	Avg. Yield/Day (Total)
765 (M)	20	12.45 (259)
781 (M)	4	23.6 (71)
808 (F)	7	11 (63)
859 (F)	3	47.3 (142)
886 (M)	3	10.7 (24)

Table 4.1 Data set sample sizes. Left, rat numbers and sex in parentheses. . Middle, number of recording days on the Ratterdam Open paradigm (note R765 was recorded on a modified version of the task in which the textured floorplates from the Beltway task were present and randomly interchanged among alleys across the course of the session). . Right, average number of cells per day, with total number of cells in parentheses.

Qualitative Analysis of Place Field Repetition

A city-block maze was used to study place field repetition. A top-down view of the track in Fig 4.1A shows the city-block arrangement of the alleys through which the rat navigates. Rats ran throughout the track for roughly one hour a day to find liquid reward dispensed into the lickports upon IR beam break, according to a pseudo-random reward schedule (Fig. 4.1B).

Next, place fields were detected within included units and the units were classified as repeating or not. The place field detection algorithm assigned each field to a region (vertical alley, horizontal alley, or intersection) based on overlap

with that region. A field could be assigned to more than one region if it overlapped significantly with multiple regions. A neuron was classified as repeating if two or more fields shared a common type of location. A neuron was classified as ‘complex’ if it displayed a repeating pattern of fields that each extended into multiple regions and classified as ‘multiple repeating’ if it had repetition in more than one type of location. An example neuron with repeating place fields is shown in Fig 4.1C. Five detected fields are shown with their boundaries overlaid. Each field is situated in a vertically oriented alley, thus constituting a repeating pattern defined by geometry, behavioral similarity, or some other variable. Note the field outlined in black (southwest, second from left) extends north and curls around the block into the intersection. If these cells are in fact modulated by the types of trajectories the animal makes, it is reasonable that some may fire along the trajectory which would yield the ‘crescent’ shape shown if the turn is, in this case, a left hand turn. Separately, on the east side of the track are two firing fields which did not meet criteria to be deemed place

A.

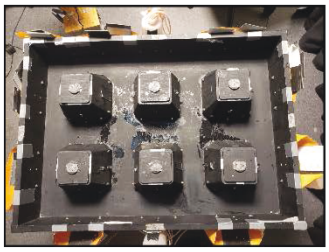

B.

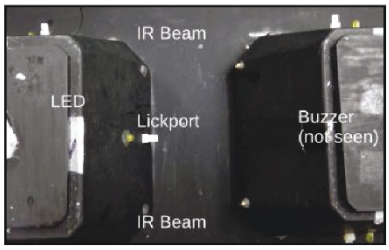
IR Beam
LED
Lickport
Buzzer
(not seen)
IR Beam

C.

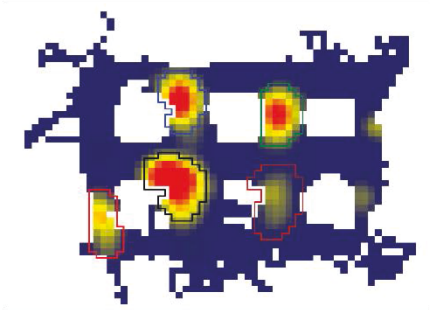

D.

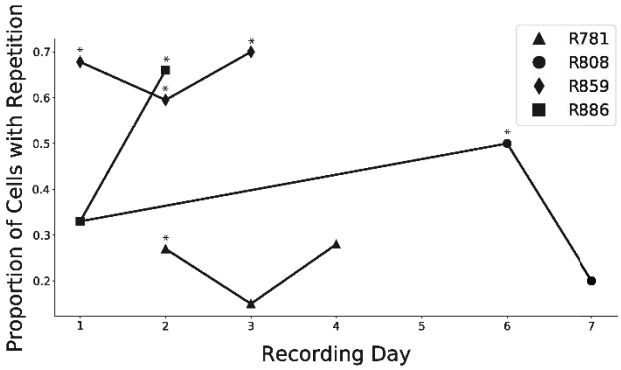
Proportion of Cells with Repetition
0.7
0.6
0.5
0.4
0.3
0.2
1
2
3
4
5
6
7
Recording Day
R781
R808
R859
R886

Fig 4.1 Overview of Ratterdam and Repetition. **A.** Top-down view of the Ratterdam apparatus in the 'open' configuration. All 17 alleys are available for traversal. The track measures 0.60 m x 0.91 m on its outer perimeter. Each alley is 14.6 cm long and 8.3 cm wide. Six large blocks, in a 2-by-3 array, define the city-block geometry, along with the outer walls. Each block is 18.4 cm on a side and 15.24 cm tall. The walls are angled backwards to mitigate camera occlusions and the tether getting caught on a corner. The edges of the blocks are chamfered (by an amount that resolves the discrepancy between the alley length and the block side length) to allow the rat more space in the intersection to make a turn. Liquid reward reservoirs are on one side of the long axis of the alley. Not shown, there is a black curtain to the West side of the track that serves as a polarizing cue. Computer and recording equipment is to the North of the image. The door is on the South left corner of the image. The recording room is 116.24 ft^2. The Ratterdam Open task consists of a single one hour session of random foraging throughout the apparatus. At any point in time, two alleys are rewarded such that when the animal breaks either IR beam a reward will be dispensed (1:1 Ensure, water, ~50 µL). Once a reward is received, a new alley is selected pseudo-randomly so as to be separated from the current alley but at least one alley. **B.** A close-up of an alley, annotated with the key features present. Each alley has an IR emitter/detector pair at each end of the alley. Upon beam break, the task control program will decide whether a reward will be delivered. In the center of the alley is a lickport with a visible light LED above. This light, along with a buzzer below the track, serves as feedback cues. A peristaltic pump is associated with each alley for the delivery of liquid reward to the lickport. **C.** An example CA1 place cell exhibiting place field repetition. Each detected field is outlined in a separate color. The fields all are within vertically-oriented alleys (including two weaker areas of firing to the right that were not defined as fields). The fields have different peak rates, consistent with preliminary data in (Spiers et al., 2015). Note that some of the fields, most prominently the black-outlined field, extend outside of the alley and curl around the corner of a block, consistent with a cell that fires as a function of a turn-related variable. The 95% percentile of firing is 4.6 Hz and defines the color saturation. **D.** Left, Amount of repetition across 11 days in four rats. Only repetition in alleys, intersections, or alleys extending into intersections were considered. The average degree of repetition seems to be rat specific; however, in all but one day the proportion of repeating cells is at least 20% of the total. Days were tested for proportion of cells with repetition. 6/11 days had a significant number of repeating cells (alpha = 0.05), a frequency which itself was significant (6/11, $p = 5.8*10^{-6}$, alpha =0.05, one-sided binomial test).

fields yet still obey the repeating pattern. Place field repetition was observed in all five rats (noting that Rat 765 completed a slight variant of the Ratterdam task). In each animal the abundance of repetition was significant (Fig 4.1D).

The experimental design defines three types of locations within Ratterdam in which place field repetition may be observed: vertical alleys, horizontal alleys, and intersections. This is an artificial, though reasonable, compartmentalization of the arena and it is possible the hippocampus is sensitive to other ways of dividing the track geometry. It should be noted that because the definition of repetition used here does not take into account repetition pattern violations, a cell is increasingly likely to be defined as repeating as its number of fields increases. Repetition was observed in all three types of locations. As mentioned above, fields could be assigned to multiple locations which increased the types of repetition observable

Varieties of Subfield Temporal Dynamics

An analysis of individual repeating subfields as a function of time revealed interesting temporal patterns of rate fluctuations. It has become increasingly clear that CA1 neurons are not always stable over time, but are often dynamic even in the absence of any obvious change in the environment (see Discussion). The temporal dynamics in repeating cells have not previously been reported. Repeating subfields exhibited a variety of temporal changes: some fields turned on or off, some ramped up or down over many minutes, some displayed mean shifts in firing (defined as an abrupt shift in the baseline activity of the field), while still others exhibited periodic behavior in their firing rate. The specific type of

behavior a field can display at a given time is termed the ‘rate regime’ of that field. Fig 4.2 shows four example repeating place cells, with the overall session rate map on the left and the time course of the field visit firing rates on

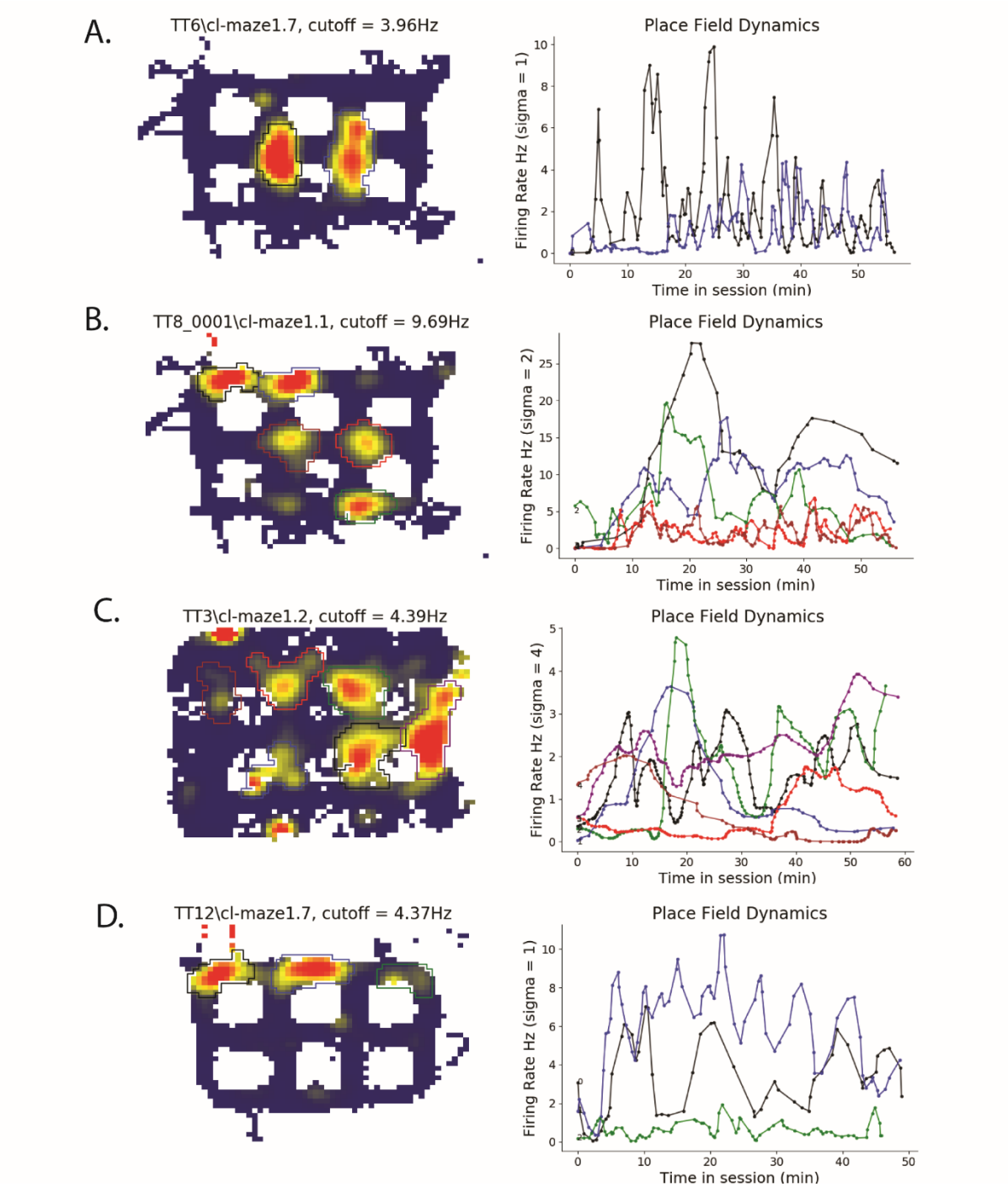

Fig 4.2. Examples of repeating place cells and temporal dynamics of subfields. Left, session rate maps with 95th percentile color map cutoff indicated. Map has been smoothed with 2d Gaussian kernel, sigma = 2. Detected place fields outlined with the field border. Right, the firing rate of each visit to a subfield is plotted as a function of time in terms of minutes into the session. The firing rate was computed as the total number of spikes emitted during a visit to a field divided by the number of occupancy samples in the same visit. Each visit was defined as the time spent in a field such that any occupancy in the field 3 seconds or later is another visit. The firing rate trace has been smoothed with a Gaussian kernel, sigma indicated on the ordinate axis. The color of the line on right corresponds to the field outlined with the same color border on left. **A.** A cell with two fields in neighboring vertical alleys. The temporal dynamics demonstrate that both fields fluctuated in their rates over time, with the right field, blue, silent for approximately the first 17 minutes. Once both fields were active their rates seem to be in anti-phase with another; when one field was waxing in its firing rate the other field tended to wane, and vice-versa. **B.** A cell with six detected fields towards the western section of a horizontal ally. Two additional fields, not meeting inclusion criteria, also follow the pattern. The field dynamics show that the cell had a low rate through the first ten minutes of the session before the rate increased across all the fields. However, around roughly minute fifteen the subfield rates diverged. The black, green, and blue fields continued to increase in rate while the brown and red fields remained at a relatively low rate. Fields in green and blue exhibited a mean rate shift, with the green field shifting to a lower rate and the blue field shifting to a higher rate. Interestingly, the fields seem to shift at roughly the same time, about 25 minutes into the session. **C.** A place field with six repeating fields in vertical alleys. The fields exhibited a complicated set of temporal dynamics. The green and black fields exhibited irregular periodic behavior with periods of roughly 20 minutes and 10 minutes, respectively. The periodicities were not sinusoidal, but rather displayed irregular periods. The red field is silent, or low rate, through the first 35 minutes of the session and then increased in rate to about 1 Hz. **D.** Three repeating fields were present in three horizontal alleys. The cell was initially quiet, or of low rate, through approximately the first four minutes. The cell then became active and the blue and black fields increased in rate while the green field remained low rate. The blue field exhibited rough periodic behavior with a period of just under 10 minutes.

the right. Figure 4.2A shows a place cell with two fields in adjacent vertical alleys. The evolution of the firing rates shows that the eastern field (blue line) is silent until about the 17 minute mark. Both fields exhibit fluctuations in the firing rates over the course of the session. Interestingly, the peaks of these rate changes appear somewhat out of phase with one another – when the eastern field has a higher firing rate the western one has a lower rate and vice-versa. This anti-phase behavior is seen across cells and forms a subset of the qualitative temporal dynamics. This may suggest a competitive interaction between the fields, although this is speculative (See Discussion).

Another pattern of rate dynamics is a mean shift, in which a field increases or decreases its rate by multiple standard deviations of its current average rate. This is seen in Fig 4.2B in which the green and blue labeled fields shift their rates down and up, respectively, by a significant percent of their running baseline. Interestingly, the shift in both fields occurs at roughly the same time (~22 mins into the session), again suggesting a possible interaction between the fields. Another specific case of mean shift is field divergence wherein the firing rate among the subfields is similar, until they diverge at a certain time point. In the same panel, three of the five fields exhibit similar dynamics until roughly 15 minutes in the session, at which point some of the fields dramatically increase their firing rate while others remain stable. This leads to a spread in firing rates that persists, with dynamics riding on top, for the duration of the session.

Some fields turn on or off at some point in the session while the cell remains active at other locations. Fig 4.2C shows a field, in red, which becomes

active at about 35 minutes in the session and remains active for the rest of the session, albeit at a low rate. It is important to note that the cell was active during the entire session at different locations; this represents a new field forming at a location that obeys the cell's repeating field pattern. That field formation and dissipation would obey the apparent pattern of repetition suggests that whatever type of input that drives repetition is present, latent, at each location that satisfies the pattern. A potentiation event may then occur and cause a field to form, gated by location due to the repetition-causing input.

Lastly, many fields exhibit periodic behavior in their rates over time. Here, the fluctuations are more periodic in nature, though not exactly sinusoidal. Fig 4.2D shows a field, in blue, that is periodic over the session with a period of slightly less than 10 minutes. It is interesting to note that another field, green, is not periodic, suggesting this is a property of the field and not the cell overall. In other words, these dynamics are spatially gated and do not simply represent a tonic input the cell is experiencing (or electrical noise being picked up by the recording system). It is crucial to note here that these effects are qualitative; given a number of fields with variable firing rates, all manner of 'patterns' between fields may be observed by chance which need not bear any relationship to biology. However, if there is a role of temporal dynamics on the place field repetition phenomenology then observing these patterns is a necessary precondition to drawing a conclusion.

Inter-field Rate Patterns

Repeating fields are often not constantly changing; periods of a stable firing rate can persist for tens of minutes before shifting, often abruptly over a few minutes, to a new firing rate. This can take various forms, some examples of which are seen in Fig 4.2. These include mean shift, ramping, field (de)activation, and long period periodicities. However, the fields within a cell usually do not change all at once (and the cells, too, seem independent in their dynamics). Thus, at any point time for many repeating cells there is a stable pattern of rates among most of the fields, with the caveat that at some points there will be a field that is undergoing a change in its rate regime. To better visualize these inter-field patterns, and their dynamics, a qualitative analysis was performed. This analysis is shown for an example unit (Fig 4.3A). Each matrix in Fig 4.3B represents the pattern of inter-field firing

A.

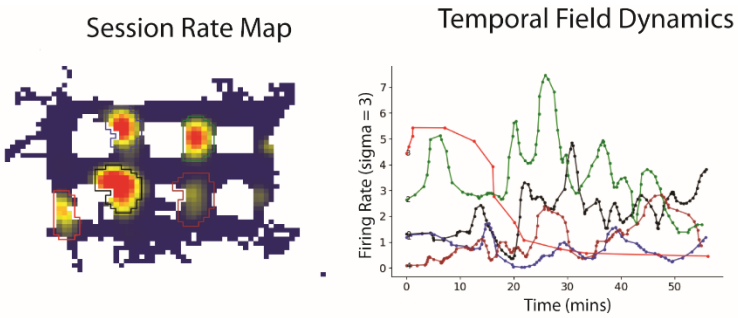
Session Rate Map
Temporal Field Dynamics
Firing Rate (sigma = 3)
Time (mins)

B.

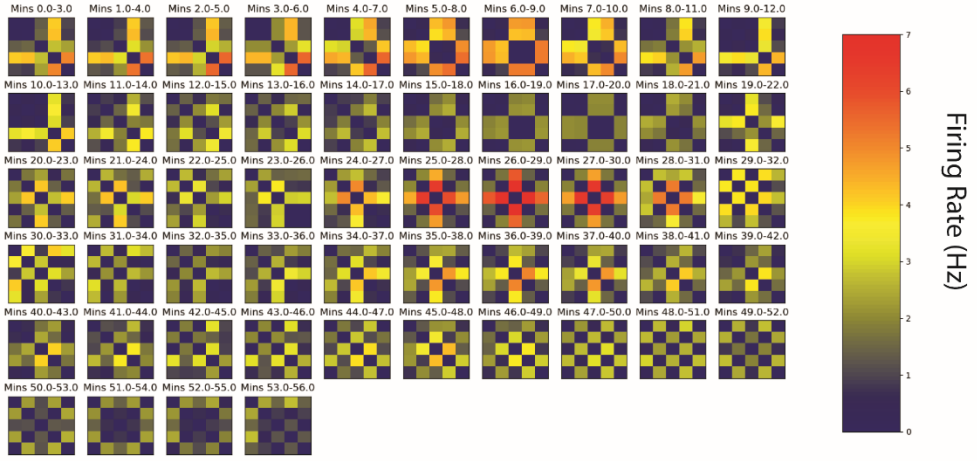
Inter-field Rate Difference (IFD) Matrices
Mins 0.0-3.0
Mins 1.0-4.0
Mins 2.0-5.0
Mins 3.0-6.0
Mins 4.0-7.0
Mins 5.0-8.0
Mins 6.0-9.0
Mins 7.0-10.0
Mins 8.0-11.0
Mins 9.0-12.0
Mins 10.0-13.0
Mins 11.0-14.0
Mins 12.0-15.0
Mins 13.0-16.0
Mins 14.0-17.0
Mins 15.0-18.0
Mins 16.0-19.0
Mins 17.0-20.0
Mins 18.0-21.0
Mins 19.0-22.0
Mins 20.0-23.0
Mins 21.0-24.0
Mins 22.0-25.0
Mins 23.0-26.0
Mins 24.0-27.0
Mins 25.0-28.0
Mins 26.0-29.0
Mins 27.0-30.0
Mins 28.0-31.0
Mins 29.0-32.0
Mins 30.0-33.0
Mins 31.0-34.0
Mins 32.0-35.0
Mins 33.0-36.0
Mins 34.0-37.0
Mins 35.0-38.0
Mins 36.0-39.0
Mins 37.0-40.0
Mins 38.0-41.0
Mins 39.0-42.0
Mins 40.0-43.0
Mins 41.0-44.0
Mins 42.0-45.0
Mins 43.0-46.0
Mins 44.0-47.0
Mins 45.0-48.0
Mins 46.0-49.0
Mins 47.0-50.0
Mins 48.0-51.0
Mins 49.0-52.0
Mins 50.0-53.0
Mins 51.0-54.0
Mins 52.0-55.0
Mins 53.0-56.0
Firing Rate (Hz)

C.

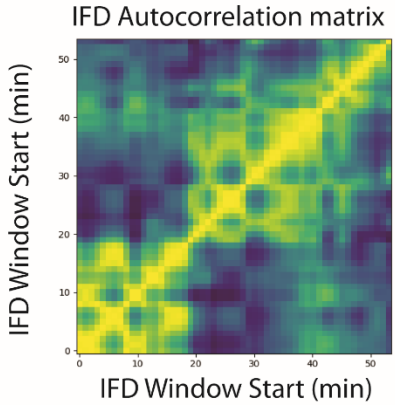
IFD Autocorrelation matrix
IFD Window Start (min)
IFD Window Start (min)

Fig 4.3 Inter-field rate patterns. A. Repeating place cell used in example IFD analysis. Left, rate map showing five detected fields in vertical alleys. Right, subfield dynamics showing different temporal modulations such as periodic behavior (blue, green) and potentiation of baseline firing (black). **B.** Set of IFD matrices. Each subplot is a symmetric matrix where the i^{th}, j^{th} entry of the k^{th} matrix is the unsigned difference between the average firing rates of subfield i and j within time window k. To account for the different number of visits between fields, and the asynchronous nature of visits, the subfields were fit to splines so that arbitrary time windows could be evaluated with an equivalent number of points in each field's window. Each matrix is symmetric and colored with the same color scale, shown right. Stable temporal patterns are shown by the similarity between successive subplots extending for some minutes (though note, that since a sliding window is used, a given matrix has some inherent correlation with the next two matrices). An example temporal pattern is seen in the first 10 minutes (first row, up until second from right). Fields 1,2 and 5 form a group with similar rate activities that is distinct from fields 3 and 4, which form a second group. This can be seen from observing the block-like pattern in IFD values within the matrix (see main text for details). Another pattern is from between about 42 minutes until 52 minutes. Fields 1,3 and 5 form a group, while fields 2 and 4 form a second group. This results in a 'checkerboard' appearance of the IDF matrix. Note that the sliding window makes it difficult to tell when a pattern begins/ends as any given minute of recording is present within three IFD plots. The existence of patterns spanning three or more subplots indicates that there are stable relationships between the fields that persist on a timescale of minutes (using the parameters in this figure. **C.** To further distill these patterns, an autocorrelation matrix was constructed from the IFD plots. Each matrix is correlated with every other matrix in the time series such that the i, j^{th} entry in the autocorrelation matrix is the correlation between i^{th} and j^{th} entry in the IFD time series. This analysis reveals a pattern of banding along the diagonal, corresponding to periods of time within which the field representations are correlated. There appear to be three main periods of correlation, beginning from 0-20 mins, 20-40 mins, and 40 min-end of the session.

rates within a sliding window and a set of matrices corresponds to the evolution of inter-field dynamics across the session (See Methods). Stable patterns of inter-field rate patterns are manifested as series of IFD plots with a similar pattern across time. There are multiple instances of patterns persisting for roughly 10 minutes over the course of the session. One pattern can be seen during approximately the first ten minutes of the session. Examining the IFD matrices during that period shows a block-like pattern of rate differences within each matrix (note the matrices are symmetric). Recall that each row corresponds to a field (as do the columns, with the joint entry being the rate difference between them). Thus, the block structure shows that fields 3 and 4 are both different from fields 1, 2 and 5 and similar to one another. In other words, there are two groups of fields – 3, 4 and 1, 2, 5 – which have similar rates within the group and distinct rates between them. In general, the visual patterns of the IFD plots can be interpreted as groups of fields with (dis)similar rates. The overall pattern in these rate differences forms a kind of ‘label’ of that period in time.

To better visualize these patterns an autocorrelation matrix was constructed wherein each IFD plot was correlated with each other one and the entry plotted in a matrix (Fig 4.3C). In this example, a series of banding patterns are visible, corresponding to periods in time within which the inputs are correlated with another. Note each value on the axes corresponds to the start of a sliding window; this is because each entry in the autocorrelation matrix is an IDF plot which is created within a sliding window. During a period of a stable rate pattern among the fields, corresponding to a particular pattern visible of the IFD

plots across time, successive IFD plots look similar to one another. Therefore, these plots will be correlated with one another during the course of a rate pattern's existence. By observing the correlation banding across the session, the periods of specific rate patterns can be seen and analyzed. There are at least three periods of high correlation in Fig 4.3C, these correspond to rate patterns seen in Fig 4.3B.

Temporal Decoding

To quantify these temporal patterns, a decoding approach was used to extract temporal information from the IFD matrices. Although successfully extracting a temporal signal does not prove that the neuron is encoding time *per se*, it does show the presence of temporal information that can be further investigated. A k-Nearest Neighbor algorithm was used to decode information. The details are found in the Methods; briefly, the decoding performance is the proportion of test matrices with a nearest neighbor in data space that is in the same temporal epoch (Fig. 4.4A). This is compared to a null distribution found via shuffling. The shuffling test shuffles the order of the visits within the field, thus destroying any temporal information present. The null hypothesis is that the ability to decode a temporal signal from the inter-field pattern is no greater than either the nominal chance value or the performance of the shuffled data. The alternative hypothesis is that a temporal signal can be extracted from the inter-field rate patterns of a repeating place cell.

An example of the decoding procedure applied to one repeating place cell is shown in Figure 4.4B. In the following data, the k-NN decoder is tested 25 times on the real data and the mean is used as the empirical performance. The

null distribution contains 1000 shuffles, each of which is decoded 25 times and the average used as single data point in the null. This is to equate the process that generates each point in the null distribution with the process of decoding the true information content. The data were divided into three minute sliding windows with an offset of one minute, while the session was divided into three epochs. The IFD

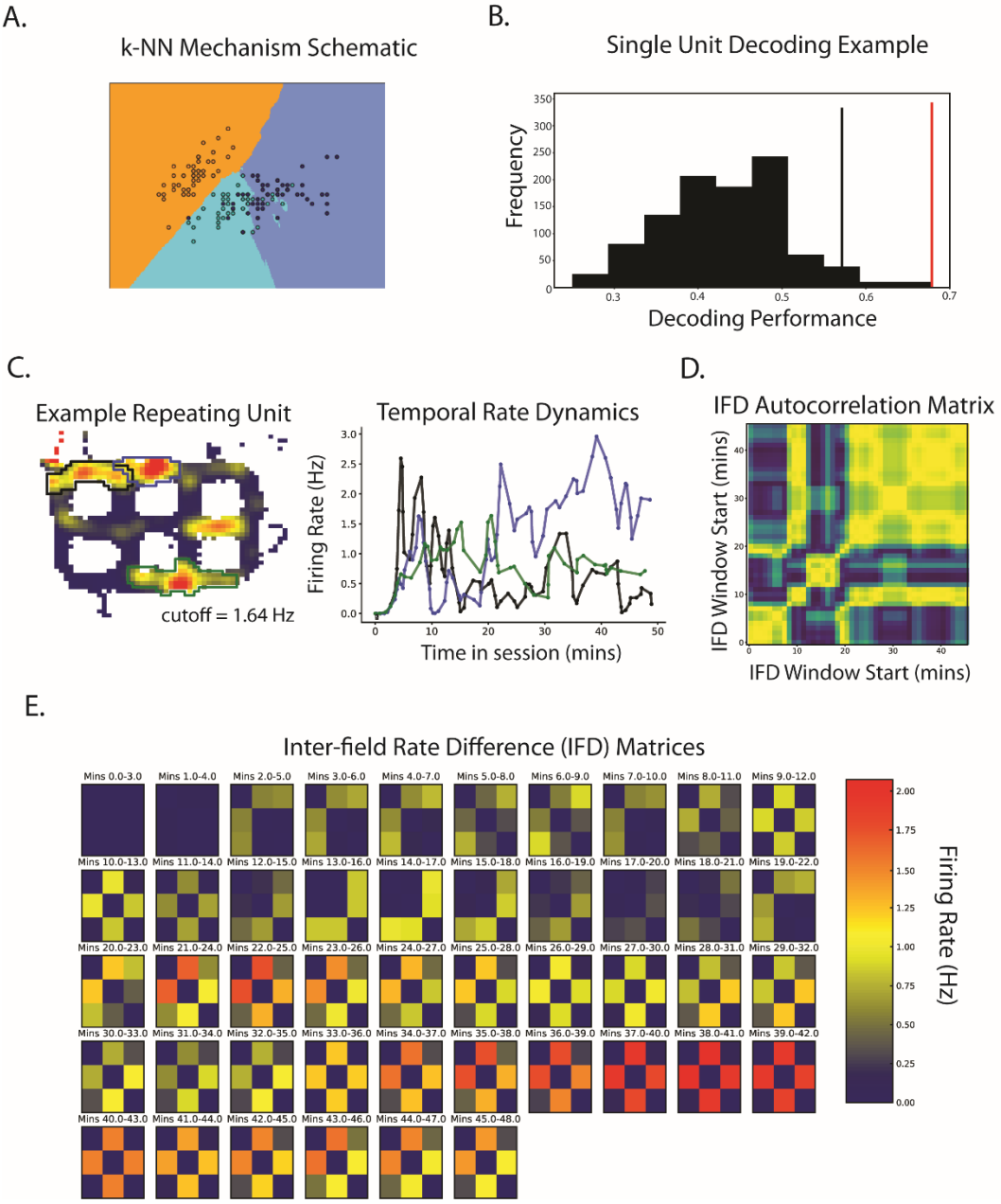

Fig 4.4 Temporal Decoding of Inter-field rate patterns. A. A schematic of mock data in a two-dimensional space illustrating kNN decoding. Image taken from sci-kit learn documentation page. (https://scikit-learn.org/stable/auto_examples/neighbors/plot_classification.html). Data points from three mock classes of data create regions within which any point in the region is closest to a member of that class. New points, or held out test points, are then assigned to one of the regions based on closest training point. The class label of the held out point is compared to the label predicted by the nearest neighbor comparison to determine a hit (label agreement) versus a miss (label mismatch). **B.** Decoding performance of one unit. Inputs to the k-NN classifier were semaphore vectors constructed with a three minute sliding window and a one minute offset. The session was divided into three epochs and test samples were tested to assess how often the two nearest neighbors in data space shared the same, real epoch label. 40% of the data were used as training and 60% testing. The k-NN classifier was run 25 times on the real data, to account for stochasticity inherent in the training/testing split. The average was used as the empirical performance. The data were then shuffled 1000 times. On each shuffle, the decoder was run 25 times and the average used as a single data point in the null distribution. Therefore, the real and shuffle data points were treated identically. The empirical performance is 67.8% while, mean of the null distribution is 47.8% and the 95th percentile is 57.1%. **C.** Left, the rate map of the example unit. Four fields are arranged within horizontal alleys. One field, green, extends into two horizontal alleys as well as an intersection. The 95th percentile of the firing rate is 1.64 Hz, which is relatively quiet for a place cell. Right, the temporal dynamics of the subfields. The blue and black fields exhibit a mean shift with an increase and decrease, respectively. The green field appears more stable, albeit with variability. **D.** Autocorrelation matrix of the semaphore vectors. Three or four epochs of high correlation are seen, lasting between several minutes to tens of minutes. These epochs correspond to periods within which the semaphore vectors are correlated with one another. It should be noted that roughly 10 minutes into the session, a pattern occurs and reemerges later from 20 minutes to the end. **E.** Plots of inter-field rate difference patterns ('semaphore' plots). Each subgraph is a three minute window in time and each successive plot is offset one minute in time from the previous. Patterns can be seen in the inter-field patterns that persist for many minutes. For instance, in minutes 2-10 there is a stable pattern present that appears as an 'L-shape' in the matrix (note the matrices are symmetric, and that due to the sliding window, the last minute of the last IFD plot to contain the L-shape pattern (minute 10), also is included in the next two IFD plots – thus the exact time of pattern transition cannot be known). Another pattern persists between minutes 12-21, appearing as an 'inverse L-shape', before transitioning. A 'checker-board' pattern exists from 21 minutes until the end of the session, however the exact firing rate within the overall 'shape' of the pattern changes over time. The k-NN classifier uses the distances in Euclidian space between these matrices to perform its classification.

vectors are divided into 40% training and 60% testing samples. Each testing sample was compared to the two nearest neighbors in data space. The null distribution is shown as a histogram (black). An individual unit is determined to contain significant temporal information in its inter-field firing patterns if the empirical performance (red bar) passes a one-sided test with a p-value = 0.05. This corresponds to exceeding the 95th percentile (black bar), which is the case in this example. The empirical performance is 67.8% (though this value is variable due to the stochastic nature of the classifier). The null distribution has an average of 47.8% and a 95th percentile of 57.1%. The fact that the null distribution is right-shifted compared to the nominal chance level of 33% could be explained by the correlations introduced by the sliding window procedure. Adjacent IFD vectors share some data and it takes, given these parameters, three successive vectors until the data is independent. Additionally, the smoothing of the data also introduces some correlation between data points. The rate map of the unit shows three repeating fields (with additional, apparent field not detected) situated in horizontal alleys (Fig 4.4C, left). The evolution of the field dynamics over time shows one field that is fairly stable (green), with a large standard deviation in the rates, and two others that increase and decrease their rates over the course of the session (blue and black, respectively) (Fig. 4.4C, right). Interestingly, both the blue and black fields show a change in their mean firing rate that occurs at roughly the same time in the session (~12 minutes). The inter-field rate patterns reveal periods of time within which the patterns remain similar to one another, separated by transition points (Fig 4.4E).

An autocorrelation analysis of these inter-field vectors shows three or four prominent periods of high autocorrelation that last between ten to twenty minutes (Fig. 4.4D). It is interesting to note a period roughly 10 minutes into the session that is highly correlated with activity later in the session. This suggests that the inter-field rate pattern at roughly 10 minutes into the session is similar in nature to the pattern seen towards the end of the session. Consistent with this, the IFD plots between 8-14 minutes in the session form a checker board pattern that appears similar to the pattern seen from 22 minutes until the end of the session (although the exact rate changes over the last twenty minutes as well).

This decoding approach is preliminary and results from only a single data set are shown as a proof-in-principle. Given the heterogeneity in the temporal dynamics seen and their time courses, the set of decoding parameters that works for one cell may fail to capture a signal in another cell. For instance, a slowly modulating signal may have the same rate in multiple epochs, especially as the session is broken into more epochs, and thus the k-NN decoder would be less accurate. Alternatively, if the sliding window is too large, then a quickly changing signal would be lost in the averaging process. A final example is a periodic signal which, by definition, looks similar across the session. These examples show how different types of temporal dynamics would require different choices of parameters. As choosing parameters for each cell based on the qualitative dynamics would be highly inappropriate, current efforts are exploring adaptive ways of extracting temporal signals from many cells in an unbiased manner.

With these caveats in mind, the k-NN decoding analysis is shown for one representative day of recording (R859 Day 2) in Figure 4.5. Forty-six units passed the inclusion criteria and were run on the classifier. The decoder used k = 2 neighbors to classify IFDs into one of three temporal epochs. Each inter-field rate vector was created from one-minute non-overlapping windows and data were split into 40% train and 60% test. The classifier was run 10 times on the data and the median performance used as the readout. This was completed once for the real data and 1000 times for the shuffled data to generate a null distribution. Fig 4.5A shows a scatter of the 95th percentile of the null

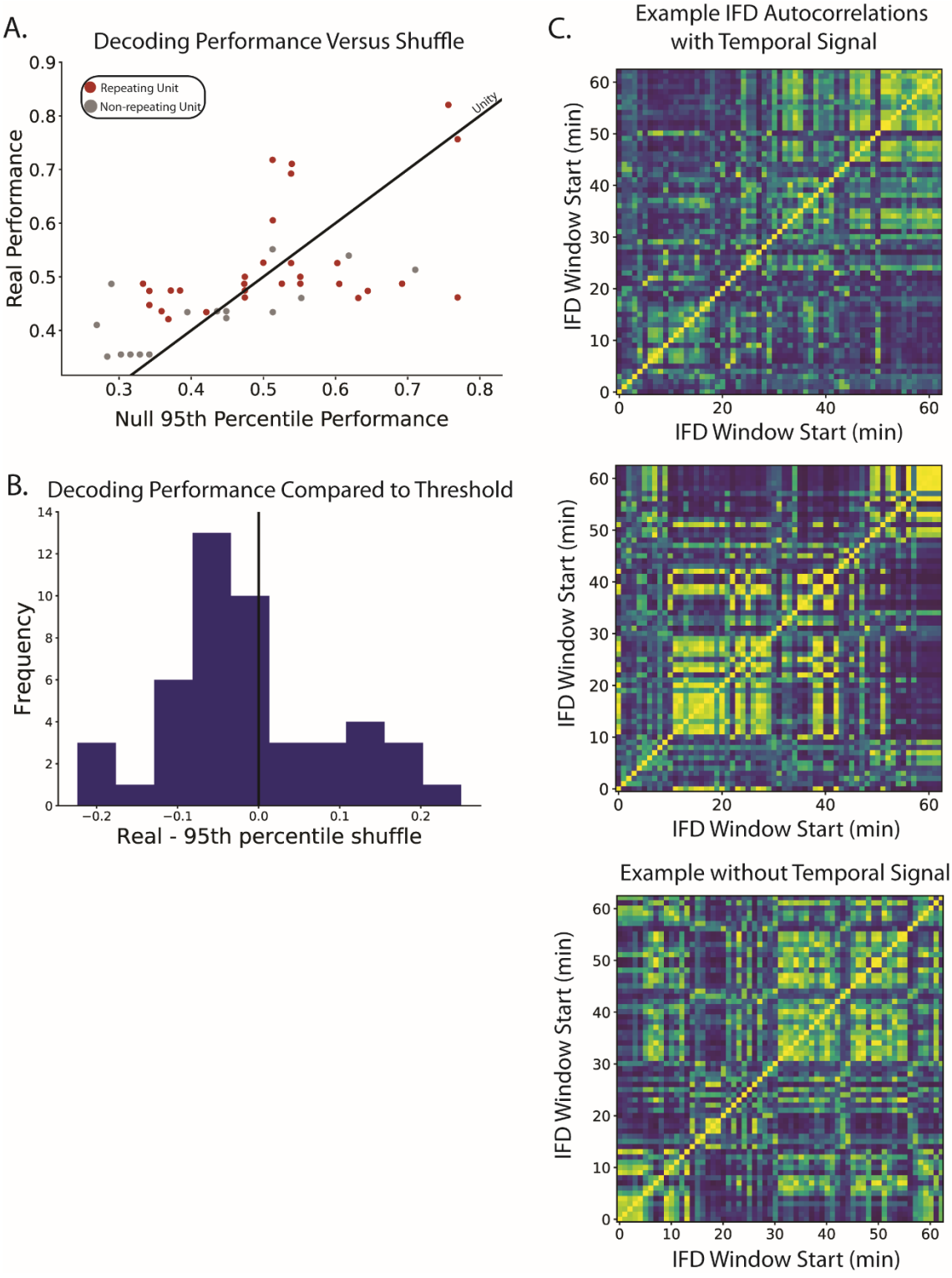
A.
Decoding Performance Versus Shuffle
Repeating Unit
Non-repeating Unit
Unity
Real Performance
Null 95th Percentile Performance
B.
Decoding Performance Compared to Threshold
Frequency
Real - 95th percentile shuffle
C.
Example IFD Autocorrelations with Temporal Signal
IFD Window Start (min)
IFD Window Start (min)
Example without Temporal Signal
IFD Window Start (min)
IFD Window Start (min)

Fig 4.5 Single Day k-NN Decoding. **A.** Scatterplot of all cells from a single day of recording used in the decoding analysis. Repeating units are shown in red and non-repeating units shown in grey. A k-NN decoder was used on each to decode which temporal epoch (n=3) a semaphore plot belonged to. X-axis shows the 95th percentile of the shuffle while y-axis shows real decoding (n=1000 runs, 10 repetitions each with a 40:60 train:test split). Points above unity in red indicate significant decoding within repeating units (14/46 one-sided binomial test $p < 3.5*10^{-9}$). **B.** Histogram of the difference between all real data and 95th percentile of the shuffle. Data to right of line at zero indicate significant performance. **C.** Two example autocorrelation matrices from two cells with significant decoding. Each pixel is the correlation between the semaphore indicated by the row with the one indicated by the column. Rows and columns refer to ordinal position of the semaphore vector in the session. Top, Blocks of higher correlation appear at least three locations in the session, around 15 minutes, 40 minutes, and 50 minutes. Band of correlation off diagonal at around 35 minutes is correlated with data later in the session, suggesting a pattern that occurs multiple times in the session. Middle**,** three large blocks of correlation on the diagonal indicate three major patterns of activity that persist for at approximately 10. Off-diagonal band near 40 minutes suggests a pattern that was present earlier in the session. Bottom, example IFD autocorrelation matrix from cell which did not have significant decoding, illustrating that the patterns seen in the autocorrelation matrices are not sufficient to indicate a

distribution against the real performance. Each point is a cell and those above unity indicate significant decoding. Note that some non-repeating cells had significant temporal decoding as well. Taking the difference between the 95th null percentile and the real performance and visualizing as a histogram shows a tail to the right of the line indicating significance (Fig 4.5B). Two example autocorrelation matrices of cells with significant temporal information are shown in 4.5C, top and middle. Each reveals bands of correlation along the diagonal, indicating periods of time with correlated inter-field activity patterns. Of note is the fact that these blocks end abruptly, suggesting there are periods within the session when the pattern changes over a short period of time. However, these patterns can also be seen in cells without significant temporal information (Fig 4.5C, bottom). This possibly indicates that an abrupt change in the inter-field rate pattern does not imply temporal information is present. Alternatively, the classifier may be able to utilize high-dimensional information that is not apparent in the autocorrelograms.

Another interesting observation is the presence of correlation bands off the diagonal, for instance around index 40 on the x-axis of the lower correlation matrix. This is consistent with a particular pattern of activity among the fields present earlier in the session re-emerging at a later time. However, given that a repeating cell usually has at most 5-6 fields, there are only so many unique patterns their rate relationships can take on and this, therefore, could be artefactual. It is possible these correlation matrices are a crude way to visualize the change in field patterns over time and that the decoder, by virtue of its high-

dimensional mechanism, is more sensitive. Additionally, the 95th percentile decoding of some of the shuffles is rather high; this could indicate a broad distribution that still has a central tendency closer to nominal chance. However, these are further indications that the k-NN analysis is preliminary in nature, though promising.

Behavioral Confounds

An alternative explanation for these data is that the cell only appears to be temporally modulated, but in fact is simply directionally-tuned, and the rat happens to enter the field in a biased manner across time. For instance, a field that waxes and wanes over the course of the session could be caused by the rat running through the field in the preferred direction during the first part of the session and the anti-preferred direction during the latter part of it.

To address this in a preliminary manner, first session-averaged occupancy maps were created to see if, on average, the animal was spending more time in a location facing a certain direction. Directional occupancy maps for a representative day show that while, overall, each location is well sampled from each direction, there are directional biases at a given location (Fig. 4.6A). For instance, the horizontal alley in the upper-right of the track has an east bias while the vertical alley to its right has a south bias.

To quantify these differences, the proportion of filtered points in each alley in the two directions of travel were subtracted from one another. In other words, for a vertical alley, the difference in the proportion of points in the alley when facing north was subtracted from the proportion facing south (Fig 4.6B). It can be seen that, on this day, there is ceiling of a 10% difference in occupancy based on

main-axis direction in an alley. This number seems to be a ceiling across days with others exhibiting a max as low as 4%.

Still, this analysis does not take into account how the rat moves through a field over time. What seems like well-balanced sampling over the course of the session may reveal behavioral biases when analyzed on a finer time-scale. To address this, time in the session was

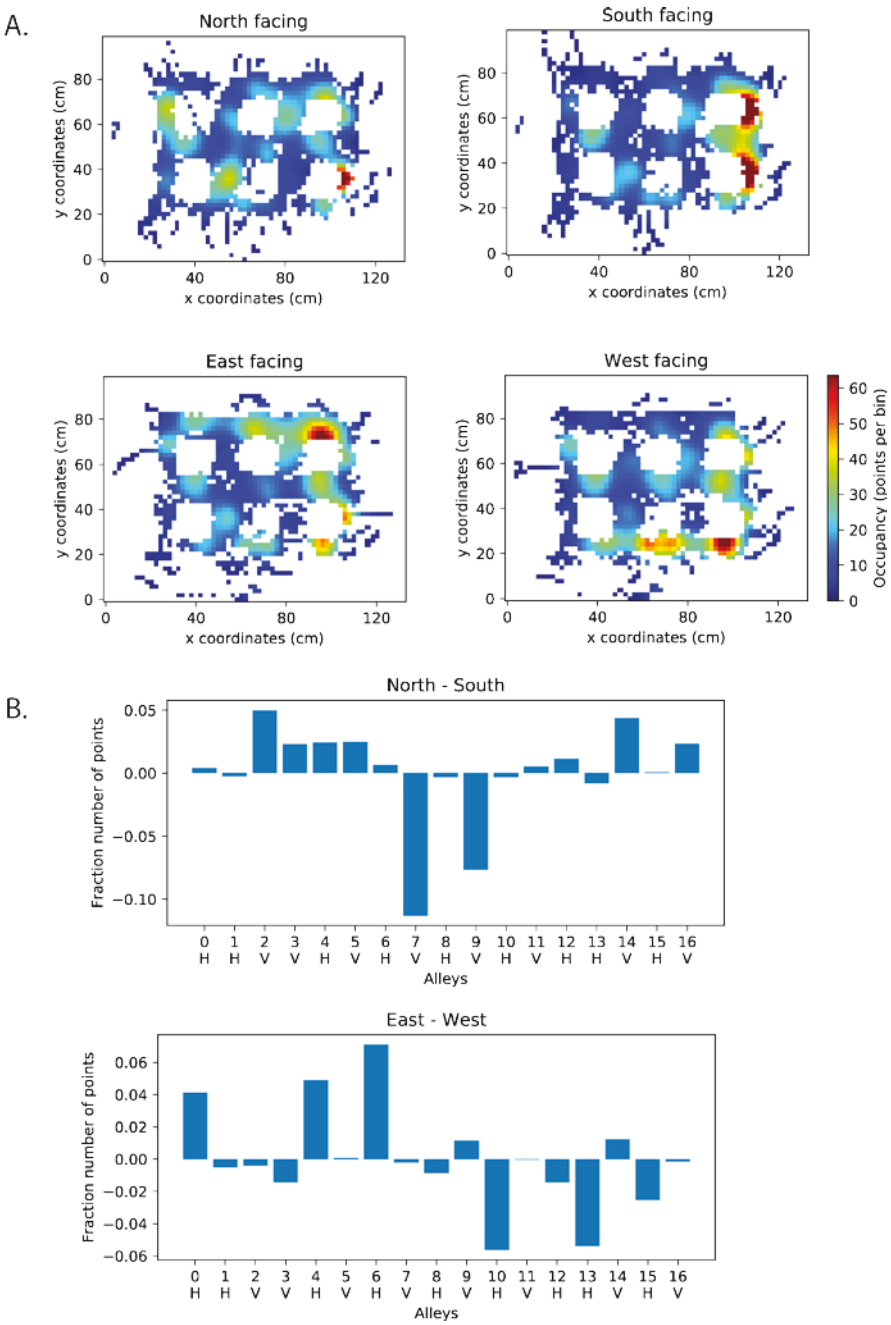

Fig 4.6 Directional bias over single recording day. **A.** Occupancy maps for each cardinal direction. A directional vector is constructed for each successive pair of occupancy points and used to assign the point to four directional categories. A 90° wedge centered on the cardinal direction ensures all points are assigned to a single category. Pixel shading shows the number of points in each bin taken from speed filtered data (3 cm/s, 50 point window size). Data are smoothed with a Gaussian kernel of two pixels. Regions with a relative directional bias over the course of the session appear as corresponding portions of two complementary plots (e.g., North versus South) with a difference in shading. **B.** For each alley, the proportion of points in excess in one direction versus the other shows a maximum variation of 10% for this day, with most alleys below 5%. The top graph shows the difference in north versus south while the bottom shows the difference between east and west. The x-axis labels display the alley number and its orientation (V, vertical; H, horizontal).

A.

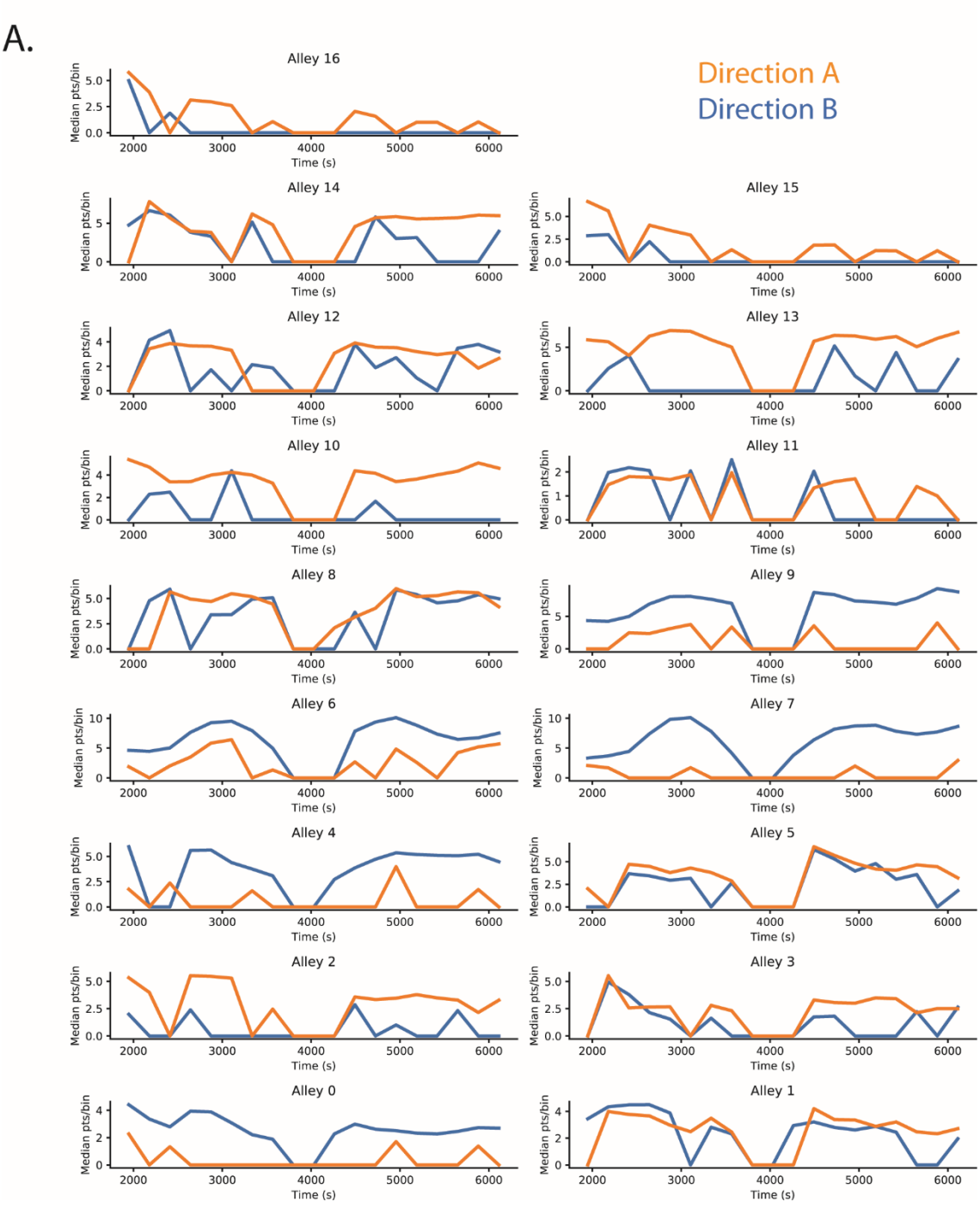
Direction A
Direction B
Alley 16
Alley 14
Alley 15
Alley 12
Alley 13
Alley 10
Alley 11
Alley 8
Alley 9
Alley 6
Alley 7
Alley 4
Alley 5
Alley 2
Alley 3
Alley 0
Alley 1
Median pts/bin
Time (s)

Fig. 4.7. Directional bias over time for each alley. A. Each subplot corresponds to a single alley with a curve for direction A (north or east, depending on alley) and another for direction B (south or west, depending on alley). The x-axis displays time in seconds (with 2000 s corresponding to the beginning of the session; zero is the time when the recording system was turned on). Each data point corresponds to the median number of occupancy samples of a one-dimensional histogram along the long axis of the alley. Each histogram contains data from a roughly three minute window. A value of zero implies that less than half of the alley was sampled from that direction during that window.

divided into roughly three minute windows. In each window, two one-dimensional occupancy histograms were created along the long axis of the alley, one for each direction through the alley. The median of each vector was computed, yielding two values for each time window, and plotted as a function of time (Fig. 4.7). Note that given the use of the median, if the alley was not traversed at least half way from a given direction then the value would be zero for that direction in that time window. The data qualitatively show that there are directional biases in the data. Some alleys, such as Alley 7, show a consistent bias where the alley is entered from a preferred direction. Others, such as Alley 11, show long periods were the alley is not fully traversed at all, but when accessed the entries are unbiased. A hypothetical pattern of data that would explain the temporal dynamics would show change in the relative bias over time. If a cell is directional then it will fire more when entered through its preferred direction and therefore changes in the entry bias would manifest in the rate as a fluctuation over time. Qualitatively, there do not appear to be cases where the pattern of entries could easily explain the temporal dynamics. However, further quantification of this is necessary.

Effect of Direction on Repeating Place Field Activity

The above discussion concerned behavioral biases interacting with directional repeating cells, but did not consider the range of possibilities of the role of directionality on repetition. It is possible there is no effect, or that all fields of a given cell are directionally tuned in the same manner. To explore this, directional rate maps were created for each cell (Fig. 4.7). On the left of each panel shows the overall ratemap while four panels on the right show the rate maps comprising

points facing in the indicated direction. The top example shows a repeating unit with six fields (three major fields, three minor) (Fig. 4.8A). Each field is located in an intersection near the corner where two perpendicular alleys meet. Comparing the East and West directional rate maps shows a strong effect of directionality across all of the fields. Each field prefers the East direction and fire very little in the opposite condition. Interestingly, the field in the intersection on the right-middle of the track is more active in the East condition compared to the overall ratemap. This suggests that differences in field rate that are observed here (and first reported in Spiers et al. 2015) may in fact reflect a weakening of the overall signal when comparing firing under a preferred condition with those of the anti-preferred conditions (here, the condition being direction). Of more interest to the present work is the fact that the center right field is also present in the North condition with a comparable rate and size; the other fields are greatly attenuated or absent. This suggests that directional tuning in repeating CA1 neurons may not a global property of the cell, but rather a subfield-specific variable. Another instance of subfield-specific directional tuning is shown in the middle panel (Fig 4.8B). Between four to six fields are arranged in vertical alleys (again, noting the rate difference between the fields). Comparing the North and South conditions shows that the bottom right and bottom middle fields are active in both conditions. However the other fields are more active in the South condition compared to the North. Thus, this field also supports the notion that individual repeating fields have some autonomy in their dynamics. This could be due to differential, spatially-gated inputs to the cell that allow different tuning at different

locations. There seem to be differences in the East and West conditions, compared to both one another and to the North South conditions. However, it is difficult to interpret the difference in firing in directions along the main axis of the alley versus the perpendicular direction given that the behaviors are expected to be different. In the last example four fields are arranged towards the northern end of vertical alleys (Fig 4.8C). The field in the upper right, and to a lesser extent the field in the lower left, are active in both conditions along the main axis of the alley. However, the field in the upper left is diminished in the South condition, suggesting a directional tuning not shared by other fields of the same cell.

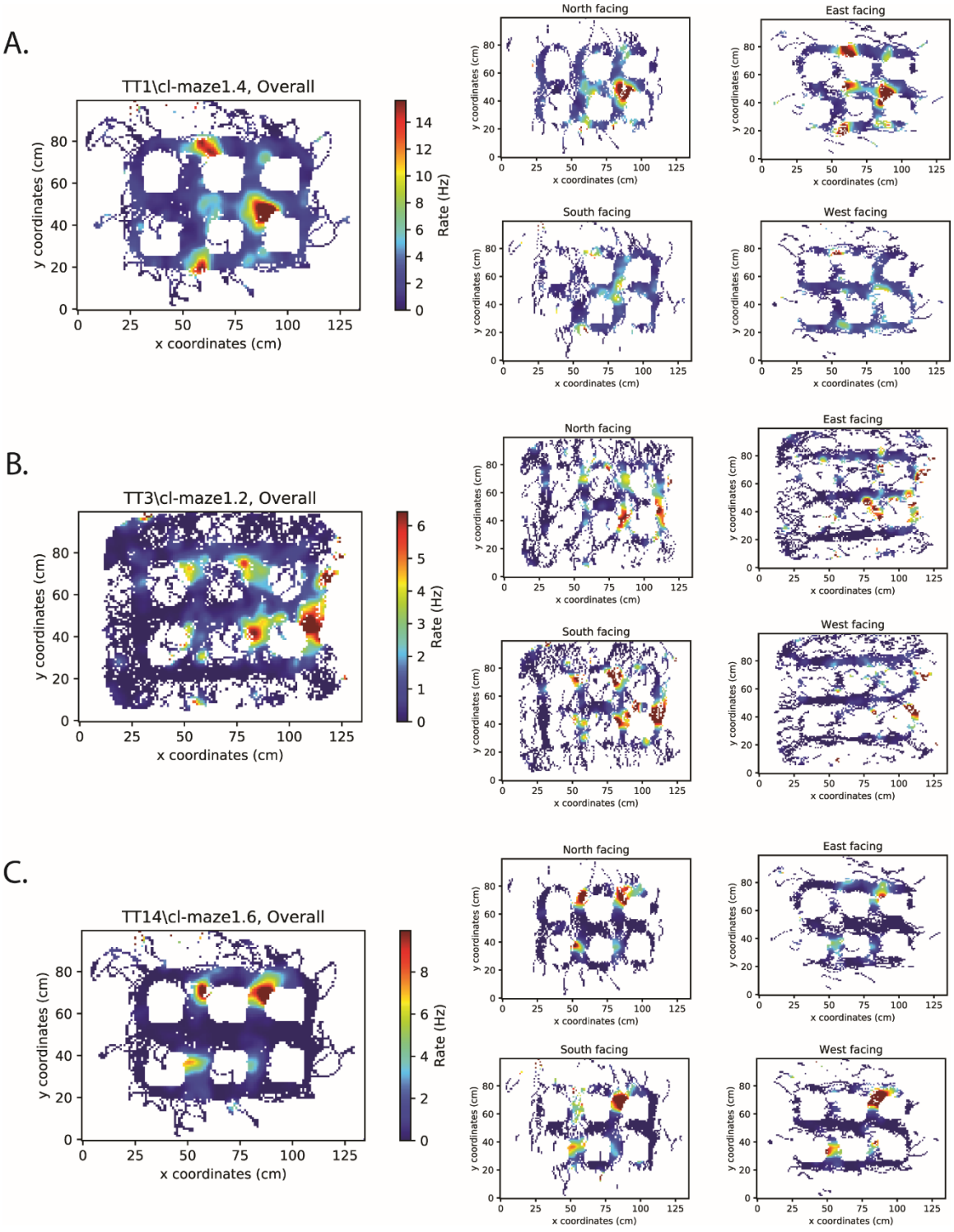
A.
TT1\cl-maze1.4, Overall
y coordinates (cm)
x coordinates (cm)
Rate (Hz)
North facing
East facing
South facing
West facing
B.
TT3\cl-maze1.2, Overall
C.
TT14\cl-maze1.6, Overall

Fig 4.8. Effect of directionality on repetition. Three repeating place cells across representative days in two rats. **All,** rate maps for given condition. Color bar saturates at 98th percentile of firing rate. **Left.** Overall rate map for a repeating CA1 place cell. **Right.** Directionally filtered rate maps for each cardinal direction. See Ch. 4 methods for details, but in brief the vector between successive speed-filtered points provides an allocentric direction which determines which directional group the point will be placed in. Each cardinal direction is the center of a 90° wedge which guarantees each point will be classified in one direction. **A, Left.** Repeating place cell with three main firing fields and three less robust firing fields in intersections near the corners of the blocking obstacles. **A, Right.** Directional filtering shows an overall preferred direction of east. All of the fields shown in the overall ratemap are present in the east filtered data. Interestingly, the middle right field is still present in the north filtered condition, while the other fields are absent, or greatly attenuated. In the south and west conditions the cell is active but at a reduced firing rate that is not clearly dependent on direction. **B, Left.** A repeating CA1 cell with six firing fields in the northern section of vertical alleys. **B, right**. Comparing the firing rate differences between directions along the main axis of the alley shows that the fields appear to not be uniformly modulated. The lower middle and right fields are present in both directions. The upper fields and left center field (centered at roughly 80, 40 on plot) are attenuated in the north condition. Any difference in the direction orthogonal to the main axis is less clear, however, center right fields appear more active in the east condition compared to the rest. **C, left.** A repeating CA1 place cell with fields in the northern part of four vertical alleys. **C, right.** Changes in movement direction between the north and south orientation reveal that the top right field (centered at roughly position 85,75) is unaffected, or affected only mildly, by directional changes while the top left field (centered at roughly position 55,70) exhibits decreased activity in the south condition compared to the north. Difference in firing in the east and west conditions is explainable by the side of the alley to which the lickport is affixed.

Discussion

These data provide new insight into how place field repetition manifests in more complicated environments and how variables such as head direction and time interact with the repetition phenomenology.

Limitations

Before discussing the implications of these findings, it is important to discuss their limitations. First, there are the limitations in the analysis. There were cases where the place field detection algorithm failed to split fields, or detected fields that a knowledgeable observer would likely decide was instead poorly tuned spatial firing. Because the algorithm provides a visual readout of its decisions, the quality of the detection for a given field is readily known; however, any need for manual oversight is a drawback, especially when needing to process many fields in a data set. Second, there is the place field repetition classification. The threshold for repetition was purposefully made liberal so as not to impose a prior belief about what these cells ought to look like. However, a consequence is that the operational definition of repetition is vague and includes a disparate set of field patterns. Lastly, there is the k-NN classifier; although it is a commonly used approach, its suitability here must be further studied. As noted in the Results section, some cells without a decodable time signal had IFD patterns qualitatively similar to those that did (and vice-versa). More work must be done to understand what signal the k-NN decoder is extracting, and possibly supplement it with another kind of classifier (possibly a random forest).

There are limitations, too, in the interpretation of the data. The main result in this chapter is the identification of temporal signals within repeating fields. However, it can be difficult to discern the difference between a genuine temporal signal and chance fluctuation over time; this problem is compounded by the number of fields a single cell can have. If a cell has several fields, then by chance there may be interesting patterns between them over time, but the generative process underlying this could be simply chance variability. The decoder technique is meant to address and quantify this, but the effort is ongoing. Another limitation is the behavioral variability in the data and whether the temporal dynamics seen reflect differences in behavior interacting with simpler tuning, such as for direction. This has been addressed in a qualitative manner, however a more thorough investigation is needed. Relatedly, there seem to be complicated relationships between directionality and field activity among some of the neurons. While this is potentially interesting in itself, any interaction this has with the observed time dynamics must be further explored.

Role of head direction in organizing repetition

The most visually striking observation in these data is that most cases of repetition seem constrained to regions of the maze sharing the same orientation. Although this requires further quantification, the potential finding comports with previous studies examining the role of head direction in place field repetition. The prevailing notion is that ambiguous head direction input promotes the emergence of repetition by failing to serve as a disambiguating signal when sensory input is similar in different locations (Grieves et al., 2016a, Harland et al. 2017). As discussed in the General and Chapter introductions, briefly, an environment

containing identical compartments will, or will not, induce repetition in CA1 neurons depending on whether the compartments are, or are not, facing in the same direction. Ablating part of the head direction system can reinstate repetition in an environment that previously did not show it (Harland et al., 2017).

A prediction of the hypothesis that head direction promotes repetition is that it would also help gate where repetition emerges. In an environment with multiple types of repeated structural components, the types of repeated motif could differ from each other in multiple ways. For instance, an environment could contain multiple square compartments as well as circular compartments that could be entered from different directions. In that case, both sensory and directional information could promote repetition within, but segregate repetition between, the types of rooms. Here, there are three types of repeated pattern (vertical alley, horizontal alley, and intersection) and the two alleys are physically identical except for their orientation. Therefore, a test of the role of head direction on repetition would be to see if direction alone can cause fields to repeat in one, but not both, types of alleys. A caveat to this is that because the track is not infinitely large, not all of the alleys of a given orientation are truly identical because some are interior to the maze while others are along the other wall.

Still, the data collected here do anecdotally support the hypothesis that the orientation alone of an alley can influence the pattern of repetition within a cell. However, a not insignificant number of cells do have fields which repeat among locations with orthogonal heading input. It is not clear whether these are cells with a weaker head direction input (which, then, is less able to gate where fields

emerge), a different kind of phenomenology, or whether head direction is simply not as constraining an input as the stronger version of this hypothesis would suggest. It is also possible technical error, such as during spike sorting, contribute to these observations by introducing unit contamination. If it is the case that the data collected show repetition preferentially occurring in regions with a similar orientation, then further support would be lent to the hypothesis that the repetition phenomenology is strongly affected by heading.

Role of directionality on subfield activity

The discussion of head direction above leads to another question: are repeating cells directional in their firing? Here, directional means that the direction of travel through a field affects the firing rate of the field; this is distinct from the discussion above of the role of head direction on the pattern of repeating field locations. It is well-known that CA1 neurons (with single fields) are often directional on linear tracks (McNaughton et al., 1983; Markus et al., 1995; Gothard et al., 1996). Frank and colleagues showed repeating place fields are affected by directionality, but did not dissociate the role of direction from trajectory type (and, indeed, concluded it was the latter that explained the changes in field activity) (Frank et al., 2000). Here, example units from repeating CA1 neurons show that there is a clear, qualitative effect of direction on the field firing. Some neurons, such as the top example in Fig 4.8, seem to be directionally tuned in a manner similar to CA1 neurons with a single field – that is, all of the fields have the same preferred direction along one axis of travel, here preferring East over West (but see below for a discussion of the implication of the North vs West condition). However, other examples show a more complicated

pattern of results. In the other two example units, the subfields did not all share the same preferred direction. This suggests that directional input to a repeating CA1 unit may be spatially gated. The unit may receive multiple directional inputs – some preferring East, West, and so on – and the relative influence of these inputs is affected by spatial inputs. This conjunction of directional and spatial inputs could allow subfields to be differentially affected by the direction of travel through a field. This would further argue, albeit somewhat indirectly, against the idea that repeating fields are indicative of a pathologically 'confused' system (in addition to the evidence that most cells are normal place cells and learning a task does not decrease the amount of repetition present). If subfields can express different preferred directions owing to spatially tuned inputs, then the system must necessarily have accurate knowledge of the rat's current allocentric position and, crucially, be providing that information to the repeating unit via synaptic input.

Another observation regarding directionality is that some fields seem stable across multiple directions while their neighboring fields are strongly affected. In this case, it isn't simply that they are differentially tuned, but rather that one field appears less sensitive overall to change in direction while other fields are more sensitive. Interestingly, in the examples shown in Fig 4.8, it seems as if the less directionally tuned field is also the strongest field in the overall rate map. This could be a trivial result of the fact that if the field is more stable across changes in traversal direction, then it will appear to be a more robust field when averaging across directions. However, this is not necessarily

the case, as a less directionally sensitive field could have a lower rate than its neighbors. These neighboring fields could have much higher rates in their preferred direction such that, even when averaging across non-preferred directions, it still results in a stronger field. These less directionally sensitive fields could be thought of as ‘anchor fields’ that remain more stable across the session in the face of variable behavior and temporal dynamics (though the latter has not yet been addressed).

Temporal dynamics and implications on circuit function

A novel observation in the present data is the presence of strong temporal changes in repeating field activity over time. Some repeating fields wax and wane over many minutes, some seem to periodically modulate in anti-phase with other fields of the same cell, while still other fields emerge or disappear while respecting the overall repeating pattern. It should be cautioned, again, that with so many fields there are bound to be all manner of empirical dynamics that are simply due to noise and chance variation. Further, the decoding approach used is in the preliminary stage of use and still needs quality assurance checks.

Identifying a temporal signal within repeating place cells would be novel, however information about time within CA1 has been reported multiple times (see Introduction). Further, given enough fields with sufficient temporal fluctuations, it is almost trivial that the pattern of firing rates at a given time would be unique. However, this does not mean this alternative hypothesis is trivial as it rests on the subfields displaying sufficient temporal modulations, which is not guaranteed and may reflect other phenomena such as field recruitment. Further, even if enough randomly fluctuating fields could yield a temporal signal, it would

not mean that the epochs could be decoded as the moment-to-moment changes would be independent due to randomness.

With these caveats, there does seem to be an ability to extract a temporal signal from a significant number of units using a nearest neighbor classifier and the dynamics in many cases are visually striking, especially the anti-phase periodicities. What, then, might be the role of these dynamics in hippocampal physiology? The fact that it may be possible to decode a temporal signal from the data would suggest that maybe these are some variant of time-encoding cells. As discussed in the introduction, it is known that CA1 neurons encode time, or at least have temporal dynamics, on timescales ranging from seconds to days. It is possible that repeating place fields also participate in these temporal ensembles, specifically those ensembles representing time on the order of minutes. However, there are at least two reasons to suspect this may not be the whole story, one involving an issue with interpretation and another involving an alternate explanation of the dynamics.

First, the ability to decode a temporal signal from the inter-field rate pattern of multiple fields is only meaningful depending on the relationship between the decoding parameters and the time course of field rate modulations. Consider a set of n random, stationary time series. They will, by definition, fluctuate over time around some mean. There will also be a time constant to these fluctuations, either a single one for the set of time series, or one for each in the set. Now consider a window in time that creates an inter-field rate difference vector (‘IFD’ vector) as was done above. The vector will be, on average, no more

similar to its neighbor in time than to a vector further away in time, as the signals are stipulated to be random and stationary. However, as the number of signals in the time series increases, it becomes increasingly probably that any given time window has a unique pattern of rate differences. This is because each time signal is independent and its noise around baseline is de-correlated from the noise of the other time signals. This is analogous to saying a television tuned to static is increasingly likely to have a unique pattern of static at any given moment, the more pixels there are on the screen. However, even though the IFD vectors will eventually become unique as the number time series comprising them increases, there will be no relationship between the pattern of a given IFD and its neighbor, because the noise is random. But now consider the time constant; it determines how slowly the noise evolves over time. If the time constant is much larger than the time window, then neighboring vectors will indeed be more similar to one another than to a more distant vector because of these temporal correlations. Therefore, time could be decoded from a random set of signals provided 1) the time constant is large and 2) there are many signals in the set. Despite this important conceptual point, there are multiple examples of rate dynamics in this data set with fast enough time constants that it should be valid, in principle, to say that there is information about time in their resulting IFD vectors and that decoding results are valid.

The second reason why time may not be the best explanatory variable is that the field dynamics may, instead, be indicative of place field recruitment processes that are temporal in nature. This will be elaborated on in the general

discussion, but briefly outlined here. A hypothesis about the origin of repetition, as discussed above, is that identical physical compartments that are accessed from the same direction cannot be adequately disambiguated owing to the similar sensory and directional information present at each location. This raises the possibility that the temporal dynamics observed here represents the CA1 network attempting to create a single firing field from multiple spatially tuned inputs and being unable to do so. In a more naturalistic environment, the cell would still be receiving multiple sources of spatially tuned input, but can use the difference in sensory and directional inputs at different allocentric locations to resolve multiple inchoate firing fields into a single, stable place field. In this, and other, apparatuses this is not possible and so multiple fields are expressed.

A wealth of information regarding the cues CA1 neurons respond to has been provided by experiments manipulating various cues in the environment as a rat navigates within it. However, some types of cues are more difficult, as a practical matter, to control than others. Additionally, one can only study cues which have already been predicted to be influential. A repeating place cell is valuable because the multiple fields allow an exploratory analysis of the explanatory variables shared among the fields. In a sense, repeating place cells allow for a within-cell comparison of the variables that control a cell's firing; some variables, such as vector relationships to landmarks, can only be studied in cells with multiple fields (or by moving the landmarks). Therefore, repeating cells offer an opportunity to reveal the attributes of the environment that control place cell firing without knowing how to manipulate the environment to reveal them.

Additionally, if it is true that repeating place fields are only seen in environments in which there are insufficient disambiguating cues to inhibit multiple fields, then these cells also offer an opportunity to study how cells are recruited to be part of the place map. As mentioned above, it is possible that repeating fields represent the CA1 system being unable to suppress activity in multiple locations and promote the emergence of a single field. If this is the case, then the temporal dynamics among these fields could allow one to study field recruitment dynamics and homeostatic processes at a population level that currently can only be studied one cell at a time.

It is plausible that repeating cells represent some aberrant physiology – place cells that behave abnormally in contrived environments. However, far from being irrelevant to the study of CA1 physiology, this may allow “atom smashing” experiments (McNaughton, personal correspondence with J.K) that utilize pathological scenarios to reveal tenets of place field physiology.

General Discussion

The hippocampus represents a great diversity of information in terms of a spatial scaffolding, a cognitive construct long referred to as a ‘cognitive map’ (O’Keefe and Nadel, 1978). The purpose of this thesis was to further explore the non-spatial ‘annotations’ to the cognitive map. The first project sought to understand whether and how rate remapping would occur in the absence of a task structure; if the cognitive map records all of (attended) experience (Morris and Frey, 1997), then no task should be necessary to observe rate remapping. A subset of CA1 neurons were identified that responded to the cues, providing a key piece of evidence that rate remapping could be a mechanism of multiplexing spatial and non-spatial information, particularly for an automatic episodic buffer. Further, the rate modulations occurred locally within the field, raising the possibility that place fields are capable of a new form of subfield computation (in addition to, e.g. phase precession (O’Keefe and Recce, 1993; Skaggs and McNaughton, 1996). In the second project, the phenomenon of place field repetition was probed, revealing a variety of interesting phenomena that deserve further characterization. Cells with multiple fields in similar location were observed to exhibit complicated dynamics in their firing rates over the course of the session. These dynamics may offer insight into another way neurons could encode time, or how the place map adapts to unusual environments. In some ways these projects explored different phenomena - studying the role of sensory cues versus complicated movement variables. However, they are united with a common purpose of understanding how the hippocampus represents information

beyond a “you-are-here” spotlight. The cognitive map is an adaptive construct which does not simply consider allocentric location. Understanding how variables related to navigation, such as the cues in an environment or the manner in which an agent moves through it, is crucial to understanding the neural mechanism of mapping.

What is stored in CA1? Indices versus Annotations

It remains unclear how detailed the non-spatial signals are within the hippocampus, and where the content of episodic memory is ultimately stored. Data, such those presented here, showing that individual items can be encoded in neural firing rates do not address whether the items are encoded as an index, devoid of granular detail, or, rather, as a representation with fine-grained sensory information. The notion that the hippocampus encodes the events of episodic memory as indices to a full representation of the memory elsewhere is a long-standing one (Teyler and DiScenna, 1986; Teyler and Rudy, 2007). Under this ‘hippocampal indexing theory’, during encoding, ensembles of hippocampal neurons are associated with distributed neocortical ensembles that represent the content of the episodic memory. While the neocortical neurons become de-correlated as new inputs impinge upon them, the hippocampal neurons are linked together via LTP to form an index that can re-instantiate the neocortical ensembles during recall. It is unclear how consistent this hypothesis is with the cognitive map theory; the distinction seems to be between local storage of information in the hippocampus versus distributed storage in neocortex. Under the cognitive map hypothesis, there is local information storage within the hippocampus. Spatial information is stored locally within the hippocampus.

Additionally, the non-spatial ‘annotations’ to the cognitive map are also stored locally – possibly containing information such as cue identity. Under the indexing hypothesis, information is stored remotely with respect to the hippocampus. If information is stored remotely, then the representation in the hippocampus is more abstract and information poor; it is a reference to information rather than the site of information storage. A paper by Tanaka and colleagues supported the indexing hypothesis by analyzing the physiology and early gene expression in mouse CA1 neurons in different environments (Tanaka et al., 2018). Neurons participating in the representation of a novel context were less spatially reliable than those that did not, suggesting to the authors a distinction between CA1 ensembles encoding space versus those encoding contextual information. The rationale for this conclusion is that, under the cognitive map hypothesis, the populations that represent spatial location and non-spatial information are identical. Therefore, the cells involved in representing non-spatial cues should also be spatially stable. However, the authors report the opposite – the cells involved in representing the novel context do not seem to be the same ones representing the environment (in a stable manner). However, it should be noted that mouse CA1 neurons are less spatially stable than place cells in rats; a more convincing study would be done in a model organism with a higher baseline spatial stability. Further, a cognitive map could still employ a less restrictive version of hippocampal indexing, so long as the index refers to the sensory content of the memory and the place map still supports fine-grained spatial encoding within the hippocampus.

It is the view expressed here that hippocampal indexing does indeed interface with a cognitive map as suggested above – the index is used for the sensory information while the map represents spatial information. A number of studies support the notion that hippocampal-neocortical interactions are essential for memory guided tasks, and that, further, these interactions are mediated via oscillatory coupling, particularly in the theta band (Brincat and Miller, 2015; Tamura et al., 2017; Shin et al., 2019 [this study analyses sharp-wave ripple-mediated hippocampal prefrontal cortex interactions (SWR-mediated HPC-PFC associations)]). In these, and related, studies, interactions between hippocampus and neocortical areas, in particular prefrontal cortex (PFC), are associated with the encoding of memory and the use of memory to guide behavior. PFC ensembles track task quantities like path chosen or choice outcome (correct/incorrect). The activity patterns between these regions are mediated via neural oscillations; hippocampus and PFC are brought into synchrony via oscillations such as the theta rhythm. However, the oscillation used depends on the computational need, as higher-frequency oscillations associated with organizing planning behavior (SWRs) can also coordinate the two regions (Shin et al., 2019). These relationships are what one would expect to see if episodic learning engaged distributed neocortical ensembles linked to hippocampal ones. If the hippocampus was the sole repository of episodic information, then it would be unclear why redundant neocortical ensembles also participate in memory encoding and recall. It is reasonable to conclude that the non-spatial component of the hippocampal cognitive map does not contain the full details of an episodic

memory, and at least some information is routed elsewhere for storage and the representation.

However, it remains unclear where exactly the balance is between local storage (in hippocampus) and indexing (using a hippocampal index to engage neocortical ensembles), for two reasons: the cues used and the time point of analysis. First, to assess what level of granularity is present within CA1 sensory representations, it would be necessary to analyze neural responses to combinations of various multimodal features – for instance, all combinations of the color, shape, and texture attributes of an object. In such a crossed design, a signal for, e.g. 'red' could potentially be extracted from a set of stimuli that vary in their colors, among other features. However, in the present design only three stimuli were used that differed from each other in multiple ways, making it impossible to tell if a cell encoding, e.g., cue A was encoding the identity of that cue or some preferred non-spatial feature thereof. The data from morph box studies could be valuable in predicting CA1 responses in such an experiment (Leutgeb et al., 2005b; Wills et al., 2005). Rats foraged for several sessions in an enclosure; during each session the walls were altered to be progressively more square-like, starting from a circle, or vice-versa. Leutgeb and co-authors reported CA1 neurons with fields that changed gradually across sessions, seemingly sensitive to each change in enclosure shape (Wills and colleagues report a different finding which could be explained by the training protocol (see Colgin et al., 2010)). This could be taken as evidence that CA1 neurons can represent fine-grained sensory detail in the environment. However, given that this was the

only change made, there is another interpretation. It is possible that the hippocampal indices are content-poor, but still have enough information that they can be ordered with respect to one another. It might be possible to say, based on looking at the index, that the representations they refer to are similar to one another without having access to the content of the representation that makes them similar. In short, hippocampal indices may allow “lexigraphical” ordering, while still not containing as much information as a local storage theory would predict. Therefore, in the Leutgeb study it is possible the graded change in CA1 responses comes from the population response moving from one stored index to another, which are all somehow organized, even though sensory aspects of the representation are unavailable (by, say, a decoder).

The second reason why the balance between local and remote (i.e. index-based) storage is unknown is the time point of analysis; it will be seen this is closely related to the concept of episodic buffers. Under indexing theory, at the time of encoding both hippocampal and neocortical neurons are engaged in the representation; over time the neocortical neurons leave the ensemble (until recalled) and the hippocampal neurons become more strongly linked. However, this proposal does not specify how much information is present within the hippocampal neurons at a given time point, and there are reasons to believe the amount of episodic information in the hippocampal ensemble is maximal at the time of encoding and decays subsequent to that, which will be proposed here. The automatic encoding hypothesis (Morris and Frey, 1997) posits that the hippocampus automatically encodes episodic information as it happens, storing it

to a short-term buffer. The information in this buffer can be used for later, offline computations, such as assisting in credit assignment. If this is the case, however, it would mean that a certain amount of episodic information must be present within the hippocampal ensemble itself, at least at the time of encoding. A hippocampal representation that serves as an index to a richer neocortical representation, but itself still contains information that will be stored in a local episodic buffer could reconcile these proposals. Further, the local hippocampal representation only needs to store this information for the lifespan of the episodic buffer. There may be, therefore, an early and late stage of episodic information storage in the hippocampus. The early and late stages of information representation within the hippocampal index may be supported by the different forms of LTP. Early LTP is a short lasting, protein-synthesis independent form of memory while late LTP is a longer lasting, protein-synthesis dependent form of LTP (Kandel et al., 2012). Early LTP may associate hippocampal and neocortical neurons during the lifespan of the episodic buffer, while late LTP may support the association of hippocampal neurons into a long-lasting index.

This discussion suggests the following model. At the time of encoding, hippocampal and neocortical ensembles are recruited; the former contains active place cells and is linked, via theta-mediated synchrony, to the neocortical ensembles that represent the content of the episodic experience (beyond its spatial location). The episodic information content in the hippocampal buffer is maximal at the point, possibly owing to the fact that the hippocampal neurons are most strongly associated with the detail-rich neocortical ensembles. After the

time of encoding, the neocortical and hippocampal neurons gradually become dissociated (and will re-associate during recall). During this stage, the ensembles are linked via early LTP. This stage corresponds to the duration of the episodic buffer, and it is the residual connection to neocortex that provides the buffer with its content. After more time, early LTP ends, the ensembles are totally disengaged, and the hippocampal ensemble has the least amount of non-spatial information. Whether any residual non-spatial information is present after this point is unknown; the work to date (including the present work) either recorded neurons as the animal was in the presence of cues – and therefore during the period of encoding or episodic buffer maintenance – or recorded neurons as animals made a memory-guided decision, which would re-instantiate the entire representation. However, the above discussion supports the notion that, at least for a time, the hippocampal index is a sparser version of the full representation that both supports the formation of long-term memory and the automatic CA1 buffer.

Infield Modulations and Computational Efficiency

The data presented here are the first to report stimulus-dependent modulations that occur on a finer spatial scale than the place field, and join other work (Itskov et al., 2011; Herzog et al., 2019) that report spatiotemporal fluctuations in CA1 activity upon cue encounter. Previous studies on rate remapping did not specify a specific pattern of rate changes that would be observed in a field; it was possible that the entire field would exhibit an additive or multiplicative gain modulation. However, the data presented here are consistent with localized fluctuations occurring within the field. This could be a

more efficient method of representation that gives the network greater storage capacity. Rather than encode all cues during the duration of an animal's encounter with them, the system could encode cues at certain points, such as reaching the cue, or leaving it. Thus the neuron would encode cue identity, but for a shorter period of time.

This may seem to run counter to the automatic recording hypothesis; if the system is only encoding certain kinds of items in the environment, such as landmarks, then by definition it is not automatically encoding the entire content of experience. This may be true under a strong version of the automatic recording hypothesis; however, it is also possible that a weaker version of the hypothesis is true that gates the automatic recording of experience to those attended locations which fall into a certain category, again regardless of reward outcome. These categories might include landmarks, defining geometric features of the environment, or other such regions that might be worth attending to without concern for whether they are rewarded. Thus, the (weaker) automatic recording hypothesis would stipulate attention and short-term encoding of all such inherently salient locations, regardless if there is any relevance to them beyond that. Put simply, even an episodic buffer tasked with faithfully encoding aspects of experience need not concern itself with every square millimeter of real estate.

Of particular importance to the present work is one potential type of inherently salient location: locations where there is more change in stimuli across time than at other locations, i.e. locations with greater experiential variance. Privileging locations where there is a greater amount of variability may be

beneficial from the standpoint of exploration versus exploitation. This distinction refers to the tradeoff between sampling opportunities known to be beneficial versus trying new choices that may be adaptive; too much of the former imposes opportunity costs, while too much of the latter risks missing available rewards (Sutton and Barto, 1992). Traditionally, locations within an environment are labeled by their reward probabilities and the agent samples them according to how it balances the exploration/exploitation tradeoff. However, the stimulus variability at a location could provide a second label for each location. To the extent the agent decides to explore a less rewarded location, considering the distribution of input variabilities across locations may increase the long-term rate of reward. The intuition for this is that locations with more change may be more likely to have a future reward than a location which is static; for a change at a location to be associated with a new reward, there have to be changes there in the first place. Therefore an agent which considers the reward distribution and the stimulus-variability distribution may achieve a larger long-term reward average than an animal that only considers reward.

The above discussion focuses on what types of cues and locations are automatically attended to, given the implications of local infield encoding. Another consideration is where this local encoding takes place relative to the cue being encoded. There are theoretical reasons to believe that boundaries where cues start and end, where landmarks are encountered, and where the environment changes (for example, the floor texture) are preferentially the site of local encoding. There is work to suggest that the distribution of place fields and the

locations of their edges respect environmental boundaries and locations such as reward sites (Wang et al., 2020; Hollup et al., 2001). If the system is sensitive to these types of locations, it is possible that the local field modulations may also occur in a manner that respects their distribution. If so, then the attributes of an environment would be coded not by their explicit representation, but by marking where they start and end (as well as their identity). This would create a compressed representation of the environment that encodes the 'episodic gradient' within an environment that can be, if needed, reconstructed into the full representation via interpolation. Encoding an episodic gradient would be a more efficient way of representing an environment while still allowing a detailed account of what items occurred within it.

In summary, the observation of cue encoding via localized fluctuations within a place field suggests intriguing possibilities for how episodic memory is encoded within CA1. Considerations of computational efficiency and utility of the map for adaptive behavior may have promoted more precise annotations to the cognitive map than would have been present if reality was more comprehensively encoded. It emphasizes what has long been known to researchers; CA1 does not create a static, rigid representation of space like a page of an atlas, but rather a flexible and adaptive cognitive construct.

Place field repetition and uncovering the representation of paths

A number of studies have supported the hypothesis that CA1 neural activity is affected by variables related to trajectory (Wood et al., 2000; Frank et al., 2000; Singer et al., 2010; Ainge et al., 2007; Ferbinteanu and Shapiro 2003; Grieves et al., 2016b). It is unclear what exactly the neurons respond to because,

first, many variables are correlated with each other (some, perfectly so). For instance, the path to a reward can be defined by the route itself, the set of allocentric (or egocentric) directions the rat faces during it, which goal is reached, the pattern of boundaries around the rat, among others. Second, the experimental designs used to date did not allow sampling from all the possible combinations of the variables above. In some of these studies, repeating cells were recorded while in others the effects were seen in single CA1 place cells. Repeating place cells offer an opportunity to better elucidate the explanatory variables underlying trajectory-related firing because the multiple fields provide a within-cell comparison. By looking at how multiple fields behave with respect to a given variable, its importance can be tested.

Representation of trajectory-related variables occurs in single-fielded CA1 neurons as well, and indeed it is in these canonical CA1 cells that most of the work has been done. Over time, CA1 recordings from an increasingly complicated set of apparatuses have shed light onto what types of path variables CA1 is attuned to. Early studies examined CA1 behavior on simple figure-eight, M-, or plus mazes in which the set of possible behaviors was limited (Wood et al., 2000; Frank et al., 2000; Ferbinteanu and Shapiro, 2003). These works characterized neurons with modulated activity based on the animal's path, but the nature of the apparatuses was too simple to dissociate, for example, coding of goal location versus path on a given trial. Further, it was unclear whether cells were tuned to single turns or more complicated trajectories. Grieves and colleagues showed strong evidence that some CA1 neurons are sensitive to the

route an animal takes to a reward (Grieves et al., 2016b) (an earlier study showed sensitivity to goal location but route and goal location were associated in their design (Ainge et al., 2007)). It is unclear how long of a route would be considered unique by the hippocampus, versus a path so long it becomes broken into parts. Segmentation of the path based on events such as reward delivery, scanning, SWR-mediated planning, or other events may occur to achieve this purpose. Indeed, some studies have reported that the theta 'look-ahead' sequence chunks the environment into pieces (Wikenheiser and Redish, 2015; Gupta et al., 2012). Interestingly, data from the Ratterdam Open design could address this question. The self-guided foraging in the present work – punctuated by rewards or self-determined pauses – creates a session comprising trajectories of different lengths around the apparatus. It is possible, in principle, to iteratively define a maximum trajectory length, in terms of number of turns through the maze and see at what point the trajectories become too long to be encoded as a single path by the hippocampus. Presupposing that there is trajectory coding in the first place, this could be tested in the following way. Begin with the shortest route length from a location, for example a single right/left turn from a particular alley. If trajectory coding is observed, i.e. a field which 'splits' depending on trajectory, then extend the route by two turns (one left, one right). Check if splitting occurs and repeat until it no longer does. In other words, the trajectory length beyond which the hippocampus no longer indicates a difference via splitting is likely the maximum route length (at least for that cell for that apparatus). .

The discussion above focuses on place cells with a single field, but of course in environments with multiple repeated spatial motifs, repetition is observed. To better understand the relationship between trajectory and repetition, consider why common apparatuses with multiple identical pieces (plus maze, T-maze, etc) do not elicit repetition. In other words, there seems to be a threshold on the number of repeating structural units in an apparatus before repetition is observed. This may be because simpler environments, despite having multiple identical parts, do not offer the opportunity to complete multiple trajectories of the same type. If the activity of repeating cells, in whole or part, can be explained by trajectory coding – and the repetition occurs because there are multiple preferred trajectories available – then by definition multiple trajectories of the same type are needed. If this interpretation is correct then the observation of repetition in more complicated mazes only (but not exclusively – Singer and co-authors saw limited repetition in a three-arm maze (Singer et al., 2010)) would not be surprising. Based on the above, it is possible that splitting, trajectory coding, and path equivalence reported in the literature are all shades of the same phenomenology, and, further, repetition is also in this category in environments with multiple available trajectories of the same type. Therefore, understanding what controls repeated cell activity may be beneficial in understanding a wider class of phenomena.

Repeating place fields, network dynamics, and competitive inhibition

An alternative interpretation of place field repetition is that it is not a natural phenomenon at all; rather, it is what happens in contrived environments

in which the hippocampal system is unable to successfully form (at most) one place field from the set of spatially-tuned inputs impinging on a CA1 neuron. Individual neurons receive input from hundreds, or even thousands, of upstream neurons. In CA1, many of these inputs are themselves spatially tuned, such as the border cells discussed in the Introduction, or modulated by various spatial and non-spatial features of the environment. Thus, as the rat moves throughout an environment, each neuron exhibits a landscape of membrane potential (Vm) with peaks and valleys corresponding to areas of the environment where more, or fewer, spatially-tuned inputs to that cell are active. For a CA1 neuron with a single place field, this landscape would appear to have a dominant peak in membrane potential corresponding to the place field. Everywhere else on the membrane potential landscape would be below some threshold, and therefore few spikes would occur at these locations. The fact that there is a threshold that can separate a single Vm hill (the place field) from the rest of the landscape is not an accident; place cells are by definition those cells which have parameters, set through the various mechanisms of place field recruitment, such that a single supra-threshold peak occurs (Epsztein et al. 2011; Harvey et al., 2009; Lee et al, 2012). Below this threshold, across the environment, are many peaks corresponding to places where the cell is receiving spatially-tuned input, but not enough to pass threshold and produce spiking. In an environment with repeating spatial features, an upstream input tuned to this repeating feature will drive multiple Vm peaks at each such location. Under normal circumstances at most one of these will become a place field because other inputs presumably inhibit

the cell (directly or indirectly) at other locations. However, the types of environments that induce place field repetition are unnatural and contrived environments. The sensory and head direction inputs are identical across multiple similar regions. Consider further that CA1 neurons do not receive identical inputs; the input fibers do not synapse in an all-to-all fashion, and therefore individual CA1 neurons will have different input patterns. Therefore there will be, through chance wiring alone, some neurons which receive even stronger border input than do other CA1 neurons. In a naturalistic environment the place field recruitment process can select a single field per cell because of the heterogeneous sensory, geometric, and self-motion cues present throughout the environment. However, in the case of an environment with repetition, and cells with unusually strong border input, the sensory and some self-motion cues do not disambiguate the environment. The border cell input is one of the few spatially-variable inputs left and it is strong enough to drive the place cell by itself. Thus, a repeating place cell is created. Therefore, the multiple fields observed in these situations are not traditional fields, in the sense that in a normal environment they would only exist as subthreshold peaks. The network dynamics that attempt to select a single place field may manifest as competitive inhibition between repeating place fields. Although speculative, it is plausible that while the process of place field recruitment occurs, a feedback process may assist in potentiating a single field and suppressing activity at other fields. The animal's behavior may play a crucial role in this, particularly if the fields are tuned to behavioral variables, such as direction or turn. As the animal moves through

the positions where these subthreshold peaks are, it will enter some fields in a preferred manner and others in an anti-preferred manner, depending on the vagaries of behavior. When the animal passes through a peak in a preferred manner the peak will be potentiated, and conversely the peak will be de-potentiated when the animal passes through in a non-preferred manner. If there is competitive inhibition between the peaks, then this may allow one field to predominate. A field that becomes potentiated could be more able to suppress the neighboring fields; conversely a de-potentiated field is less able to do so (and the discrepancy could be amplified if a potentiated field inhibits a field that has been de-potentiated). Under normal circumstances, this process terminates when one peak predominates and becomes the place field.

However, this process is contingent on having disambiguating inputs (e.g. head direction, sensory inputs) that assist in the field selection process. These inputs are different at different peaks, and so they contribute to the membrane potential differences between peaks that ultimately result in field selection. Because these inputs are not sufficiently different between peaks in an environment that promotes repetition, the peaks never become different enough for one to be selected. However, the inter-field competitive inhibition still occurs. Thus, in a repeating environment, these competitive interactions persist without conclusion and cause fields to wax and wane in their firing rates. The temporal dynamics observed in this data set may very well be the signature of these competitive interactions. If the pattern of inter-field rate dynamics could be explained in terms of competitive interactions – possibly by fitting the behavior to

a model – then place field repetition could be recast as an opportunity to study dynamics at the population level that previously could only be studied unit by unit (with the caveat that now that the dynamics cause spiking, the network behavior is altered compared to if the dynamics were subthreshold).

Place Field Repetition as Efficient Coding

This discussion may lead one to believe place field repetition is simply a pathological case found in peculiar environments. The arguments related to learning made by Grieves and colleagues would support this view (but again, c.f. Singer et al. 2010). This may be the case; however there are other interpretations of the data, as well. It is possible that place field repetition reflects an efficient coding strategy in environments that can be represented by a 'basis set' of locations. A repeating environment could be represented by a set of signals, each of which responds to one of the repeating patterns. The combination of these signals could be decoded to reveal the exact position. For instance, in Chapter 4, the open Ratterdam apparatus consists of twenty-nine locations (seventeen alleys and twelve intersections) arranged in a city-block grid. However, this arena could also be expressed as a basis set of three features: vertical alleys, horizontal alleys, and intersections. It is possible that neurons could respond to one of these elementary features, and location within the maze could be deciphered by reading out combinations of such units. The hippocampus recruits a number of neurons to tile an environment. However, the number of neurons needed scales linearly with the size of the environment. If there are additional complexities present (task variables, non-spatial cues, etc.) then more neurons are needed to reflect those variables as well as spatial

location. However, if neurons instead encoded one of the elementary parameters that define a symmetric/repeating environment such as Ratterdam, then far fewer neurons would be needed. A certain number of ‘column cells’ and ‘row cells’ could exist and a given pair, in principle, could uniquely define an alley. Thus, the presence of place field repetition may be an adaptation to environments with a structure that can be exploited for computational efficiency. However, it is speculative as to what environments existed in the evolutionary history of the rodent lineage that would benefit from such a representation.

Conclusion

The results of this thesis, concerning rate remapping and place field repetition, provide insight into how the content of experience is incorporated into the CA1 place map. Place cells are not a spotlight saying ‘you-are-here’ – this has been known since the earliest reports of their existence (see ‘misplace’ units, O’Keefe, 1976). However, the striking nature of the place field – one of the clearest signals in the entire nervous system – understandably drew disproportionate attention to the purely spatial computations performed by the place map. But evidence has accumulated that all manner of non-spatial cues are also recorded by the map: CS signals, odors, sounds, textures, tastes, rewards, internal motivational state, time, turns the animal is about to make, turns the animals has just made, trajectory, direction, match-status, trial type, and surely more yet to be reported. This has led to the suggestion that space is not really what the hippocampal system represents; it is an arbitrary associator and space simply happens to be a ubiquitous variable (Cohen and Eichenbaum, 1993; Wood et al., 1999; Aronov et al., 2017; Itskov et al., 2011; Herzog et al.,

2019; Hollup et al., 2001; Kennedy and Shapiro, 2009; Manns and Eichenbaum, 2009; MacDonald et al., 2011; Ferbinteanu and Shapiro, 2003; Wood et al., 2000; Markus et al., 1995). While an expansive view of what such a flexible network can do is well-taken, the view expressed here is that it is no coincidence that every electrode ever implanted into the hippocampus has revealed a spatial signal; this is a fundamental variable upon which other representations are overlaid. Indeed, this is the central thesis of the cognitive map theory; that such a binding of space and content allows episodic memory to be adaptively encoded.

Among the non-spatial variables encoded within the place map, there is a distinction between sensory variables, those related to abstract operant categories like trial type, and those quasi-spatial ones such as trajectory. The presence of more abstract variables, and particularly those related to paths and movements, suggests that the map does not simply ‘drop a pin’ to indicate the presence of some cue (although that simplified terminology has been used throughout this work for its intuitive value). It seems to be the case that place fields are not simply ‘pixels’ in some cognitive atlas, but rather are part of dynamic representations of the world and how we interact with it. A place field at a start box clearly encodes a location. But when that field’s activity is gated by the route the animal takes to a goal, then it is clear the hippocampal place system is more than a verisimilar map. It may be topographical, metric-based, and Euclidian (as O’Keefe and Nadel proposed). But it is also concerned with what sorts of locations are important, how the sensory environment changes around us, how we move through the world, and even how pieces of the world

relate to one another. It is less a transcription of world onto tissue, and more an adaptive interaction between a complex, changing world and a small seahorse-shaped patch of tissue trying to successfully navigate within it.

Appendix

A1 Histology

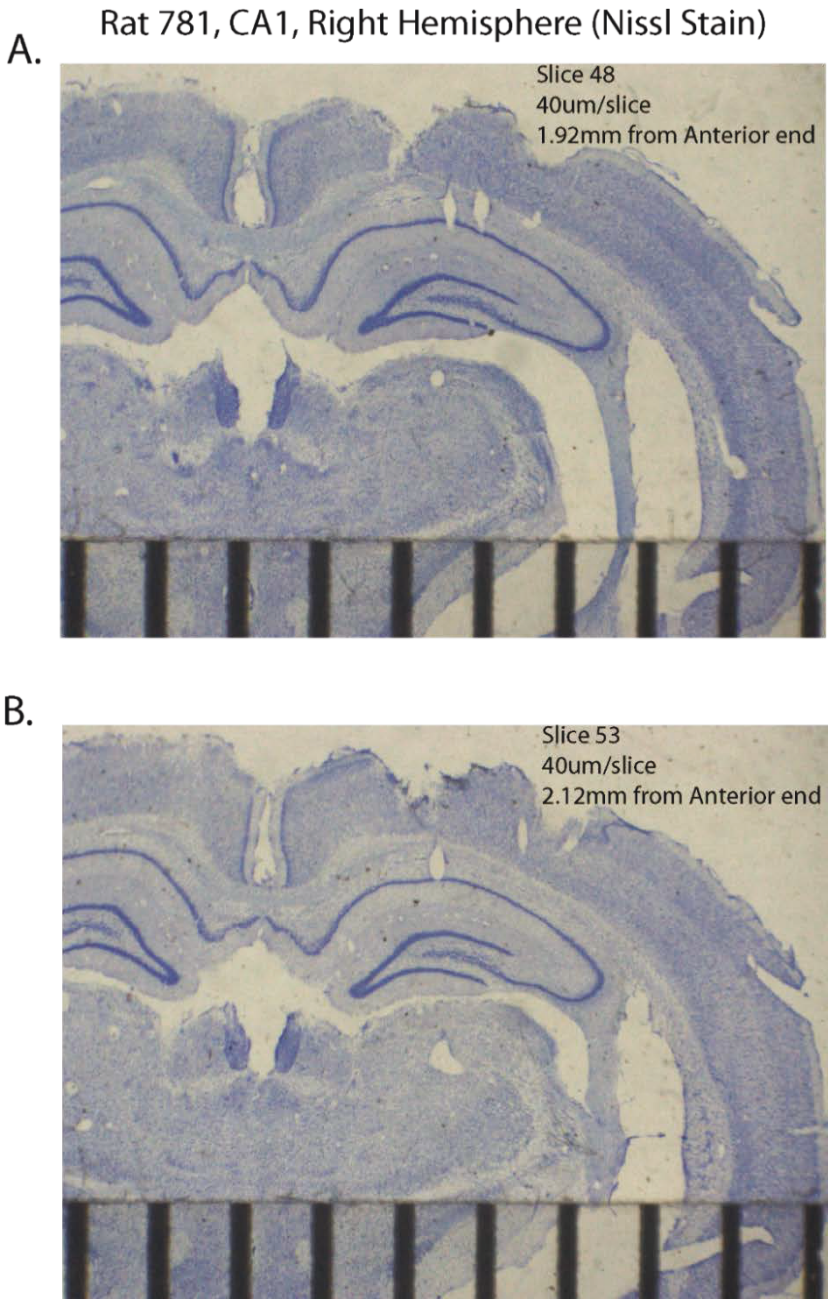

Fig A1-1. Histology from R781. Both panels are 40 µm slices, Nissl stained from the right hemisphere CA1. Tears in/near CA1 layer indicate location of tetrode tracks. Black scale bars are in mm. **A.** Two tetrode tracks are visible in intermediate CA1 at 1.92 mm along the anterior-posterior axis (A-P axis), starting from anterior. **B.** One tetrode track visible in intermediate CA1 at 2.12 mm A-P.

A.

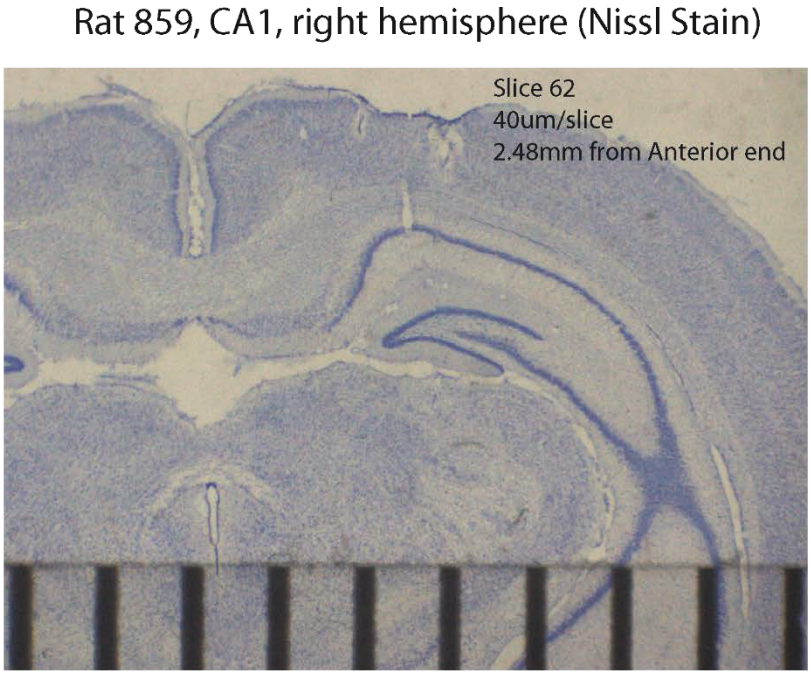

B.

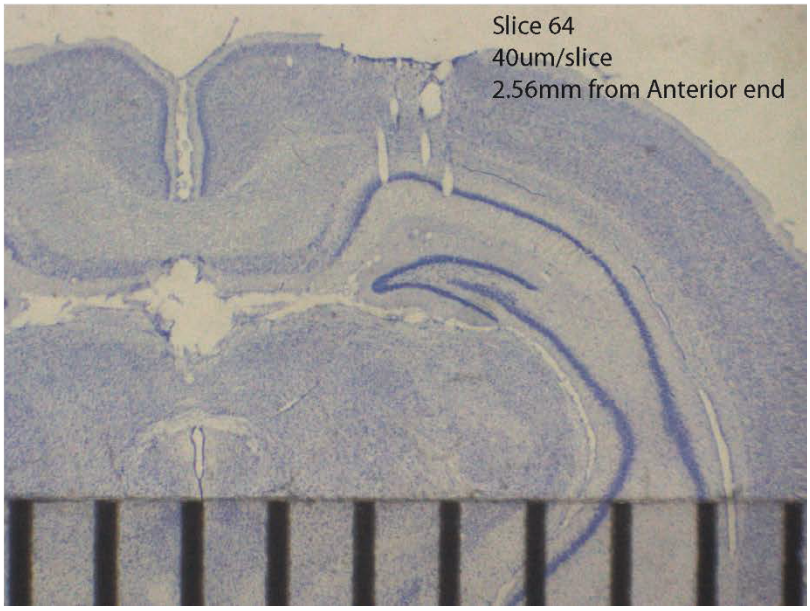

Fig A1-2. Histology from R859. Both panels are 40 μm slices, Nissl stained from the right hemisphere CA1. Tears in/near CA1 layer indicate location of tetrode tracks. Black scale bars are in mm. **A.** One tetrode track is visible in proximal CA1 at 2.48 mm along the anterior-posterior axis (A-P axis), starting from anterior. **B.** Three tetrode tracks are visible in/near proximal CA1 at 2.56 mm A-P.

A2 Pilot Experiment: Match-to-sample task on a T-maze

This appendix describes a pilot experiment that led to the experiment described in Chapter 3 of the main text. These pilot data were presented at the 2018 Society for Neuroscience Conference

Citation:

(**Hockeimer, W** and Knierim, J.J. “Firing Rate Modulations May Encode Surface Texture Cues Within The Place Cell Map Of Hippocampal CA1 Neurons” Society for Neuroscience. San Diego. 2018.)

Abstract

The hippocampus is thought to instantiate a cognitive map that multiplexes spatial and non-spatial information (O’Keefe and Nadel, 1978; Leutgeb et al., 2005a; Wood et al., 1999; Herzog et al., 2019; Manns and Eichenbaum, 2009). However, this hypothesis has not been fully tested. To explore this idea further, pilot electrophysiological data from hippocampal CA1 were collected from a rat trained on a match-to-sample task. The data revealed a significant subset of neurons that responded to differences in the task cues (18/94 neurons, $p < 8.88*10^{-7}$, one-sided binomial test, alpha = 0.05). The effect of stimulus was potentially affected by directionality and turn choice, although these effects were not quantified. These data support the hypothesis that CA1 neurons multiplex spatial and non-spatial information, and justified further data collection, using a different experimental design, which were reported in Chapter 3.

Introduction

The background for the pilot data has been introduced in the General Introduction and the Chapter 3 Introduction. In brief, the hypothesis to be tested was that stable place fields would modulate their firing in a stimulus-dependent manner. This hypothesis would be supported by identifying a statistically significant subpopulation of neurons that displayed a significant difference in firing rate through the spatial extent of the field in a stimulus-dependent manner.

Methods

A single rat was trained to perform a match-to-sample task. The stimuli were removable floorplates with different tactile and visual qualities (note, these were not the same stimuli used in Chapter 3). On each trial, a stimulus was present on each arm and the stem of a T-maze (Fig A2-1A); one of the stimuli on the arms would match that of the stem and indicate the presence of reward at that arm.

Pre-training proceeded in stages (note, multiple rats were trained on this task, while only one was implanted with a hyperdrive). First, a rat was acclimated to the apparatus and the reward locations, with reward dispensed regardless of arm choice. On each trial, the rat began in a start box, ran down the stem to the decision point (the section joining the arms with the stem) and made a decision to go down the right or left arms. After the trial was over the rat returned to the start box. Next, two matching stimuli were placed on the stem and the rewarded arm; from here on, choosing the arm with the non-matching stimulus was defined as an incorrect choice and resulted in a timeout. After the rat learned to follow the

stimulus, a non-matching distractor was placed on the non-rewarded arm, but at a distance from the matching one. Over trials and days, the distractor was moved closer to the matching stimulus until they met in the middle of the stimulus on the arm (Fig A2-1A). Three stimuli were used; across trials, the choice of stimuli, rewarded arm, and the combination between reward and stimulus were automatically counterbalanced. A Python script controlled the task while an Arduino script/microcontroller controlled the task hardware.

A hyperdrive was built and implanted as described in the General Methods section. A permutation test was used to analyze a significant texture response as described in Chapter 3. Given the potential role of directionality and arm choice on CA1 activity, data were sorted multiple ways. Trials were grouped according to the arm chosen and labeled with what texture was present on one of the arms of the T-maze. For instance, one possible grouping was all trials where the right arm was chosen, grouped by what texture was present on the stem. Finally, each trial was divided into outbound and inbound trajectories, which were concatenated together. A schematic of the ways in which trials were divided, sorted by choice and texture location, is shown in Fig A2-1B. Each trial was linearized and divided into the portions of the trial on the stem, right arm, and left arm (noting that only one arm will be sampled beyond the middle of the arm based on how decisions are defined). Fig A2-1D, top, shows the way the trial is broken down; the grey lines show the arm boundaries and the red line divides outgoing and inbound trajectories.

Results

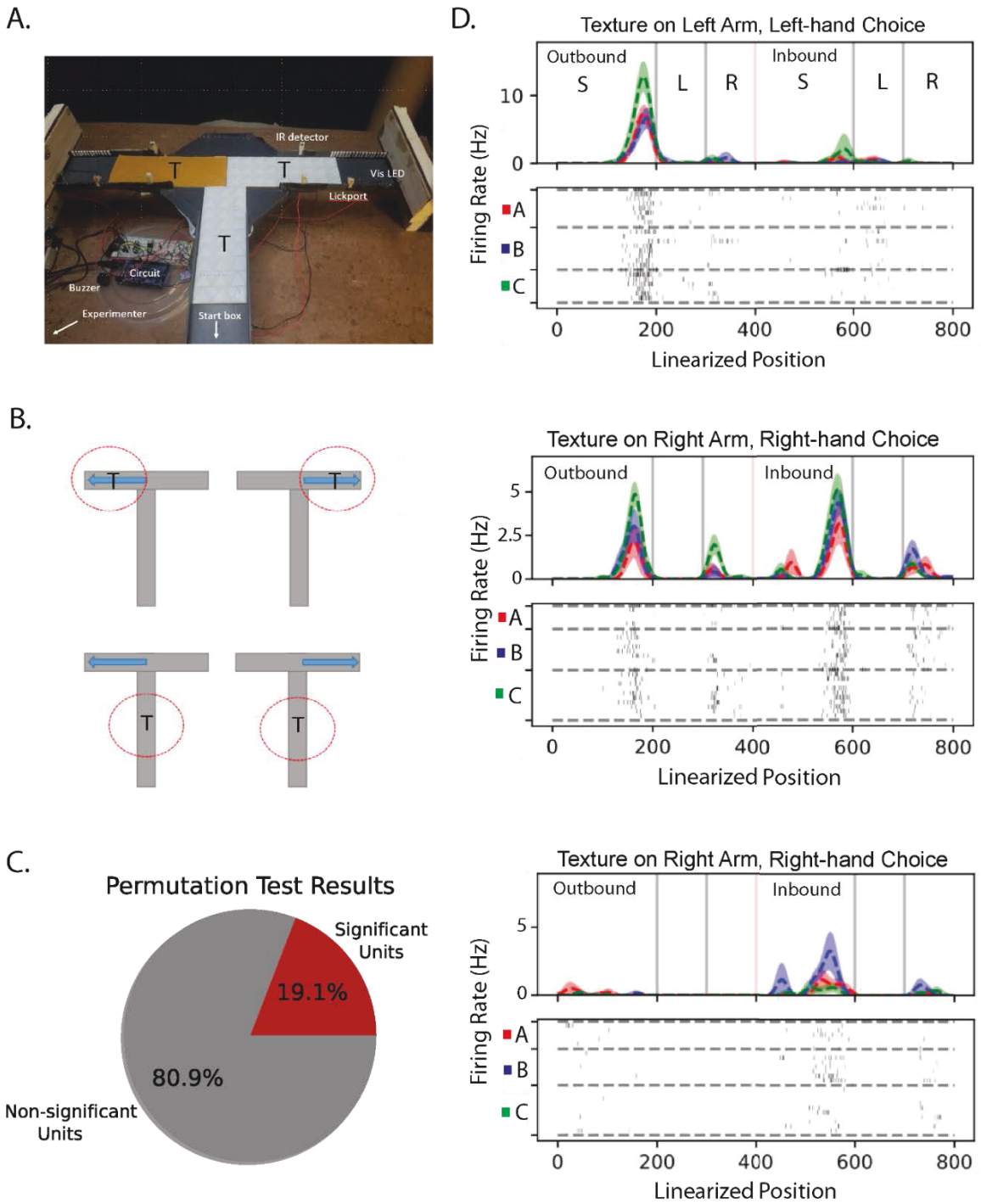

A single rat was implanted with a hyperdrive in CA1. Data were pooled across days and examined for an effect of stimulus on firing rate. The data for each cell and for each trial were grouped as described in the Methods. A significant number of neurons displayed significant effects on firing rate of texture

Fig A2-1. T-maze Pilot Data. **A**. Annotated picture of the T-maze task. Photo is taken from start box position. An example trial is shown with a match stimulus on the right arm ("T" indicates texture positions). Two IR emitter-detector pairs, on each arm, were triggered when an animal made a decision. The visible LED and buzzer served as feedback cues. Not shown, a blocking card that kept the rat in an incorrectly chosen arm for a timeout period. **B**. Schematic showing how trials were organized for analysis. A single day typically consisted of 60 trials. These were grouped into categories based on the arm chosen and labeled according to a single texture location. In other words, a single grouping might divide all trials based on what texture was present on the stem when the rat went left. Another way of grouping would do so based on the texture on the left arm. These groupings would be identical when the matching texture was on the left arm (and the animal chose correctly). **C.** Pie chart showing the proportion of neurons, across days, which had significant texture information according to a permutation test. **D.** Three example units with significant texture information. In each, the top panel shows the average firing rate from the trials grouped according to the label on top, +/- the standard error of the mean. On bottom, the raster plots for each trial, grouped by the texture present on the arm indicated in the label. The x-axis corresponds to the linearized position. The outgoing stem, left, and right arms are concatenated with the incoming stem, left, and right arms on a scale from 0-800 bins. Grey lines show the arm boundaries (see top) and the red line shows boundary between outbound and inbound journeys, defined as the rat's encounter with the lickport. Top, CA1 cell with directional firing field, more active on the outbound journey compared to the inbound. Within the outbound journey, the cell fired more when texture C was present compared to the other stimuli. Middle, cell with field at the end of the stem, extending onto the right arm. The neuron fired more for texture C at the end of the stem on the outbound journey compared to the inbound journey. Bottom, Directional cell with field at the end of the stem on the inbound journey. The cell fired predominantly when texture B was present compared to the other textures.

based on the permutation test (Fig A2-1C; 18/94 neurons, $p < 8.88*10^{-7}$, one-sided binomial test, alpha = 0.05). At a single-unit level, the fields exhibited complicated firing rate patterns based on texture, with variables such as direction and choice seeming to gate the rate remapping effect (although these were not specifically quantified).

Three example units are shown in Fig A2-1D that passed the permutation test. In each set of panels, the top panel shows the average firing rate, +/- the standard error of the mean, of trials under each texture, according to the grouping definition labeled. For instance, in the top panel the trials were divided

into groups based on whether A, B, or C were present on the left arm and the animal made a left choice. The bottom shows raster plots for each trial.

In the first example, a neuron has a single field at the distal end of the stem (from the start box) with some activity on the right arm (Fig A2-1D, top). The field is directional; the cell fires as the animal walks down the stem, but is much quieter as the animal passes through the same location on the return journey. The firing when texture C was present was greater than the firing when the other textures were present. Further, this example shows that the neuron fired in the decision area of the apparatus – at the end of the stem near the beginning of the arms – in a stimulus-dependent manner. In the second example, trials were organized based on the texture present on the right arm when the animal made a right-hand choice. This cell had a field on the end of the stem, which also extended onto the right arm (Fig A2-1D, middle). The firing field on the stem was less directionally tuned than in the previous example; the cell fired in that location regardless of the direction of travel. However, on the outbound journey, the cell fired more strongly when texture C was present compared to the other two. Further, the section of the firing field on the right arm seemed to be more texture-selective than the main field; in this region, the cell fired on only three trials between both A and B conditions, but fired on all trials when C was present (although, on three of them the firing was either weak or spatially-shifted with respect to the majority of C trials). Given that these trials were organized based on the texture on the right arm when the animal chose that arm, this cell appeared to fire for texture C when it was the texture about to be chosen. In the

last example, a neuron with a directional field was present on the stem, with a preference for inbound travel (Fig A2-1D, bottom). On the trajectory back to the start box, the cell fired reliably when texture B was present, and less so when textures A or B were present.

Discussion

These data support the rate remapping hypothesis that CA1 neurons encode non-spatial cues in the firing rate envelopes of stable spatial fields. A significant number of neurons exhibited a significant texture effect, based on a permutation test per unit and binomial test on the responsive subpopulation. The discussion of the rate remapping hypothesis is discussed in the Chapter 3 discussion and the General Discussion. However, further topics merit discussion given the differences between this task and that of the one in Chapter 3.

The different ways of organizing trials made clear, anecdotally, the fact that these CA1 neurons were sensitive not only to texture, but to other variables such as direction and arm choice. Specifically, these other variables seemed to gate the presence of a texture signal. This raises the intriguing possibility that rate remapping may interact with the trajectory coding discussed in Chapter 4. The three examples in Fig A2-1D are organized, in part, by the arm choice. It is well-known that the path an animal takes can affect place field firing (Wood et al. 2000; Frank et al., 2000; Grieves et al., 2016b). The fact that stimulus encoding is only visible when sorting trials according to trajectory indicates that this encoding could interact with the representation of trajectory. It is possible that the encoding of trajectory is sensitive to cues along the trajectory; in this case, the

CA1 neuron is not only responding to the topographical features of the route, but also the features of the route as the animal experiences it. This would comport well with the cognitive map theory; it is not simply locations that are encoded, but pieces of the world as we move through and experience them.

References

Ainge, J. A., et al. “Hippocampal CA1 Place Cells Encode Intended Destination on a Maze with Multiple Choice Points.” *Journal of Neuroscience*, vol. 27, no. 36, Sept. 2007, pp. 9769–79. *DOI.org (Crossref)*, doi:10.1523/JNEUROSCI.2011-07.2007.

Alme, Charlotte B., et al. “Place Cells in the Hippocampus: Eleven Maps for Eleven Rooms.” *Proceedings of the National Academy of Sciences*, vol. 111, no. 52, Dec. 2014, pp. 18428–35. *DOI.org (Crossref)*, doi:10.1073/pnas.1421056111.

Amaral, D. G., and M. P. Witter. “The Three-Dimensional Organization of the Hippocampal Formation: A Review of Anatomical Data.” *Neuroscience*, vol. 31, no. 3, Jan. 1989, pp. 571–91. *DOI.org (Crossref)*, doi:10.1016/0306-4522(89)90424-7.

Amaral, David, and Pierre Lavenex. *Hippocampal Neuroanatomy.* Oxford University Press, 2007.

Anderson, Michael I., and Kathryn J. Jeffery. “Heterogeneous Modulation of Place Cell Firing by Changes in Context.” *The Journal of Neuroscience*, vol. 23, no. 26, Oct. 2003, pp. 8827–35. *Crossref*, doi:10.1523/JNEUROSCI.23-26-08827.2003.

Andersen, Per, et al., eds. *The hippocampus book*. Oxford university press, 2006.

Aronov, Dmitriy, et al. “Mapping of a Non-Spatial Dimension by the Hippocampal–Entorhinal Circuit.” *Nature*, vol. 543, no. 7647, Mar. 2017, pp. 719–22. *DOI.org (Crossref)*, doi:10.1038/nature21692.

Barry, Caswell, and Neil Burgess. “Learning in a Geometric Model of Place Cell Firing.” *Hippocampus*, vol. 17, no. 9, Sept. 2007, pp. 786–800. *DOI.org (Crossref)*, doi:10.1002/hipo.20324.

Bostock, Elizabeth, et al. “Experience-Dependent Modifications of Hippocampal Place Cell Firing.” *Hippocampus*, vol. 1, no. 2, 1991, pp. 193–205. *Wiley Online Library*, doi:10.1002/hipo.450010207.

Brandon, Mark P., et al. “New and Distinct Hippocampal Place Codes Are Generated in a New Environment during Septal Inactivation.” *Neuron*, vol. 82, no. 4, May 2014, pp. 789–96. *DOI.org (Crossref)*, doi:10.1016/j.neuron.2014.04.013.

Brincat, Scott L., and Earl K. Miller. “Frequency-Specific Hippocampal-Prefrontal Interactions during Associative Learning.” *Nature Neuroscience*, vol. 18, no. 4, Apr. 2015, pp. 576–81. *DOI.org (Crossref)*, doi:10.1038/nn.3954.

Buzsáki, György. “Hippocampal Sharp Waves: Their Origin and Significance.” *Brain Research*, vol. 398, no. 2, Elsevier, 1986, pp. 242–252.

Cai, Denise J., et al. “A Shared Neural Ensemble Links Distinct Contextual Memories Encoded Close in Time.” *Nature*, vol. 534, no. 7605, June 2016, pp. 115–18. *DOI.org (Crossref)*, doi:10.1038/nature17955.

Carpenter, Francis, et al. “Grid Cells Form a Global Representation of Connected Environments.” *Current Biology*, vol. 25, no. 9, May 2015, pp. 1176–82. *DOI.org (Crossref)*, doi:10.1016/j.cub.2015.02.037.

Colgin, Laura L., et al. “Attractor-Map Versus Autoassociation Based Attractor Dynamics in the Hippocampal Network.” *Journal of Neurophysiology*, vol. 104, no. 1, July 2010, pp. 35–50. *Crossref*, doi:10.1152/jn.00202.2010.

Cowen, S. L., and D. A. Nitz. “Repeating Firing Fields of CA1 Neurons Shift Forward in Response to Increasing Angular Velocity.” *Journal of Neuroscience*, vol. 34, no. 1, Jan. 2014, pp. 232–41. *DOI.org (Crossref)*, doi:10.1523/JNEUROSCI.1199-13.2014.

Csicsvari, Jozsef, et al. “TFast Network Oscillations in the Hippocampal CA1 Region of the Behaving Rat.” *The Journal of Neuroscience*, vol. 19, no. 16, Aug. 1999, pp. RC20–RC20. *DOI.org (Crossref)*, doi:10.1523/JNEUROSCI.19-16-j0001.1999.

Delacour, J. “Two Neuronal Systems Are Involved in a Classical Conditioning in the Rat.” *Neuroscience*, vol. 13, no. 3, Nov. 1984, pp. 705–15. *DOI.org (Crossref)*, doi:10.1016/0306-4522(84)90090-3.

Derdikman, Dori, et al. “Fragmentation of Grid Cell Maps in a Multicompartment Environment.” *Nature Neuroscience*, vol. 12, no. 10, Oct. 2009, pp. 1325–32. *DOI.org (Crossref)*, doi:10.1038/nn.2396.

Deshmukh, Sachin S., and James J. Knierim. “Representation of Non-Spatial and Spatial Information in the Lateral Entorhinal Cortex.” *Frontiers in Behavioral Neuroscience*, vol. 5, 2011. *Crossref*, doi:10.3389/fnbeh.2011.00069.

Edwards, Charles Henry, et al. *Differential Equations & Linear Algebra*. London, 2001.

Eichenbaum, H., et al. “Cue-Sampling and Goal-Approach Correlates of Hippocampal Unit Activity in Rats Performing an Odor-Discrimination Task.” *The Journal of Neuroscience*, vol. 7, no. 3, Mar. 1987, pp. 716–32. *DOI.org (Crossref)*, doi:10.1523/JNEUROSCI.07-03-00716.1987.

Eichenbaum, Howard, and others. *Memory, Amnesia, and the Hippocampal System*. MIT press, 1993.

Epsztein, Jérôme, et al. “Intracellular Determinants of Hippocampal CA1 Place and Silent Cell Activity in a Novel Environment.” *Neuron*, vol. 70, no. 1, Apr. 2011, pp. 109–20. *DOI.org (Crossref)*, doi:10.1016/j.neuron.2011.03.006.

Ergorul, Ceren, and Howard Eichenbaum. "The hippocampus and memory for “what,”“where,” and “when”." *Learning & Memory* 11.4 (2004): 397-405.

Fenton, André A., Gyorgy Csizmadia, and Robert U. Muller. "Conjoint control of hippocampal place cell firing by two visual stimuli: I. The effects of moving the stimuli on firing field positions." *The Journal of General Physiology* 116.2 (2000): 191-210.

Ferbinteanu, Janina, and Matthew L. Shapiro. “Prospective and Retrospective Memory Coding in the Hippocampus.” *Neuron*, vol. 40, no. 6, Dec. 2003, pp. 1227–39. *DOI.org (Crossref)*, doi:10.1016/S0896-6273(03)00752-9.

Fortin, Norbert J., et al. “Critical Role of the Hippocampus in Memory for Sequences of Events.” *Nature Neuroscience*, vol. 5, no. 5, May 2002, pp. 458–62. *DOI.org (Crossref)*, doi:10.1038/nn834.

Frank, Loren M., et al. “Trajectory Encoding in the Hippocampus and Entorhinal Cortex.” *Neuron*, vol. 27, no. 1, July 2000, pp. 169–78. *DOI.org (Crossref)*, doi:10.1016/S0896-6273(00)00018-0.

Fuhs, Mark C., et al. “Influence of Path Integration Versus Environmental Orientation on Place Cell Remapping Between Visually Identical Environments.” *Journal of Neurophysiology*, vol. 94, no. 4, Oct. 2005, pp. 2603–16. *DOI.org (Crossref)*, doi:10.1152/jn.00132.2005.

Fujisawa, Shigeyoshi, et al. “Behavior-Dependent Short-Term Assembly Dynamics in the Medial Prefrontal Cortex.” *Nature Neuroscience*, vol. 11, no. 7, July 2008, pp. 823–33. *DOI.org (Crossref)*, doi:10.1038/nn.2134.

Fyhn, Marianne, et al. “Hippocampal Remapping and Grid Realignment in Entorhinal Cortex.” *Nature*, vol. 446, no. 7132, Mar. 2007, pp. 190–94. *DOI.org (Crossref)*, doi:10.1038/nature05601.

Goodale, Melvyn A., and A. David Milner. "Separate visual pathways for perception and action." (1992): 20-25.

Gothard, Katalin M., William E. Skaggs, and Bruce L. McNaughton. "Dynamics of mismatch correction in the hippocampal ensemble code for space: interaction between path integration and environmental cues." *Journal of Neuroscience* 16.24 (1996): 8027-8040.

Grieves, Roddy M, Éléonore Duvelle, et al. “A Boundary Vector Cell Model of Place Field Repetition.” *Spatial Cognition & Computation*, vol. 18, no. 3, July 2018, pp. 217–56. *DOI.org (Crossref)*, doi:10.1080/13875868.2018.1437621.

Grieves, Roddy M., Éléonore Duvelle, et al. “Field Repetition and Local Mapping in the Hippocampus and the Medial Entorhinal Cortex.” *Journal of Neurophysiology*, vol. 118, no. 4, Oct. 2017, pp. 2378–88. *DOI.org (Crossref)*, doi:10.1152/jn.00933.2016.

(b) Grieves, Roddy M, Emma R. Wood, et al. “Place Cells on a Maze Encode Routes Rather than Destinations.” *ELife*, vol. 5, June 2016. *Crossref*, doi:10.7554/eLife.15986.

(a) Grieves, Roddy M., Bryan W. Jenkins, et al. “Place Field Repetition and Spatial Learning in a Multicompartment Environment.” *Hippocampus*, vol. 26, no. 1, 2016, pp. 118–34. *Wiley Online Library*, doi:10.1002/hipo.22496.

Gupta, Anoopum S., et al. “Segmentation of Spatial Experience by Hippocampal Theta Sequences.” *Nature Neuroscience*, vol. 15, no. 7, July 2012, pp. 1032–39. *Crossref*, doi:10.1038/nn.3138.

Hafting, Torkel, et al. “Microstructure of a Spatial Map in the Entorhinal Cortex.” *Nature*, vol. 436, no. 7052, Aug. 2005, pp. 801–06. *DOI.org (Crossref)*, doi:10.1038/nature03721.

Harland, Bruce, et al. “Lesions of the Head Direction Cell System Increase Hippocampal Place Field Repetition.” *Current Biology*, vol. 27, no. 17, Sept. 2017, pp. 2706-2712.e2. *DOI.org (Crossref)*, doi:10.1016/j.cub.2017.07.071.

Harris, Kenneth D., et al. *Spike Train Dynamics Predicts Theta- Related Phase Precession in Hippocampal Pyramidal Cells*. 2002, p. 4.

Hartley, Tom, et al. “Modeling Place Fields in Terms of the Cortical Inputs to the Hippocampus.” *Hippocampus*, vol. 10, no. 4, 2000, pp. 369–79. *Wiley Online Library*, doi:10.1002/1098-1063(2000)10:4<369::AID-HIPO3>3.0.CO;2-0.

Harvey, Christopher D., et al. “Intracellular Dynamics of Hippocampal Place Cells during Virtual Navigation.” *Nature*, vol. 461, no. 7266, Oct. 2009, pp. 941–46. *DOI.org (Crossref)*, doi:10.1038/nature08499.

Hastie, Trevor, et al. *The Elements of Statistical Learning: Data Mining, Inference, and Prediction*. Springer Science & Business Media, 2009.

Hayman, Robin, et al. “Anisotropic Encoding of Three-Dimensional Space by Place Cells and Grid Cells.” *Nature Neuroscience*, vol. 14, no. 9, Sept. 2011, pp. 1182–88. *DOI.org (Crossref)*, doi:10.1038/nn.2892.

Hayman, Robin M. A., et al. “Context-Specific Acquisition of Location Discrimination by Hippocampal Place Cells.” *European Journal of Neuroscience*, vol. 18, no. 10, Nov. 2003, pp. 2825–34. *DOI.org (Crossref)*, doi:10.1111/j.1460-9568.2003.03035.x.

Herzog, Linnea E., et al. “Interaction of Taste and Place Coding in the Hippocampus.” *The Journal of Neuroscience*, vol. 39, no. 16, Apr. 2019, pp. 3057–69. *DOI.org (Crossref)*, doi:10.1523/JNEUROSCI.2478-18.2019.

Hirase, Hajime, et al. “Firing Rate and Theta-Phase Coding by Hippocampal Pyramidal Neurons during ‘Space Clamping’: Theta Phase of Hippocampal Pyramidal Cells.” *European Journal of Neuroscience*, vol. 11, no. 12, Dec. 1999, pp. 4373–80. *DOI.org (Crossref)*, doi:10.1046/j.1460-9568.1999.00853.x.

Hollup, Stig A., et al. “Accumulation of Hippocampal Place Fields at the Goal Location in an Annular Watermaze Task.” *The Journal of Neuroscience*, vol. 21, no. 5, Mar. 2001, pp. 1635–44. *DOI.org (Crossref)*, doi:10.1523/JNEUROSCI.21-05-01635.2001.

Holscher, Christian, et al. “Learned Association of Allocentric and Egocentric Information in the Hippocampus.” *Experimental Brain Research*, vol. 158, no. 2, Sept. 2004. *DOI.org (Crossref)*, doi:10.1007/s00221-004-1896-z.

Hopfield, John J. "Neurons with graded response have collective computational properties like those of two-state neurons." *Proceedings of the national academy of sciences* 81.10 (1984): 3088-3092.

Høydal, Øyvind Arne, et al. “Object-Vector Coding in the Medial Entorhinal Cortex.” *Nature*, vol. 568, no. 7752, Apr. 2019, pp. 400–04. *DOI.org (Crossref)*, doi:10.1038/s41586-019-1077-7.

Itskov, Pavel M., et al. “Hippocampal Representation of Touch-Guided Behavior in Rats: Persistent and Independent Traces of Stimulus and Reward Location.” *PLoS ONE*, edited by Ehsan Arabzadeh, vol. 6, no. 1, Jan. 2011, p. e16462. *DOI.org (Crossref)*, doi:10.1371/journal.pone.0016462.

Jacobs, N. S., et al. “Critical Role of the Hippocampus in Memory for Elapsed Time.” *Journal of Neuroscience*, vol. 33, no. 34, Aug. 2013, pp. 13888–93. *DOI.org (Crossref)*, doi:10.1523/JNEUROSCI.1733-13.2013.

Jensen, Ole, and John E. Lisman. "Position reconstruction from an ensemble of hippocampal place cells: contribution of theta phase coding." *Journal of neurophysiology* 83.5 (2000): 2602-2609.

Kandel, Eric R., et al. *Principles of Neural Science*. McGraw-hill New York, 2000.

Kennedy, P. J., and M. L. Shapiro. “Motivational States Activate Distinct Hippocampal Representations to Guide Goal-Directed Behaviors.” *Proceedings of the National Academy of Sciences*, vol. 106, no. 26, June 2009, pp. 10805–10. *DOI.org (Crossref)*, doi:10.1073/pnas.0903259106.

Kentros, C. “Abolition of Long-Term Stability of New Hippocampal Place Cell Maps by NMDA Receptor Blockade.” *Science*, vol. 280, no. 5372, June 1998, pp. 2121–26. *DOI.org (Crossref)*, doi:10.1126/science.280.5372.2121.

Knierim, James J. “Dynamic Interactions between Local Surface Cues, Distal Landmarks, and Intrinsic Circuitry in Hippocampal Place Cells.” *The Journal of Neuroscience*, vol. 22, no. 14, July 2002, pp. 6254–64. *DOI.org (Crossref)*, doi:10.1523/JNEUROSCI.22-14-06254.2002.

Knierim, James J. “Hippocampus and Memory: Can We Have Our Place and Fear It Too?” *Neuron*, vol. 37, no. 3, Elsevier, 2003, pp. 372–374.

Kraus, Benjamin J., et al. “Hippocampal ‘Time Cells’: Time versus Path Integration.” *Neuron*, vol. 78, no. 6, June 2013, pp. 1090–101. *DOI.org (Crossref)*, doi:10.1016/j.neuron.2013.04.015.

Lee, D., et al. “Hippocampal Place Fields Emerge upon Single-Cell Manipulation of Excitability During Behavior.” *Science*, vol. 337, no. 6096, Aug. 2012, pp. 849–53. *DOI.org (Crossref)*, doi:10.1126/science.1221489.

Lee, Heekyung, et al. “Neural Population Evidence of Functional Heterogeneity along the CA3 Transverse Axis: Pattern Completion versus Pattern Separation.” *Neuron*, vol. 87, no. 5, Sept. 2015, pp. 1093–105. *DOI.org (Crossref)*, doi:10.1016/j.neuron.2015.07.012.

Lenck-Santini, Pierre-Pascal, et al. “Place-Cell Firing Does Not Depend on the Direction of Turn in a Y-Maze Alternation Task: Place Cells and Memory.” *European Journal of Neuroscience*, vol. 13, no. 5, Mar. 2001, pp. 1055–58. *DOI.org (Crossref)*, doi:10.1046/j.0953-816x.2001.01481.x.

(b) Leutgeb, Jill K., et al. “Progressive Transformation of Hippocampal Neuronal Representations in ‘Morphed’ Environments.” *Neuron*, vol. 48, no. 2, Oct. 2005, pp. 345–58. *DOI.org (Crossref)*, doi:10.1016/j.neuron.2005.09.007.

(a) Leutgeb, S. “Independent Codes for Spatial and Episodic Memory in Hippocampal Neuronal Ensembles.” *Science*, vol. 309, no. 5734, July 2005, pp. 619–23. *Crossref*, doi:10.1126/science.1114037.

Lever, Colin, et al. “Long-Term Plasticity in Hippocampal Place-Cell Representation of Environmental Geometry.” *Nature*, vol. 416, no. 6876, Mar. 2002, pp. 90–94. *Crossref*, doi:10.1038/416090a.

Lisman, John. "The theta/gamma discrete phase code occuring during the hippocampal phase precession may be a more general brain coding scheme." *Hippocampus* 15.7 (2005): 913-922.

Lisman, John E., and Ole Jensen. "The theta-gamma neural code." *Neuron* 77.6 (2013): 1002-1016.

Ludvig, Nandor. “Place Cells Can Flexibly Terminate and Develop Their Spatial Firing. A New Theory for Their Function.” *Physiology & Behavior*, vol. 67, no. 1, Aug. 1999, pp. 57–67. *DOI.org (Crossref)*, doi:10.1016/S0031-9384(99)00048-7.

MacDonald, Christopher J. *Hippocampal ``Time Cells'' Bridge the Gap in Memory for Discontiguous Events | Elsevier Enhanced Reader*. *reader.elsevier.com*, doi:10.1016/j.neuron.2011.07.012. Accessed 12 July 2020.

Manns, J. R., and H. Eichenbaum. “A Cognitive Map for Object Memory in the Hippocampus.” *Learning & Memory*, vol. 16, no. 10, Sept. 2009, pp. 616–24. *DOI.org (Crossref)*, doi:10.1101/lm.1484509.

Manns, Joseph R., et al. “Gradual Changes in Hippocampal Activity Support Remembering the Order of Events.” *Neuron*, vol. 56, no. 3, Nov. 2007, pp. 530–40. *Crossref*, doi:10.1016/j.neuron.2007.08.017.

Markus, Etan J., et al. "Interactions between location and task affect the spatial and directional firing of hippocampal neurons." *Journal of Neuroscience* 15.11 (1995): 7079-7094.

Marr, David. “Simple Memory: A Theory for Archicortex.” *Philosophical Transactions of the Royal Society B: Biological Sciences*, vol. 262, no. 841, pp. 23–81. *Zotero*, doi:http://doi.org/10.1098/rstb.1971.0078.

McKenzie, Sam, et al. “Hippocampal Representation of Related and Opposing Memories Develop within Distinct, Hierarchically Organized Neural Schemas.” *Neuron*, vol. 83, no. 1, July 2014, pp. 202–15. *DOI.org (Crossref)*, doi:10.1016/j.neuron.2014.05.019.

McNaughton, Bruce L., Carol A. Barnes, and J. J. E. B. R. O'Keefe. "The contributions of position, direction, and velocity to single unit activity in the hippocampus of freely-moving rats." *Experimental brain research* 52.1 (1983): 41-49.

Milner, Brenda. “Disorders of Learning and Memory after Temporal Lobe Lesions in Man.” *Neurosurgery*, vol. 19, no. CN_suppl_1, Oxford University Press, 1972, pp. 421–446.

Milner, Nrenda, et al. “Further Analysis of the Hippocampal Amnesic Syndrome: 14-Year Follow-up Study of H.M.” *Neuropsychologia*, vol. 6, no. 3, Sept. 1968, pp. 215–34. *DOI.org (Crossref)*, doi:10.1016/0028-3932(68)90021-3.

Minsky, ML, et al. *Computers and Thought*. 1963.

Modi, Mehrab N., et al. “CA1 Cell Activity Sequences Emerge after Reorganization of Network Correlation Structure during Associative Learning.” *ELife*, vol. 3, Mar. 2014, p. e01982. *DOI.org (Crossref)*, doi:10.7554/eLife.01982.

Moita, Marta A. P., et al. “Hippocampal Place Cells Acquire Location-Specific Responses to the Conditioned Stimulus during Auditory Fear Conditioning.” *Neuron*, vol. 37, no. 3, Feb. 2003, pp. 485–97. *Crossref*, doi:10.1016/S0896-6273(03)00033-3.

Morris, R. G. M., and U. Frey. “Hippocampal Synaptic Plasticity: Role in Spatial Learning or the Automatic Recording of Attended Experience?” *Philosophical Transactions of the Royal Society of London. Series B: Biological Sciences*, edited by N. Burgess and J. Oapos;Keefe, vol. 352, no. 1360, Oct. 1997, pp. 1489–503. *DOI.org (Crossref)*, doi:10.1098/rstb.1997.0136.

Muller, Robert. “A Quarter of a Century of Place Cells.” *Neuron*, vol. 17, no. 5, Nov. 1996, pp. 813–22. *DOI.org (Crossref)*, doi:10.1016/S0896-6273(00)80214-7.

Muller, Ru, and Jl Kubie. “The Effects of Changes in the Environment on the Spatial Firing of Hippocampal Complex-Spike Cells.” *The Journal of Neuroscience*, vol. 7, no. 7, July 1987, pp. 1951–68. *DOI.org (Crossref)*, doi:10.1523/JNEUROSCI.07-07-01951.1987.

O’Keefe, J., and J. Dostrovsky. “The Hippocampus as a Spatial Map. Preliminary Evidence from Unit Activity in the Freely-Moving Rat.” *Brain Research*, vol. 34, no. 1, Nov. 1971, pp. 171–75. *DOI.org (Crossref)*, doi:10.1016/0006-8993(71)90358-1.

O’Keefe, J., and A. Speakman. “Single Unit Activity in the Rat Hippocampus during a Spatial Memory Task.” *Experimental Brain Research*, vol. 68, no. 1, Sept. 1987. *DOI.org (Crossref)*, doi:10.1007/BF00255230.

O’Keefe, John. “Place Units in the Hippocampus of the Freely Moving Rat.” *Experimental Neurology*, vol. 51, no. 1, Jan. 1976, pp. 78–109. *DOI.org (Crossref)*, doi:10.1016/0014-4886(76)90055-8.

O'Keefe, John. "Hippocampal neurophysiology in the behaving animal." (2007).

O’Keefe, John, and Neil Burgess. “Dual Phase and Rate Coding in Hippocampal Place Cells: Theoretical Significance and Relationship to Entorhinal Grid Cells.” *Hippocampus*, vol. 15, no. 7, 2005, pp. 853–66. *DOI.org (Crossref)*, doi:10.1002/hipo.20115.

O'Keefe, John and Neil Burgess. “Geometric Determinants of the Place Fields of Hippocampal Neurons.” *Nature*, vol. 381, no. 6581, May 1996, pp. 425–28. *DOI.org (Crossref)*, doi:10.1038/381425a0.

O’Keefe, John, and Lynn Nadel. *The Hippocampus as a Cognitive Map*. Clarendon Press ; Oxford University Press, 1978.

O'Keefe, John, and Michael L. Recce. "Phase Relationship between Hippocampal Place Units and the EEG Theta Rhythm." *Hippocampus*, vol. 3, no. 3, July 1993, pp. 317–30. *DOI.org (Crossref)*, doi:10.1002/hipo.450030307.

Olds, J., et al. "Learning Centers of Rat Brain Mapped by Measuring Latencies of Conditioned Unit Responses." *Journal of Neurophysiology*, vol. 35, no. 2, Mar. 1972, pp. 202–19. *DOI.org (Crossref)*, doi:10.1152/jn.1972.35.2.202.

Pastalkova, E., et al. "Internally Generated Cell Assembly Sequences in the Rat Hippocampus." *Science*, vol. 321, no. 5894, Sept. 2008, pp. 1322–27. *DOI.org (Crossref)*, doi:10.1126/science.1159775.

Ranck, James B. "Behavioral Correlates and Firing Repertoires of Neurons in the Dorsal Hippocampal Formation and Septum of Unrestrained Rats." *The Hippocampus*, Springer, 1975, pp. 207–244.

Ranck Jr, JB, et al. "Single Neuron Recording in Behaving Mammals: Bridging the Gap between Neuronal Events and Sensory-Behavioral Variables." *Behavioral Approaches to Brain Research*, Oxford University Press London/New York, 1983, pp. 62–93.

Reichenbach, Hans, and others. *Experience and Prediction: An Analysis of the Foundations and the Structure of Knowledge*. University of Chicago press Chicago, 1938.

Robinson, Nick T. M., et al. "Medial Entorhinal Cortex Selectively Supports Temporal Coding by Hippocampal Neurons." *Neuron*, vol. 94, no. 3, May 2017, pp. 677-688.e6. *DOI.org (Crossref)*, doi:10.1016/j.neuron.2017.04.003.

Samsonovich, Alexei, and Bruce L. McNaughton. "Path Integration and Cognitive Mapping in a Continuous Attractor Neural Network Model." *The Journal of Neuroscience*, vol. 17, no. 15, Aug. 1997, pp. 5900–20. *DOI.org (Crossref)*, doi:10.1523/JNEUROSCI.17-15-05900.1997.

Savelli, Francesco, et al. "Influence of Boundary Removal on the Spatial Representations of the Medial Entorhinal Cortex." *Hippocampus*, vol. 18, no. 12, Dec. 2008, pp. 1270–82. *DOI.org (Crossref)*, doi:10.1002/hipo.20511.

Scoville, W. B. "The Limbic Lobe in Man." *Journal of Neurosurgery*, vol. 11, no. 1, Jan. 1954, pp. 64–66. *DOI.org (Crossref)*, doi:10.3171/jns.1954.11.1.0064.

Scoville, William Beecher, and Brenda Milner. "LOSS OF RECENT MEMORY AFTER BILATERAL HIPPOCAMPAL LESIONS." *Journal of Neurology, Neurosurgery, and Psychiatry*, vol. 20, no. 1, Feb. 1957, pp. 11–21.

Shannon, C. E. *A Mathematical Theory of Communication*. p. 55.

Shapiro, Matthew L., et al. "Cues That Hippocampal Place Cells Encode: Dynamic and Hierarchical Representation of Local and Distal Stimuli."

Hippocampus, vol. 7, no. 6, 1997, pp. 624–42. *Wiley Online Library*, doi:10.1002/(SICI)1098-1063(1997)7:6<624::AID-HIPO5>3.0.CO;2-E.

Sharp, Patricia E. “Subicular Place Cells Expand or Contract Their Spatial Firing Pattern to Fit the Size of the Environment in an Open Field but Not in the Presence of Barriers: Comparison with Hippocampal Place Cells.” *Behavioral Neuroscience*, vol. 113, no. 4, 1999, pp. 643–62. *DOI.org (Crossref)*, doi:10.1037/0735-7044.113.4.643.

Shin, Justin D., et al. “Dynamics of Awake Hippocampal-Prefrontal Replay for Spatial Learning and Memory-Guided Decision Making.” *Neuron*, vol. 104, no. 6, Dec. 2019, pp. 1110-1125.e7. *DOI.org (Crossref)*, doi:10.1016/j.neuron.2019.09.012.

Singer, A. C., et al. “Experience-Dependent Development of Coordinated Hippocampal Spatial Activity Representing the Similarity of Related Locations.” *Journal of Neuroscience*, vol. 30, no. 35, Sept. 2010, pp. 11586–604. *DOI.org (Crossref)*, doi:10.1523/JNEUROSCI.0926-10.2010.

Skaggs, William E., and Bruce L. McNaughton. “Spatial Firing Properties of Hippocampal CA1 Populations in an Environment Containing Two Visually Identical Regions.” *The Journal of Neuroscience*, vol. 18, no. 20, Oct. 1998, pp. 8455–66. *DOI.org (Crossref)*, doi:10.1523/JNEUROSCI.18-20-08455.1998.

Skaggs, William E, and Bruce L. McNaughton. *Theta Phase Precession in Hippocampal Neuronal Populations and the Compression of Temporal Sequences*. p. 24.

Solstad, Trygve, et al. “Representation of Geometric Borders in the Entorhinal Cortex.” *Science*, vol. 322, no. 5909, Dec. 2008, pp. 1865–68. *DOI.org (Crossref)*, doi:10.1126/science.1166466.

Spiers, H. J., et al. “Place Field Repetition and Purely Local Remapping in a Multicompartment Environment.” *Cerebral Cortex*, vol. 25, no. 1, Jan. 2015, pp. 10–25. *DOI.org (Crossref)*, doi:10.1093/cercor/bht198.

Squire, Larry R. “Declarative and Nondeclarative Memory: Multiple Brain Systems Supporting Learning and Memory.” *Journal of Cognitive Neuroscience*, vol. 4, no. 3, MIT Press, 1992, pp. 232–243.

Stewart, Sarah, et al. “Boundary Coding in the Rat Subiculum.” *Philosophical Transactions of the Royal Society B: Biological Sciences*, vol. 369, no. 1635, Feb. 2014, p. 20120514. *DOI.org (Crossref)*, doi:10.1098/rstb.2012.0514.

Sutton, Richard S., et al. *Introduction to Reinforcement Learning*. MIT press Cambridge, 1998.

Tamura, Makoto, et al. “Hippocampal-Prefrontal Theta-Gamma Coupling during Performance of a Spatial Working Memory Task.” *Nature Communications*, vol. 8, no. 1, Dec. 2017, p. 2182. *DOI.org (Crossref)*, doi:10.1038/s41467-017-02108-9.

Tanaka, Kazumasa Z., et al. “The Hippocampal Engram Maps Experience but Not Place.” *Science*, vol. 361, no. 6400, July 2018, pp. 392–97. *DOI.org (Crossref)*, doi:10.1126/science.aat5397.

Taxidis, Jiannis, et al. "Differential Emergence and Stability of Sensory and Temporal Representations in Context-Specific Hippocampal Sequences." *Neuron* 108.5 (2020): 984-998.

Terada, Satoshi, et al. “Temporal and Rate Coding for Discrete Event Sequences in the Hippocampus.” *Neuron*, vol. 94, no. 6, June 2017, pp. 1248-1262.e4. *DOI.org (Crossref)*, doi:10.1016/j.neuron.2017.05.024.

Teyler, Timothy J., and Pascal DiScenna. *The Hippocampal Memory Indexing Theory*. p. 8.

Teyler, Timothy J., and Jerry W. Rudy. “The Hippocampal Indexing Theory and Episodic Memory: Updating the Index.” *Hippocampus*, vol. 17, no. 12, Dec. 2007, pp. 1158–69. *DOI.org (Crossref)*, doi:10.1002/hipo.20350.

Tolman, Edward C. "Cognitive maps in rats and men." *Psychological review* 55.4 (1948): 189.

Tsao, Albert, et al. “Integrating Time from Experience in the Lateral Entorhinal Cortex.” *Nature*, vol. 561, no. 7721, Sept. 2018, pp. 57–62. *DOI.org (Crossref)*, doi:10.1038/s41586-018-0459-6.

Tulving, Endel. “Precis of Elements of Episodic Memory.” *Behavioral and Brain Sciences*, vol. 7, no. 2, Cambridge University Press, 1984, pp. 223–238.

Wang, Cheng, et al. “Egocentric Coding of External Items in the Lateral Entorhinal Cortex.” *Science*, vol. 362, no. 6417, Nov. 2018, pp. 945–49. *DOI.org (Crossref)*, doi:10.1126/science.aau4940.

Wang, Chia-Hsuan, et al. “Hippocampal Place Cells Encode Local Surface-Texture Boundaries.” *Current Biology*, vol. 30, no. 8, Apr. 2020, pp. 1397-1409.e7. *DOI.org (Crossref)*, doi:10.1016/j.cub.2020.01.083.

Wiebe, Sherman P., and Ursula V. Stäubli. “Dynamic Filtering of Recognition Memory Codes in the Hippocampus.” *The Journal of Neuroscience*, vol. 19, no. 23, Dec. 1999, pp. 10562–74. *DOI.org (Crossref)*, doi:10.1523/JNEUROSCI.19-23-10562.1999.

Wiener, Si, et al. “Spatial and Behavioral Correlates of Hippocampal Neuronal Activity.” *The Journal of Neuroscience*, vol. 9, no. 8, Aug. 1989, pp. 2737–63. *DOI.org (Crossref)*, doi:10.1523/JNEUROSCI.09-08-02737.1989.

Wikenheiser, Andrew M., and A. David Redish. “Hippocampal Theta Sequences Reflect Current Goals.” *Nature Neuroscience*, vol. 18, no. 2, Feb. 2015, pp. 289–94. *DOI.org (Crossref)*, doi:10.1038/nn.3909.

Wills, T. J. “Attractor Dynamics in the Hippocampal Representation of the Local Environment.” *Science*, vol. 308, no. 5723, May 2005, pp. 873–76. *Crossref*, doi:10.1126/science.1108905.

Wilson, M., and B. McNaughton. “Dynamics of the Hippocampal Ensemble Code for Space.” *Science*, vol. 261, no. 5124, Aug. 1993, pp. 1055–58. *DOI.org (Crossref)*, doi:10.1126/science.8351520.

Wood, Emma R., Paul A. Dudchenko, R. Jonathan Robitsek, et al. “Hippocampal Neurons Encode Information about Different Types of Memory Episodes Occurring in the Same Location.” *Neuron*, vol. 27, no. 3, Sept. 2000, pp. 623–33. *DOI.org (Crossref)*, doi:10.1016/S0896-6273(00)00071-4.

Wood, Emma R., Paul A. Dudchenko, and Howard Eichenbaum. “The Global Record of Memory in Hippocampal Neuronal Activity.” *Nature*, vol. 397, no. 6720, Feb. 1999, pp. 613–16. *DOI.org (Crossref)*, doi:10.1038/17605.

Ziv, Yaniv, et al. “Long-Term Dynamics of CA1 Hippocampal Place Codes.” *Nature Neuroscience*, vol. 16, no. 3, Mar. 2013, pp. 264–66. *DOI.org (Crossref)*, doi:10.1038/nn.3329.

Curriculum Vitae for Ph.D Candidates

Johns Hopkins University School of Medicine

William Hockeimer November, 2020

Educational History

Johns Hopkins University Neuroscience Training Program, Baltimore, Maryland, Ph.D in Neuroscience (2014-2021)

Mentor: Dr. James Knierim. Dissertation Title: Non-spatial Information Encoding in Hippocampal CA1

University of Michigan, Ann Arbor, B.Sc (2009-2013)

High Honors, Neuroscience, Minor in Philosophy (Mind and Meaning)
Honors Thesis Mentor: Dr. Michael Sutton
Thesis Title: *"Mechanistic Target of Rapamycin is Necessary for Changes in Dendritic Spine Morphology Underlying Long-Term Potentiation"*

Saint Joseph's Preparatory School, Philadelphia, Pennsylvania (Class of 2009)

Publications and Posters

Hockeimer, W and Knierim, J.J. "CA1 neurons encode Non-spatial cues as a conjunction of location and cue identity" Society for Neuroscience. Chicago. 2019.

Hockeimer, W and Knierim, J.J. "Firing Rate Modulations May Encode Surface Texture Cues Within The Place Cell Map Of Hippocampal CA1 Neurons" Society for Neuroscience. San Diego. 2018.

Henry, F. E. (co-first author), **Hockeimer, W**. (co-first author), Chen, A., Mysore, S. P., & Sutton, M. A. (2017). Mechanistic target of rapamycin is necessary for changes in dendritic spine morphology associated with long-term potentiation. *Molecular Brain*, *10*(1), 1-17.

Kaplan, C. M., Saha, D., Molina, J. L., **Hockeimer, W**. D., Postell, E. M., Apud, J. A., ... & Tan, H. Y. (2016). Estimating changing contexts in schizophrenia. *Brain*, *139*(7), 2082-2095.

Hockeimer, W, Henry, F, and Sutton, M. "Mechanistic Target of Rapamycin is Necessary for Changes in Dendritic Spine Morphology Underlying Long-Term Potentiation." MiSfN Poster Presentation. Michigan Chapter of the Society for Neuroscience. Detroit. 2013.

Seavey, M, Lu, L., Stump, K., Wallace, N., **Hockeimer, W.**, M. O'Kane, T., Ruggeri, B., and Dobrzanski, P. “Therapeutic Efficacy of CEP-33779, a Novel Selective JAK2 Inhibitor, in a Mouse Model of Colitis-induced Colorectal Cancer” *Mol Cancer Ther* April 2012 11:984-993.

Hockeimer, W.. “Modern Approaches in Artificial Intelligence: fuzzy logic, neural nets and the future of intelligence” 2nd Annual Eastern Michigan University Undergraduate Philosophy Conference.

Awards and Leadership

2014-2018 – Volunteer, Project BRIDGE, Baltimore, Maryland
2015-2018 – Graduate Research Fellowship Program Fellow, National Science Foundation
2011-2013 – Co-Editor-in-Chief, University of Michigan Undergraduate Research Journal
2006 – Calvert Award, American Entomological Society (poster: “PCR Amplification of mitochondrial DNA from a Mexican Geometrine Moth Species.”)